



**Laboratory For Atmospheric and Space Physics**  
 LASP Mission Operations and Data Systems Division  
 University of Colorado  
 Boulder, Colorado

<p><b>GOES-R EXIS</b></p> <p><b>Ground Processing Algorithms (CDRL 080)</b></p> <p><b>Document No. 109620</b></p>
---

**Approvers List**

Prepared By	Donald L. Woodraska, PhD, EXIS Data Processing Lead
Reviewers	Frank Eparvier, PhD, EXIS Principal Investigator/Lead Scientist
Configuration Management	

Rev	Change Description	By
A	Initial draft release	DLW
B	Updated based on IPT comments	DLW
C	Update based on Harris/AER telecons	DLW
D	Update for courtesy deliver	DLW
E	Updated	DLW
F	Updated for minor change in EUVS-A, B. Algorithm changes in EUVS-C based on calibration analysis	DLW
G	Update to correct typographical errors from TIM and include content for flags	DLW

H	Update to include Technical Memos #1-5	DLW
---	--	-----

## 0.1 Table of Contents

0.1	Table of Contents .....	iii
0.2	Table of Tables .....	vii
0.3	Table of Figures.....	vii
0.4	Reference Documents.....	viii
0.5	Applicable Documents.....	viii
0.6	Acronyms/Abbreviations.....	viii
0.7	Definitions.....	x
1.0	Overview .....	1
1.1	Scope .....	2
1.2	Context .....	2
2.0	Selected High Level Requirements.....	3
2.1	Key Requirements .....	3
2.2	Document Requirements.....	4
3.0	Processing EXIS Data .....	5
3.1	Process Startup .....	5
3.2	Main Process Flow .....	5
3.2.1	Pseudocode .....	7
4.0	XRS Algorithm Description .....	9
4.1	Detector Measurement Input .....	9
4.2	Detector Details .....	11
4.2.1	Integration Rate .....	11
4.2.2	Saturation Values.....	11
4.3	Mathematical Description and Algorithm Design.....	11
4.3.1	Solar Minimum Diodes, $A_1$ and $B_1$ .....	12
4.3.2	Solar Maximum Diodes, $A_{2j}$ and $B_{2j}$ .....	14
4.3.3	Dependency Analysis .....	17
4.4	XRS Algorithm Steps.....	18
4.4.1	Packet Decomposition .....	20
4.4.1.1	Temperature Conversions .....	21
4.4.2	Lookup_1-AU .....	22
4.4.3	Signal, $\bar{S}$ .....	22
4.4.4	Integration time, $\Delta t$ (and application of time stamp).....	22
4.4.4.1	Timing Details.....	23
4.4.5	Gain, $G$ .....	24
4.4.5.1	Inputs & Dependencies .....	24
4.4.5.1.1	Preflight Gain Temperature Dependence, $G_{\text{preflight}}$ .....	24
4.4.5.1.2	Calibration Table for Time Dependence, $f_G$ .....	25
4.4.5.1.3	Calibration Table for Linearity, $f_{\text{Lin}}$ .....	26
4.4.5.1.4	Table Details .....	26
4.4.5.1.5	Maintenance.....	26
4.4.5.2	Output.....	26
4.4.5.3	Implementation Recommendations .....	27
4.4.6	Evaluate $C'$ .....	27
4.4.6.1	$C_{\text{Dark}}$ .....	27
4.4.6.1.1	Electrometer Offset, $C_{\text{elect}}$ .....	27
4.4.6.1.2	Thermal Contribution to Dark, $C_{\text{therm}}$ .....	28
4.4.6.1.3	Background, $C_{\text{rad}}$ .....	28
4.4.7	Responsivity, $R_C$ .....	29
4.4.8	Field of View (FOV).....	29
4.4.9	XRS Ratio .....	30
4.5	XRS Output .....	30
4.6	XRS Measurement Flag Details .....	37
4.6.1	Flags Set in Telemetry Decomposition .....	37

4.6.1.1	Special Note about Pointing Flags .....	38
4.6.1.2	Special Note about DataNotGood Flags .....	40
4.6.2	Flags Set After Evaluation of Eq. 4.3 .....	40
4.6.3	Flags Set After Evaluation of Eq. 4.12 .....	40
4.6.4	Flags Set After Evaluation of Eq. 4.9 and Eq. 4.18 .....	41
4.6.4.1	DataNotGoodA .....	41
4.6.4.2	DataNotGoodB .....	41
4.6.4.3	RatioNotGood .....	41
5.0	EUVS Algorithm Description .....	41
5.1	Detector Measurement Input .....	42
5.2	Mathematical Description and Algorithm Design .....	43
5.2.1	Dependency Analysis .....	45
5.3	EUVS-A Algorithm Steps .....	46
5.3.1	Packet Decomposition .....	50
5.3.2	Lookup_1au .....	51
5.3.3	Signal, S .....	51
5.3.4	Integration time, $\Delta t$ .....	51
5.3.5	Gain .....	51
5.3.6	Flatfield .....	51
5.3.7	Scattered Light .....	51
5.3.8	Order Sorting .....	52
5.3.9	Dark .....	52
5.3.10	Mask .....	52
5.3.11	Responsivity .....	52
5.3.12	Field of View .....	52
5.3.13	Degradation .....	53
5.3.14	Sum over Lines .....	53
5.4	EUVS-A Output .....	53
5.5	EUVS-A Measurement Flag Details .....	57
5.5.1	Flags Set in Telemetry Decomposition .....	58
5.5.1.1	Special Note about Pointing Flags .....	58
5.5.1.2	Special Note about DataNotGood Flags .....	59
5.5.2	Flags Set After Evaluation of Eq. 5.2 .....	60
5.6	EUVS-B Algorithm Steps .....	60
5.6.1	Hydrogen Lyman-alpha and Geocorona .....	61
5.7	EUVS-B Output .....	62
5.8	EUVS-C Mathematical Description and Algorithm Design .....	66
5.8.1	Data Encoding .....	66
5.8.1.1	EUVS-C Pixel Mode 0 and 1, Data Minus Reference .....	66
5.8.1.2	EUVS-C Pixel Mode 2, Data Only .....	67
5.8.1.3	EUVS-C Pixel Mode 3, Reference Only .....	67
5.8.2	Algorithm Concept .....	67
5.8.3	Dependency Analysis .....	70
5.9	EUVS-C Algorithm Steps .....	71
5.9.1	Packet Decomposition .....	73
5.9.2	Signal, S .....	74
5.9.3	Integration time, $D_t$ .....	74
5.9.4	Dark Background, $D_{BG}$ .....	75
5.9.4.1	Electronic Offset, $D_{Offset}$ .....	75
5.9.4.2	Thermal Dark, $D_{Therm}$ .....	76
5.9.5	Flatfield .....	76
5.9.6	Linearity .....	76
5.9.7	Scattered Light .....	76
5.9.8	Lookup Wavelength .....	76
5.9.9	Integrate Features .....	77
5.9.9.1	Lines, h, k .....	77

5.9.9.2	Wings, red and blue.....	77
5.9.10	Calculate Ratio.....	78
5.10	EUVS-C Output.....	78
5.11	EUVS-C Measurement Flags.....	82
5.11.1	Flags Set in Telemetry Decomposition.....	82
5.11.1.1	Special Note about Pointing Flags.....	83
5.11.1.2	Special Note about DataNotGood Flags.....	83
5.11.2	Flags Set After Evaluation of Eq. 5.12.....	84
5.11.3	Flags Set After Evaluation of Eq. 5.17.....	84
6.0	Creating the Spectrum.....	84
6.1	Proxy Model Inputs.....	85
6.2	Proxy Model Mathematical Description and Algorithm Design.....	85
6.3	Proxy Model Algorithm Steps.....	88
6.3.1	Solar Minimum Reference.....	88
6.3.2	Averaging to Create Proxies.....	88
6.3.2.1	Daily Averages.....	89
6.3.3	Spectral Bins.....	89
6.4	Proxy Model Output.....	90
6.5	EUVS Data Product.....	90
7.0	GPDS System Description.....	97
8.0	SPS Processing.....	97
8.1	Detector Measurements.....	97
8.2	Mathematical Description.....	98
8.2.1	Implementation Recommendation.....	100
8.2.2	Dependency Analysis.....	100
8.3	SPS Algorithm Steps.....	101
8.3.1	Packet Decomposition.....	101
8.3.2	Signal, $S$ .....	101
8.3.3	Integration Time.....	102
8.3.4	Gain, $G$ .....	102
8.3.5	Dark, $C_{\text{Dark}}$ .....	102
8.3.5.1	Electrometer Offset, $C_{\text{elect}}$ .....	102
8.3.5.2	Thermal Contribution to Dark, $C_{\text{therm}}$ .....	102
8.3.6	Implementation Recommendations.....	102
8.4	EXIS Orientation and Roll Angle.....	104
9.0	Maintaining Calibration, Long-Term Stability.....	105
9.1	Daily Calibration Analysis Routines.....	105
9.1.1	Flatfield.....	105
9.1.1.1	EUVS-A and EUVS-B.....	106
9.1.1.2	EUVS-C.....	106
9.1.2	Dark Electrometer Offset.....	107
9.1.3	Relative Gain.....	107
9.1.4	Degradation Bootstrap Algorithm.....	110
9.1.5	EUVS-A Filter Degradation.....	111
9.2	Other Calibration Analysis Routines.....	114
9.2.1	Cruciform and FOV.....	114
9.2.2	Inter-comparisons.....	115
9.2.3	EUVS-C Flatfield.....	115
9.3	Special Routines.....	115
9.3.1	Accuracy.....	115
9.3.1.1	XRS Accuracy.....	116
9.3.1.2	EUVS-A Accuracy.....	117
9.3.1.3	EUVS-B Accuracy.....	118
9.3.1.4	EUVS-C Accuracy.....	118
9.3.1.5	EUVS Product Accuracy.....	119
9.3.2	Signal to Noise.....	119

9.3.2.1	XRS Signal to Noise .....	119
9.3.2.2	EUVS Signal to Noise.....	120
Appendix A	- GPDS Description.....	A-1
Appendix B	- Polynomial Conversions .....	B-1
Appendix C	- Calibration Coefficients and Lookup Tables .....	C-1
Appendix D	- Astronomical Unit Correction (1-AU) .....	D-2
Appendix E	- Time.....	E-3
Appendix F	- Spacecraft Telemetry.....	F-3

## 0.2 Table of Tables

Table 1 Reference Documents .....	viii
Table 2 Applicable Documents.....	viii
Table 3 Acronyms.....	x
Table 4 EXIS Components: Packets per integration and integration rate. ....	3
Table 5 Diode telemetry order and ASIC relationship .....	10
Table 6 XRS Measurement Equation Variables .....	17
Table 7 XRS measurement flags.....	31
Table 8 XRS data product variables .....	37
Table 9 EUVS-A and EUVS-B Measurement Equation Variables .....	45
Table 10 EUVS-A diode telemetry order and ASIC relationship.....	50
Table 11 EUVS-A measurement flags.....	54
Table 12 EUVS-A data product variables .....	57
Table 13 EUVS-B diode telemetry order and ASIC relationship.....	61
Table 14 EUVS-B measurement flags.....	63
Table 15 EUVS-B data product variables.....	65
Table 16 EUVS-C Measurement Equation Variables .....	69
Table 17 Mg II h and k fit parameter initial guesses .....	77
Table 18 Wing weights around the Mg II lines .....	78
Table 19 EUVS-C measurement flags.....	79
Table 20 EUVS-C data product variables.....	82
Table 21 Solar Emissions Measured by EXIS.....	85
Table 22 Proxy Data Availability Cases.....	88
Table 23 Spectral bin ranges.....	90
Table 24 EUVS measurement flags.....	93
Table 25 EUVS data product contents.....	97
Table 26 EUVS absolute filter step numbers and positions. ....	114
Table 27 GPDS Hardware Description.....	A-1

## 0.3 Table of Figures

Figure 1. EXIS main processing flow.....	6
Figure 2. XRS mechanical layout with ASIC 1 on the right and ASIC 2 on the left. Solar North and East-West convention will be verified during instrument testing to ensure the directions are correct. ....	10
Figure 3 XRS dependency graph .....	17
Figure 4 XRS rooted dependency tree.....	18
Figure 5. XRS GPA Overview.....	19
Figure 6. XRS functions .....	20
Figure 7. The pointing flag nested regions represented as rectangles. ....	39
Figure 8. EUVS-A, EUVS-B, & EUVS-C spectral measurements .....	42
Figure 9 EUVS-A, B dependency graph.....	45
Figure 10 EUVS-A, B Rooted dependency tree.....	46
Figure 11. EUVS-A and EUVS-B Algorithm Overview.....	47
Figure 12. EUVS-A (and EUVS-B) functions.....	48

Figure 13. EUVS-A 30.4 diode layout..... 49  
 Figure 14. EUVS-A diode layout..... 49  
 Figure 15. EUVS-A cathode numbers are fortuitously in wavelength order..... 50  
 Figure 16. EUVS-B diode layout..... 60  
 Figure 17 EUVS-C dependency graph ..... 70  
 Figure 18 EUVS-C rooted dependency tree ..... 71  
 Figure 19 EUVS-C algorithm flow..... 72  
 Figure 20. EUVS-C functions..... 73  
 Figure 21. Model Spectrum Algorithm Flow ..... 86  
 Figure 22 SPS diode layout on the flex circuit. .... 99  
 Figure 23 SPS dependency graph ..... 100  
 Figure 24 SPS rooted dependency tree ..... 101  
 Figure 25. SPS Processing Flow ..... 103  
 Figure 26. SPS Functions..... 104

## 0.4 Reference Documents

Document Ref	Title
103767	EXIS Software Development and Management Plan
109124	EXIS Irradiance Uncertainty Budget

**Table 1 Reference Documents**

## 0.5 Applicable Documents

Document Ref	Title
417-R-EXISCDRL-0114	Geostationary Operational Environmental Satellite (GOES) GOES-R Series EUVS XRS Irradiance Sensors (EXIS) Contract Data Requirements List (CDRL)
417-R-EXISSOW-0113	GOES-R EXIS Statement of Work (v2.1)
417-R-EXISPORD-0116	GOES-R EXIS Performance and Operational Requirements Document (v2.0)
109743	GOES-R EXIS Command and Telemetry Handbook (CDRL 43)
104904	GOES-R EXIS Calibration Program Plan (CDRL 78)
130766	GOES-R EXIS Calibration Data Books (CDRL 79)
110933	GOES-R EXIS Processor FPGA Design Specification

**Table 2 Applicable Documents**

## 0.6 Acronyms/Abbreviations

Acronym	Meaning
APID	Application Identifier
ASIC	Application Specific Integrated Circuit
CCSDS	Consultative Committee on Space Data Systems
CDRL	Contract Deliverable Requirements List
CDR	Critical Design Review
CM	Configuration Management
CMD	Command
COTS	Commercial Off-The-Shelf



CPU	Central Processing Unit
CSC	Computer Software Component
CSCI	Computer Software Configuration Item
CSU	Computer Software Unit
DN	Data Number
DSA	Design Status Assessment
EEPROM	Electrically Erasable Programmable Read-Only Memory
EUV	Extreme Ultraviolet
EUVS	Extreme Ultraviolet Sensor
EVE	EUV Variability Experiment
EXEB	EUVS and XRS Electronics Box
EXIS	EUVS XRS Irradiance Sensors
EXISE	EXIS Emulator
FPGA	Field Programmable Gate Array
FSW	Flight Software
FUV	Far Ultraviolet
GCC	GNU C Compiler
GNU	GNU's Not Unix
GOES-R	Geostationary Operational Environmental Satellite, R-Series
GOTS	Government Off-The-Shelf
GPA	Ground Processing Algorithm
GPDS	Ground Processing Demonstration System
GSE	Ground Support Equipment
GSFC	Goddard Space Flight Center
GSW	Ground Software
I&T	Integration and Test
ICD	Interface Control Document
IDL	Interactive Data Language
I/O	Input/Output
LASP	Laboratory for Atmospheric and Space Physics
LED	Light Emitting Diode
MUV	Middle Ultraviolet
NASA	National Aeronautics and Space Administration
NOAA	National Oceanic and Atmospheric Administration
NPR	NASA Procedure Requirements
OASIS-CC	Operations And Science Instrument Support-Command and Control
OIS	OASIS-CC Interface System
OTS	Off-the-Shelf
PCI	Peripheral Component Interconnect
PDPR	Preliminary Design Peer Review
PDR	Preliminary Design Review
PLT	Post-Launch-Test
PROM	Programmable Read-Only Memory
QA	Quality Assurance
RAM	Random Access Memory
ROM	Read-Only Memory
RTVM	Requirements Traceability Verification Matrix
S/C	Spacecraft
SAT	Software Acceptance Test
SDMP	Software Development and Management Plan
SLOC	Source Lines Of Code
SPS	Solar Position Sensor
SQA	Software Quality Assurance

SQAE	Software Quality Assurance Engineer
SRAM	Static Random-Access Memory
SSE	Software Systems Engineer
SSIM	Spacecraft Simulator/Emulator
STOL	Standard Test and Operations Language
SUN	Stanford University Network
SUVI	Solar Ultraviolet Imager
SVN	Subversion
TIMED	Thermosphere Ionosphere Mesosphere Energetics and Dynamics
TLM	Telemetry
XRS	X-Ray Sensor

**Table 3 Acronyms**

## 0.7 Definitions

**System:** A system is a collection of software that implements a major function. The EXIS ground processing system is one example of a system.

**Computer Software Configuration Item (CSCI):** A CSCI is a collection of software that performs a subsystem level function or shares a common purpose within a system. The EXIS ground processing system contains several CSCIs.

**Computer Software Component (CSC), Package, or Class:** A CSC is a collection of subprograms, data structures, and data elements that are common to a file or group of closely related files (i.e. a source program and its associated header file). The EXIS ground processing CSCIs consist of multiple CSCs.

**Computer Software Unit (CSU):** A CSU is a named subprogram, task, function, data structure, or data element. Each CSC consists of one or more units.

**Static Parameters:** These parameters are only updated if it's determined that there is an error, or possibly a hardware failure.

**Semi-static Parameters:** These parameters may be updated throughout the life of the mission to maintain product quality. This usually involves detailed analysis by a person or persons.

**Dynamic Parameters:** These parameters "evolve" from the initial delivery. The algorithms update parameters of this type automatically, possibly off-line.

## 1.0 Overview

The Geostationary Operational Environmental Satellite (GOES) Program is a joint effort of NASA and the National Oceanic and Atmospheric Administration (NOAA). NOAA has operated the GOES series since 1975 for the purpose of providing continuous Earth imaging and sounding data. Beginning with GOES-M in 2001, the satellites have also provided short-wavelength solar imaging and irradiance measurements. GOES-R+ is the latest planned series, consisting of four missions scheduled to begin launching in 2014.

Each satellite in the GOES-R series includes a set of three operational instruments that provides information on solar activity and the effects of the Sun on the earth and near earth space environment. These are the Solar Ultraviolet Imager (SUVI) (built by Lockheed Martin Advanced Technology Center), and the Extreme Ultraviolet Sensor (EUVS) and the X-ray Sensor (XRS) built by the Laboratory for Atmospheric and Space Physics (LASP) at the University of Colorado. The EUVS and XRS are packaged together in one flight element, the EUV and X-Ray Irradiance Sensors, or EXIS. In addition to the EUVS and XRS science components, EXIS also contains the EUVS and XRS Electronics Box (EXEB). Up to a total of four EXIS instruments are planned to fly, one on each GOES-R+ series Observatory. Two have been contracted to LASP.

EXIS provides UV and X-ray irradiance measurements of the full solar disk. The three EUVS channels denoted A, B, and C, give coverage in the bands of 25-31nm (0.6 nm resolution), 117-141nm (0.6 nm with 1.0 nm resolution near 140 nm) and 275-285nm (0.1 nm resolution). The XRS contains two active and two inactive channels: channel A covering 0.05-0.4nm, channel B covering 0.1-0.8nm, and "dark" diode channels to allow background subtraction. To span the full dynamic range of the sun in these wavelengths both XRS A and B measurements are each split between a solar minimum channel and a solar maximum channel (quadrant detectors). The solar maximum channels also provide a means for estimating flare locations on the solar disk. From the EUVS A, B, C and XRS A, B, a reconstruction of the full spectrum between 5 nm and 127 nm will be possible (through a model). In addition to the science components, an engineering component called the Solar Position Sensor (SPS) provides the solar pointing information for the science channels using a quad diode which is very similar to the XRS solar maximum channels, but sensitive to longer wavelength light. Pointing information is needed to process the data from all of the science channels, and the SPS is designed to provide this information. If SPS is not available, then the SUVI guide telescope pointing could be used, but this needs to be calibrated to the EXIS science reference boresight.

The EUVS and XRS science components are controlled by an FPGA that interfaces with the flight software that is resident on the EXEB. The EXIS Flight Software (FSW) distributes and executes commands, maintains the health and safety of the instrument, and gathers, formats, and provides instrument telemetry to the spacecraft. The EXIS Ground Software (GSW) provides the capability for the instrument operations team to monitor the instrument's health, to command instrument activities, and to

receive and archive telemetry. An EXIS Emulator (EXISE), capable of simulating EXIS operations, and a Spacecraft Simulator (SSIM) will be developed to assist in testing; this equipment is supported by GSE software.

The ground processing algorithms (GPAs) are defined as sets of ordered instructions that describe how to create the level 1B data. These algorithms for EXIS are described in this document (CDRL 80, or LASP document 109620). The GPAs will be demonstrated to be feasible through the creation of prototype software. This prototype code will be demonstrated using a computer system called the Ground Processing Demonstration System (GPDS).

The purpose of this document is to define the ground processing algorithms (GPA) associated with the EXIS instrument. Prototype GPA software will be developed at LASP and will demonstrate the algorithm feasibility which will culminate in a demonstration.

## 1.1 Scope

This document satisfies CDRL 080 and only pertains to the ground processing system. It is the responsibility of the NOAA Ground Segment Contractor to implement these algorithms on the system that will be used in flight operations. These algorithms will be prototyped on readily available computer systems and implemented as a "proof of concept" on the Ground Processing Demonstration System (GPDS). This hardware used in the GPDS, the algorithms, and the prototype code is described in this document.

It is imperative that the reader understands that the GPA software developed by LASP is *not* mission-critical software, and will not be used in flight. Rather, the software developed by LASP will demonstrate that the requirements *could* be met if properly implemented in the processing ground system that will be used in flight. We believe the LASP prototype software is of sufficient quality to support flight operations, but knowledge of the details of the production systems, and potential liability concerns likely preclude that possibility. A third party institution will use the algorithms described in this document as the basis for implementing the GPA to support flight operations.

## 1.2 Context

This section describes the context of the GPA using the GPDS as an example. The GPA implementation details are presented in terms of the GPDS implementation throughout this document. It is understood that the Ground System Contractor's system and environment may have additional/different capabilities to leverage. For the GPDS, we implement a complete packet processing interface that is outside the scope of the GPA, but useful for testing and developing the GPA. The Ground System Contractor will have to perform this task for all of the instruments, so there is undoubtedly a different mechanism for providing data to the GPA.

The GPA uses level 0 telemetry data from the instrument. The GPDS receives this detector data (and engineering data) as packets from the EXIS instrument. The packets are sorted by APID and decomposed into useable quantities. Certain engineering telemetry items are required to properly create the XRS irradiances and EUVS irradiance spectrum (Level 1B product). These items must be extracted from telemetry packets and converted into engineering units (degrees C, etc.)

When an XRS packet is received (with a nominal 1 second integration time), it is passed into the XRS processing algorithm, which produces the calibrated irradiances from a single measurement. Similarly, when one EUVS-A or EUVS-B packet is received (with a nominal 1 second integration time), it is passed into the corresponding EUVS-A or EUVS-B processing algorithm in order to produce a calibrated measurement. For the EUVS-C, multiple packets are needed due to the larger detector array. This information is summarized in Table 4. Note that the Level 1B irradiance spectrum (EUVS product) is derived from a model that uses the irradiances measured by EUVS and XRS over a 30-second interval. The algorithm is designed to produce one EUVS spectrum every 30 seconds (see the EXIS230 requirement).

	EXIS Components				
	EUVS-A	EUVS-B	EUVS-C	XRS	SPS
Packets per integration	1	1	8	1	1
Nominal integration rate	1 second	1 second	5 seconds, to be updated during PLT	1 second	0.25 second
Processing function name	Euvs_a. processData	Euvs_b. processData	Euvs_c. processData	Xrs. processData	Sps. processData

**Table 4 EXIS Components: Packets per integration and integration rate.**

## 2.0 Selected High Level Requirements

### 2.1 Key Requirements

The Contractor (LASP) **shall** provide Ground Processing Algorithms (GPAs) to produce data to be compliant with the requirements specified in the EXIS PORD. [EXISSOW161 3.1.3.0-1]

Interpretation: Delivery of this document to the GOES-R project will partially satisfy the requirement. A demonstration using prototype software running on the GPDS will demonstrate that the ground segment contractor could implement the algorithm in order to meet performance requirements.

A measurement **shall** be obtained with a time cadence of 3 seconds or faster such that the irradiance accuracy requirement in EXISPORD80 is met over a 3 second interval. [EXISPORD88]

Interpretation: This describes the cadence of the XRS algorithm output. The XRS is expected to nominally operate at 1.0 seconds, and calibrated irradiance can only be created for 1.0 second integrations. The XRS can be operated with other integration rates ranging from 0.25-64 seconds in 0.25 second increments, but no irradiance can be calculated except at 1.0 seconds. XRS-A and B are further required to have exposures that differ by less than 0.1 seconds. [EXISPORD91]

The EXIS contribution to the XRS data latency **shall** be no more than 1 second. [EXISPORD89]

Interpretation: The GPA allocation is currently set to 0.5 seconds.

A measurement of the solar irradiance **shall** be obtained every 30 seconds. [EXISPORD130]

Interpretation: This describes the cadence of the EUVS spectrum creation. Detector operation is independent of the EUVS data product. The expected integration rate for EUVS-A and EUVS-B is 1 second, but it could range from 0.25-64 seconds in 0.25 second increments. The EUVS-C integration rate will be adjusted on orbit during PLT to its final operational rate. During I&T, it will be operated at a 5 second integration rate. The goal is to have 30 seconds of measurement data to drive the proxy model, which creates the spectrum. The data are averaged to 30 seconds to create proxy inputs to the spectral model every 30 seconds.

The EXIS contribution to the EUVS data latency **shall** be no more than 5 seconds. [EXISPORD131]

Interpretation: The GPA allocation is 4.0 seconds. Since the 3 EUVS channel integration rates are independent of each other and independent of the algorithm output, the latency is only applicable to the spectrum creation portion of the algorithm.

## 2.2 Document Requirements

The Ground Processing Algorithm Document **shall** be complete and detailed, preferably in Unified Modeling Language, such that a third party can generate executable code that correctly implements the algorithms. [EXISCDRL570]

The Ground Processing Algorithm Document **shall** include narrative descriptions of each routine, and include equations, figures and other supporting information where appropriate, in order to clearly convey the intent and context of the processing. [EXISCDRL571]

The Ground Processing Algorithm Document **shall** be written so as to mirror the intended structure of the resulting computer source code. The document should include structural information such as hierarchy charts and data flow diagrams. [EXISCDRL572]

The Ground Processing Algorithm Document **shall** include algorithm specifications including data interface definitions, flow charts, and pseudocode for each routine. [EXISCDRL573]

The Ground Processing Algorithm Document **shall** provide a complete description of all required datasets (e.g. initial gain and bias terms, detector maps), preferably in Extensible Markup Language (XML). [EXISCDRL574]

The Ground Processing Algorithm Document **shall** describe the hardware used to test the algorithm and the measured performance of the algorithms on the test hardware (e.g., CPU and Memory utilization, Latency). [EXISCDRL575]

### **3.0 Processing EXIS Data**

For EXIS development, integration, and testing a main program is used to instantiate objects and control the processing. The main portion also manages proxy arrays so information can be shared in a thread-safe manner. This program is useful for supporting modular development, and for performing timing tests.

#### **3.1 Process Startup**

The program startup involves establishing a socket connection to the server over a port. The code is outside the scope of the GPA but is briefly described here for completeness. The server runs a version of the OTS product called OIS. OIS is setup to allow multiple client connections to the same server socket. Once the client has established the connection, the server will begin forwarding CCSDS packets as they are received. The current OIS version forwards all packets with no filtering applied.

#### **3.2 Main Process Flow**

The main program is written in a file called `process_exis_threads.cpp` (a non-threaded version is also provided for comparison called `process_exis.cpp`). The non-threaded version provides an alternative example, and is useful for comparison. The main program loop and other processing elements are described graphically in Figure 1. The XRS, EUVS-A, EUVS-B, and EUVS-C processing threads all use processed SPS data. The proxy model thread uses processed data from the XRS, EUVS-A, EUVS-B, and EUVS-C threads. Each thread reads calibration data and writes processed data to a disk for later offline analysis. Offline data analysis is critical to maintaining the calibration of the products.

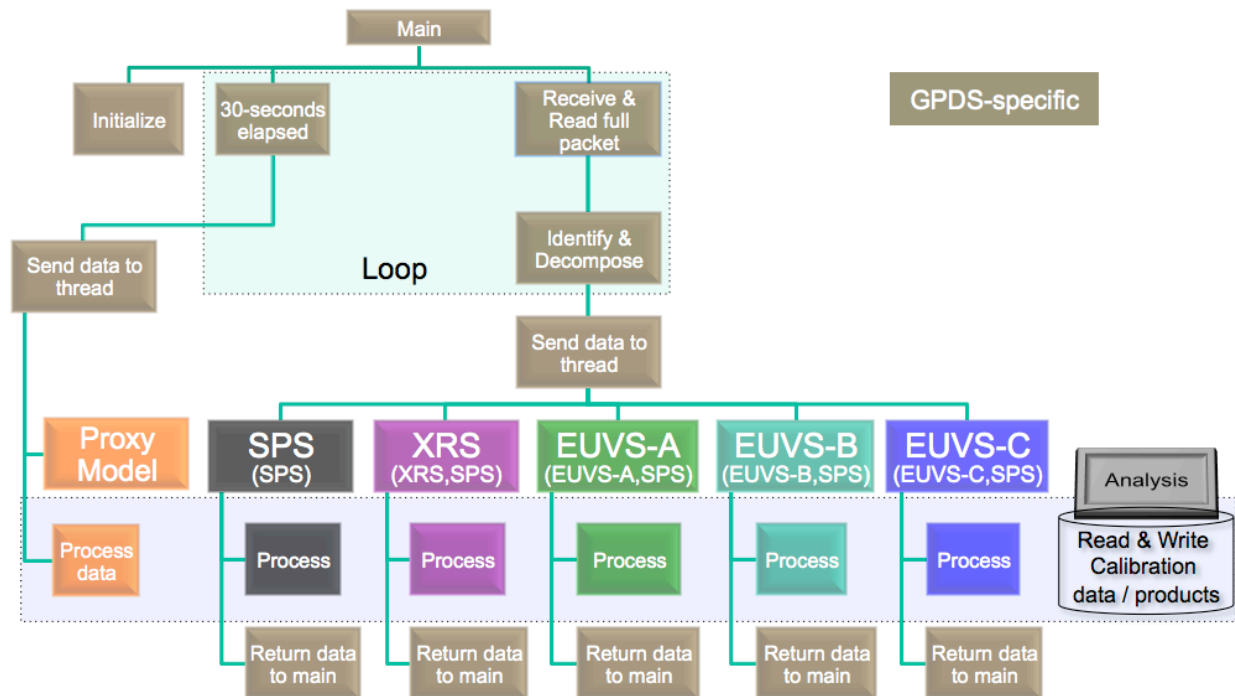


**Figure 1. EXIS main processing flow.**

Reading a packet from the socket connection involves using the system read function. First the primary CCSDS header is read. The data length field is used to determine the remaining bytes to read for the current packet, which are then also read. Once the whole packet is read, the APID is compared to the expected values for XRS, EUVS-A, EUVS-B, EUVS-C, and SPS. If the packet does not match one of these known values it is discarded. The EXIS produces several other CCSDS housekeeping-related packets that are not needed to produce data products, so these are discarded. Rather than create a custom OIS which forwards only science channel packets, we are leveraging the existing OIS. The details of receiving packets are expected to be different for the ground system contractor, but this description provides context for the methods used in the GPDS.

Once the packet is known and identified by APID, it is then ready to verify the checksum and then be processed. Each EXIS packet has an 8-bit checksum contained in byte #19 (first byte after the secondary header). The checksum algorithm is rudimentary and can be summarized as a 0xFF seeded bitwise exclusive “OR” of all bytes starting at #20 through the end of the packet. Instead of pseudocode, we provide the IDL code used to calculate the checksum from the data simulator software.

```

result = 'ff'xb ; set the initial checksum seed value

; arr is a bytearray of the packet data starting at byte #20

for i=0L,n_elements(arr)-1 do result XOR= arr[i]
    
```



If the calculated checksum does not match the checksum reported in byte #19, then the packet should be ignored, and a warning should be issued. This indicates that something went wrong between flight software calculation of the checksum and the GPA calculation of the checksum. This is an anomalous situation, and the packet should not be used. The ground system contractor will need to implement recovery procedures from such a case.

The portion that creates the level 1b spectrum runs based on the packet time, and is initiated every 30 seconds at the 0 and 30 second mark of each minute. For the GPDS, we attempt to produce reproducible test results. To achieve this, the 30-second spectrum creation code is triggered based on examination of the packet time from every packet received. When the first packet in the next interval is detected, proxy model processing is started. The main program (thread) retains the data used to create the level 1b model spectrum. Since EUVS A, B, C, SPS, and XRS channels each have their own cadence that is independently set by command, one must expect that the channels are not operating in a synchronized fashion. We assume all packets are received in time order, the way that the instrument generates them.

The main loop is infinite, so there is no normal program exit condition. It can be manually broken by user intervention, such as at the end of a test.

### 3.2.1 Pseudocode

This section contains pseudocode to describe the processing flow. Threaded calculation is indicated with start/end text to show that the child threads handle all the processing details. The main thread only waits if a thread is busy.

```
int main()
{
    //Initialization

    //Open a socket connection to OIS.

    while(true) //Loop Forever
    {
        if (30 seconds has elapsed)
        {
            #START_THREAD // spectrum
            spectrum.createSpectrum();
            #END_THREAD
        }
        //Read as much data from the socket as possible and place it in a buffer.

        if (buffer contains a full packet)
        {
            switch(apid)
            {
                case XRS:
                {
                    while(XRS thread is busy)
                    {
```

```
        // issue warning message, thread is busy;
        usleep(DELAY);
    }
    xrs.extractPacket(packet); //load data into object
    #START_THREAD // xrs
    xrs.processData();
    #END_THREAD
}

case EUVS_A:
{
    while(EUVS_A thread is busy)
    {
        // issue warning message, thread is busy;
        usleep(DELAY);
    }
    euvs_a.extractPacket(packet); //load data into object
    #START_THREAD // euvs_a
    euvs_a.processData();
    #END_THREAD
}

case EUVS_B:
{
    while(EUVS_B thread is busy)
    {
        // issue warning message, thread is busy;
        usleep(DELAY);
    }
    euvs_b.extractPacket(packet); //load data into object
    #START_THREAD // euvs_b
    euvs_b.processData();
    #END_THREAD
}

case EUVS_C:
{
    // Add partial packets to the packet queue
    euvs_c_buffer[apid - EUVS_C_APID_START] = packet;

    if(All 8 packets were received || the sequence counter has changed)
    {
        while(EUVS_C thread is busy)
        {
            // issue warning message, thread is busy;
            usleep(DELAY);
        }
        euvs_c.extractPacket(euvs_c_buffer); //load data into object
        // clear the euvs_c_buffer
        #START_THREAD // euvs_c

        euvs_c.processData();
        #END_THREAD
    } //end if
}

case SPS:
{
    while(SPS thread is busy)
    {
```

```

        // issue warning message, thread is busy;
        usleep(DELAY);
    }
    sps.extractPacket(packet); //load data into object
    #START_THREAD // sps
    sps.processData();
    #END_THREAD
}
// Remove the packet from buffer
} //end switch
} //end if
} //end while loop

// Note: This part of the code is reached by signal interrupt.
// Close the file pointers, socket connection, and free any dynamically allocated memory

return SUCCESS;
} //end of main

```

The EUVS product uses data from all of the EXIS science channels; none of which are expected to be synchronous. It is unclear how (or if) this is affected by missing/dropped data. The NCEI customer has requested 30-second intervals defined by 0-second and 30-second UTC boundaries.

The following sections describe the processing algorithm for each packet type, the creation of the level 1b spectrum, and the offline analysis necessary to maintain the calibration.

## 4.0 XRS Algorithm Description

### 4.1 Detector Measurement Input

The XRS has two channels, A (0.05-0.4 nm) and B (0.1-0.8 nm). The purpose of the algorithm is to produce the solar irradiance from each channel. Each channel is comprised of 6 diode measurements: a dark diode, a solar minimum diode (denoted by subscript 1, i.e.  $A_1$  or  $B_1$ ), and a solar maximum quadrant diode set ( $A_{2j}$  or  $B_{2j}$ ). For the purpose of this discussion, we will address only the A channel. To increase the dynamic range of the measurement, the diodes have different fixed-size apertures that stagger the dynamic ranges of the diodes. The  $A_1$  diode is expected to provide good measurements for low solar activity, but may saturate during solar maximum and large flares. The  $A_{2j}$  diode set is expected to provide good measurements during high solar activity, but may “bottom-out” during solar minimum conditions. Both  $A_1$  and  $A_{2j}$  are needed to span the large dynamic range of XRS. The same concept is implemented for the B channel diodes.

The mechanical diode placement is shown in Figure 2. The top-left quad diode is the solar max ( $A_{2j}$ ) channel for A, and the top-right diode is the solar min channel,  $A_1$ . The second row shows the solar min channel for B on the left, and the solar max channel for B on the right. The bottom two diodes are the dark diodes for A and B.

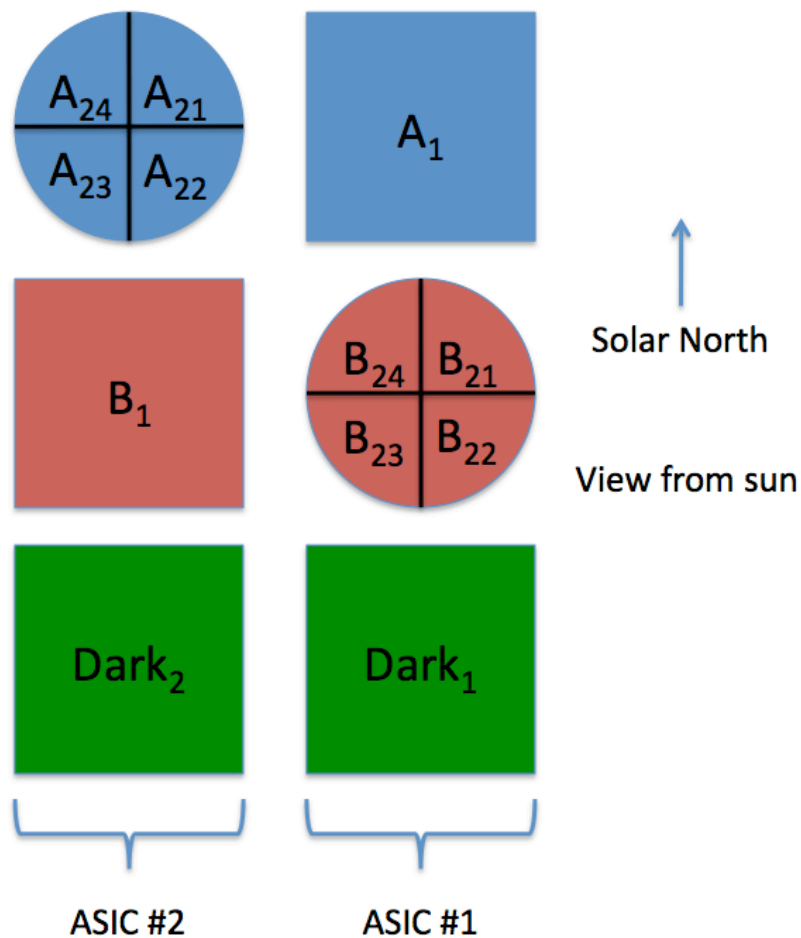


Figure 2. XRS mechanical layout with ASIC 1 on the right and ASIC 2 on the left. Solar North and East-West convention will be verified during instrument testing to ensure the directions are correct.

Telemetry Order	Diode Description	ASIC
1	Dark <sub>1</sub> – Dark diode on ASIC 1	1
2	B <sub>21</sub>	1
3	B <sub>22</sub>	1
4	B <sub>23</sub>	1
5	B <sub>24</sub>	1
6	A <sub>1</sub> – Solar minimum channel	1
7	A <sub>21</sub>	2
8	A <sub>22</sub>	2
9	A <sub>23</sub>	2
10	A <sub>24</sub>	2
11	B <sub>1</sub> – Solar minimum channel	2
12	Dark <sub>2</sub> – Dark diode on ASIC 2	2

Table 5 Diode telemetry order and ASIC relationship

## 4.2 Detector Details

### 4.2.1 Integration Rate

The XRS detector is expected to be operated at an integration rate of 1.0 seconds during science collection of solar data. Any integration time that is not 1.0 seconds may be calibration data and if it is used to generate science products, then the data cannot be guaranteed to meet EXIS PORD88 requirement.

### 4.2.2 Saturation Values

The hardware clock that samples the signal runs at 1 MHz (1 microsecond sampling), however, there is an 11 ms period where the detector is not collecting measurement information. A hardware counter increments by 1 during each microsecond if a signal was measured. The maximum exposure time for a 1 second integration with an 11 ms dead time is therefore 989 ms. When saturated, the XRS diode values will be 989,000 DN (Data Numbers) when operated at the nominal 1.0 second integration rate, which corresponds to the maximum number of detections (1 per microsecond) during the exposure period.

Since there are only 20 bits allocated for each diode, the maximum possible number that can be represented is 1,048,575 DN ( $2^{20}-1$ ), which is larger than the maximum possible 989,000 DN value at a 1.0 second integration rate.

For integration rates that are shorter than 1 second (not recommended), a similar concept applies and the 11 ms dead time is a constant.

For integration rates that are longer than 1 second (not recommended), the situation is more complex. The detector values do not stick at the maximum value. The counters are allowed to continue counting and can exceed the maximum number that can be represented in 20 bits. For a 2.0 second integration, the maximum possible number realized in hardware would be 1,978,000 (2,000,000 - 11,000), which gets truncated to 940,425 DN when the low 20 bits are used to create the packet contents. This leads to a counter-intuitive behavior where the saturation for 2.0 seconds is less than the saturation value for 1 second. The upper limit from the electronics is based on the fixed 1 MHz clock, the fixed 11 ms dead time, the fixed 20-bit readout, and the variable integration time in units of quarter seconds (from 1-256). An expression to calculate the saturation value in DN for any integration rate is  $[(intTime+1)*250000 - 11000] < (2^{20}-1)$ .

## 4.3 Mathematical Description and Algorithm Design

The complete measurement equation for XRS is broken into separate equations for clarity. The quadrant diodes require an extra step, so the next section describes the solar minimum diodes, and the following subsection describes the quadrant (solar maximum) diodes.

### 4.3.1 Solar Minimum Diodes, A<sub>1</sub> and B<sub>1</sub>

First the current is calculated. Note that this section is only valid for the solar minimum diodes, A<sub>1</sub> and B<sub>1</sub>.

$$C_{A1} = \frac{S_{A1}}{\Delta t} \cdot G_{A1}$$

Eq. 4.1

$$C_{B1} = \frac{S_{B1}}{\Delta t} \cdot G_{B1}$$

Eq. 4.2

$$G_{A1} = G_{preflight,A1} \cdot f_{G,A1} \cdot f_{Lin,A1}$$

$$G_{B1} = G_{preflight,B1} \cdot f_{G,B1} \cdot f_{Lin,B1}$$

The total gain shown in Eq. 4.2 has a preflight calibration component that depends on temperature, an in-flight time-dependent term, and a signal-dependent linearity term. Details are in section 4.4.5.

$$C'_{A1} = C_{A1} - C_{Dark,A1}$$

Eq. 4.3

$$C'_{B1} = C_{B1} - C_{Dark,B1}$$

Eq. 4.3 shows the calculation of the corrected currents. The two dark diodes are used to create the dark correction associated with background radiation. The whole dark correction involves a series of terms shown in Eq. 4.4 through Eq. 4.6. One term is related to the in-situ dark diode measurements,  $S_{Dark}$  averaged from both dark diodes. To reduce the effect of large random spikes on the dark diodes, the dark diodes data numbers are averaged over the previous 60 seconds (configurable as `dark_diode_interval` in LUT). The telemetry order for all of the diodes is listed in Table 5. The dark diode variables are represented by the subscript *Dark*. The mechanical layout is shown in Figure 2. Essentially, the dark diode measurement is converted into a reference radiation value that is then scaled for the other diodes (those that measure sunlight) using a proportionality constant  $k$ . Initially, the  $k$  values are set to 1.0 and will be updated using in-flight measurements of particle events during a period when all diodes are in darkness.

$$C_{Dark,A1} = C_{elect,A1} + C_{therm,A1} + C_{Rad,A1}$$

Eq. 4.4

$$C_{Dark,B1} = C_{elect,B1} + C_{therm,B1} + C_{Rad,B1}$$

Eq. 4.5

$$C_{rad,A1} = k_{A1} \cdot \langle C_{rad,Dark} \rangle$$

$$C_{rad,B1} = k_{B1} \cdot \langle C_{rad,Dark} \rangle$$

Eq. 4.6

$$C_{rad,Dark1} = \frac{\langle S_{Dark1} \rangle_{60} \cdot G_{Dark1}}{\Delta t} - C_{elect,Dark1} - C_{therm,Dark1}$$

$$C_{rad,Dark2} = \frac{\langle S_{Dark2} \rangle_{60} \cdot G_{Dark2}}{\Delta t} - C_{elect,Dark2} - C_{therm,Dark2}$$

$$\langle C_{rad,Dark} \rangle = (W_{Dark1} \cdot C_{rad,Dark1}) + (W_{Dark2} \cdot C_{rad,Dark2}) \text{ and always } \geq 0$$

Since the dark tables (exis\_fm1\_xrs\_dark\_asic1/2temp\_a/b/aside.cal) are reported in units of DN, they must be converted to currents by then dividing by  $\Delta t$  and multiplying by the same gain terms from Eq. 4.2. This is identical to the procedure shown in Eq. 4.1. The dark tables represent the sum of  $C_{elect}$  and  $C_{therm}$ .

Now  $C'$  can be evaluated. For compatibility with the quadrant diode equations that follow (see section 4.3.2), we introduce a  $C''$  term which is identical to  $C'$ .

Note that if  $\langle C_{rad,Dark} \rangle$  is less than zero it should be replaced with zero. Negative particle radiation will lower the current on the other diodes unnecessarily, but this could happen due to random noise during periods when very little particle radiation is detectable. The  $W_{Dark}$  terms are initially set to 0.5 so it is equivalent to an average. If one of the diodes deviates from expectations, its weight can be changed in the LUT without changing the code.

**Eq. 4.7**

$$C''_{A1} = C'_{A1}$$

$$C''_{B1} = C'_{B1}$$

The responsivity involves the assumed spectral shape,  $\Phi$ , and the instrument response function,  $\varepsilon$  as shown in Eq. 4.8.

**Eq. 4.8**

$$R_{C,A1} \equiv \frac{A_{A1} \cdot \int_0^{\infty} \Phi(\lambda) \cdot \varepsilon_{A1}(\lambda) d\lambda}{\int_{\lambda_{min,A1}}^{\lambda_{max,A1}} \Phi(\lambda) d\lambda}$$

$$R_{C,B1} \equiv \frac{A_{B1} \cdot \int_0^{\infty} \Phi(\lambda) \cdot \varepsilon_{B1}(\lambda) d\lambda}{\int_{\lambda_{min,B1}}^{\lambda_{max,B1}} \Phi(\lambda) d\lambda}$$

Note that  $R_c$ , bandpass-corrected responsivities, are computed during pre-flight calibration and are not expected to change on orbit, thus it is applied as a constant. This equation is provided for completeness. These values of  $R_c$  are Static Parameters that are provided in the calibration data book (CDRL 79, the GOES-R EXIS Calibration Data Books).

**Eq. 4.9**

$$E_{A1} = \frac{C''_{A1}}{R_{C,A1} \cdot f_{FOV,A1}}$$

$$E_{B1} = \frac{C''_{B1}}{R_{C,B1} \cdot f_{FOV,B1}}$$

The irradiance,  $E$ , represents the irradiance at the spacecraft, so it is appropriate for terrestrial applications, such as ionospheric modeling.

### 4.3.2 Solar Maximum Diodes, $A_{2j}$ and $B_{2j}$

First the currents are calculated. Note that  $j$  is the quadrant diode number, 1, 2, 3, or 4. The first step is to convert the raw signals for the diodes into currents.

$$C_{A2j} = \frac{S_{A2j}}{\Delta t} \cdot G_{A2j}$$

**Eq. 4.10**

$$C_{B2j} = \frac{S_{B2j}}{\Delta t} \cdot G_{B2j}$$

$$G_{A2j} = G_{preflight,A2j} \cdot f_{G,A2j} \cdot f_{Lin,A2j}$$

**Eq. 4.11**

$$G_{B2j} = G_{preflight,B2j} \cdot f_{G,B2j} \cdot f_{Lin,B2j}$$

There are 8 equations represented in Eq. 4.10 and 8 more in Eq. 4.11, since each quadrant diode is calculated separately. The total gain in Eq. 4.11 has a preflight calibration component that depends on temperature, an in-flight time-dependent term, and a signal-dependent linearity term. Details are in section 4.4.5.

$$C'_{A2j} = C_{A2j} - C_{Dark,A2j}$$

**Eq. 4.12**

$$C'_{B2j} = C_{B2j} - C_{Dark,B2j}$$

The corrected currents are shown in Eq. 4.12. The corrected current shall be stored in the XRS product for use by higher level processing in calculating the flare location (the description of that level 2+ algorithm is beyond the scope of this document). The two dark diodes are used to create a portion of the dark correction. The dark correction involves a series of terms shown in Eq. 4.13 through Eq. 4.15. One of them is related to the in-situ dark diode measurement,  $S_{Dark}$  averaged from both dark diodes. The telemetry order for all of the diodes is listed in Table 5. The dark diode variables are represented by the subscript *Dark*. The mechanical layout is shown in Figure 2. Essentially, the dark diode measurement is converted into a reference radiation value that is then scaled for all of the other diodes using  $k_{ij}$ . Initially,



$k_{i,j}$  are set to 1.0 for the solar minimum diodes, and 0.25 for the quadrant diodes. This will be updated using in-flight measurements.

$$\begin{aligned} \text{Eq. 4.13} \quad C_{Dark,A2j} &= C_{elect,A2j} + C_{therm,A2j} + C_{Rad,A2j} \\ C_{Dark,B2j} &= C_{elect,B2j} + C_{therm,B2j} + C_{Rad,B2j} \end{aligned}$$

$$\begin{aligned} \text{Eq. 4.14} \quad C_{rad,A2j} &= k_{A2j} \cdot \langle C_{rad,Dark} \rangle \\ C_{rad,B2j} &= k_{B2j} \cdot \langle C_{rad,Dark} \rangle \end{aligned}$$

$$\begin{aligned} \text{Eq. 4.15} \quad C_{rad,Dark1} &= \frac{\langle S_{Dark1} \rangle_{60} \cdot G_{Dark1}}{\Delta t} - C_{elect,Dark1} - C_{therm,Dark1} \\ C_{rad,Dark2} &= \frac{\langle S_{Dark2} \rangle_{60} \cdot G_{Dark2}}{\Delta t} - C_{elect,Dark2} - C_{therm,Dark2} \\ \langle C_{rad,Dark} \rangle &= (W_{Dark1} \cdot C_{rad,Dark1}) + (W_{Dark2} \cdot C_{rad,Dark2}) \text{ and always } \geq 0 \end{aligned}$$

Note that Eq. 4.15 is the same as Eq. 4.6, since the in-situ radiation background contribution is the same. Also note that the  $S_{Dark}$  is averaged over the previous 60 seconds to reduce the effect of possible random spikes. If  $\langle C_{rad,Dark} \rangle$  is less than zero it should be replaced with zero.

The corrected currents,  $C'$  can now be evaluated. The corrected currents are summed to create the total current for the short and long wavelength bands.

$$\begin{aligned} \text{Eq. 4.16} \quad C''_{A2} &= \sum_{j=1}^4 C'_{A2j} \\ C''_{B2} &= \sum_{j=1}^4 C'_{B2j} \end{aligned}$$

Eq. 4.16 shows the total current from adding the  $A_{2j}$  or  $B_{2j}$  quadrant diodes. The responsivity involves the assumed spectral shape,  $\Phi$ , and the instrument response function,  $\varepsilon$  as shown in Eq. 4.17.

$$\text{Eq. 4.17} \quad R_{C,A2} \equiv \frac{A_{A2} \cdot \int_0^{\infty} \Phi(\lambda) \cdot \varepsilon_{A2}(\lambda) d\lambda}{\int_{\lambda_{min,A2}}^{\lambda_{max,A2}} \Phi(\lambda) d\lambda}$$

$$R_{C,B2} \equiv \frac{A_{B2} \cdot \int_0^{\infty} \Phi(\lambda) \cdot \varepsilon_{B2}(\lambda) d\lambda}{\int_{\lambda_{min,B2}}^{\lambda_{max,B2}} \Phi(\lambda) d\lambda}$$

Note that  $R_C$  is computed in pre-flight and is not expected to change on orbit, thus it is applied as a constant. This equation is provided for completeness. The calibrated values will be provided in the calibration data book (CDRL 79).

$$E_{A2} = \frac{C''_{A2}}{R_{C,A2} \cdot f_{FOV,A2}}$$

**Eq. 4.18**

$$E_{B2} = \frac{C''_{B2}}{R_{C,B2} \cdot f_{FOV,B2}}$$

The irradiance,  $E$ , represents the irradiance at the spacecraft, so it is appropriate for terrestrial applications. For heliophysics applications, a 1-AU correction will be supplied as a multiplicative factor; however, the 1-AU factor will not be applied to the level 1b product data. The 1-AU correction is discussed in Appendix D -Astronomical Unit Correction.

The spectral model (described in section 6.0) uses the primary irradiances from the XRS-A and XRS-B.

The variable descriptions are summarized in Table 6.

Variable	Description	Units
$A_{A1}, A_{A2}, A_{B1}, A_{B2}$	Aperture areas	m <sup>2</sup>
j	Quadrant diode number	NA
S	Signal	Data Number (DN) / integration
G	Gain (includes linearity)	Coulombs / DN
$\Delta t$	Integration time	Seconds / integration
$f_G$	Long-term gain calibration adjustment to compensate for in-flight changes	Dimensionless
$G_{preflight}$	Pre-flight gain correction for temperature	Coulombs / DN
$f_{Lin}$	Linearity	Dimensionless
C	Corrected current	Coulombs / second or Amps
$C_{Dark}$	Total Dark correction with offsets	Amps
$C_{elect}$	Temperature dependent electrical offset based on commanded value	Amps
$C_{therm}$	Thermal contribution to dark from the diode material	Amps
k	Scaling factor for radiation dark	Dimensionless
$C_{rad}$	Radiation background	Amps
C'	Dark corrected current	Amps
C''	Measurement current with sum over quads	Amps
$\Phi$	Assumed spectral shape	W/m <sup>2</sup> /nm
$\varepsilon$	Instrument response function	Amps / W

$R_C$	Responsivity	Amps $m^2 / W$
$f_{FOV}$	Field of view	Dimensionless
$E$	Irradiance	$W/m^2$

**Table 6 XRS Measurement Equation Variables**

Generally, each term in the measurement equations that needs to be calculated will have a corresponding function call. This supports a modular design. Certain functions will need some engineering data in order to determine the result. For example, the gain needs the temperature, and the FOV needs pointing information. All required processing information to produce level 1b products is provided within the EXIS telemetry packets. (Telemetry packet definitions will be described in EXIS CDRL 43, Command and Telemetry Handbook). However, the orientation of the instrument relative to the solar north axis is needed in higher level processing in order to determine solar flare location correctly.

### 4.3.3 Dependency Analysis

The terms in the measurement equations for XRS are inter-related. The dependency is shown graphically in Figure 3.

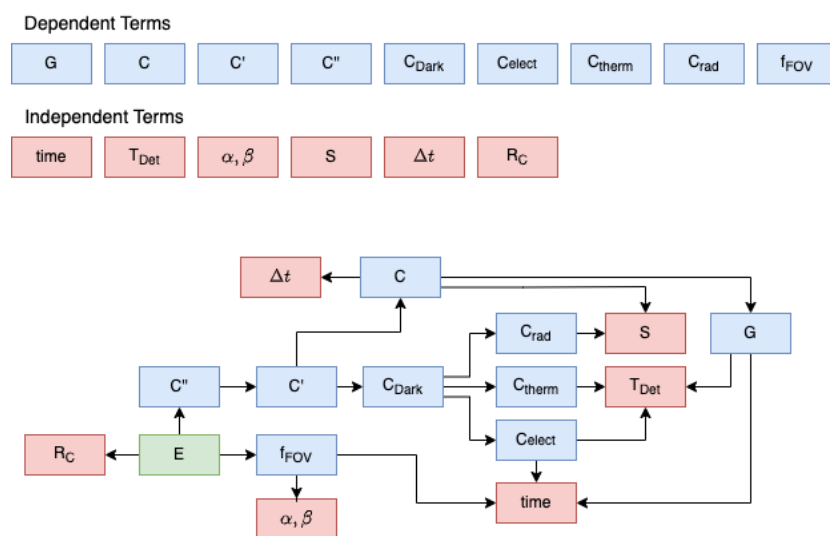


**Figure 3 XRS dependency graph**

The dependency graph is useful for identifying the connectedness of the terms in the measurement equations. The acyclic property of the graph ensures that no terms are dependent in a way that would cause an infinite loop.

Reversing the arrows of Figure 3 creates a rooted-tree as shown in Figure 4. This elucidates the acyclic property and shows that all paths will eventually terminate with the irradiance.

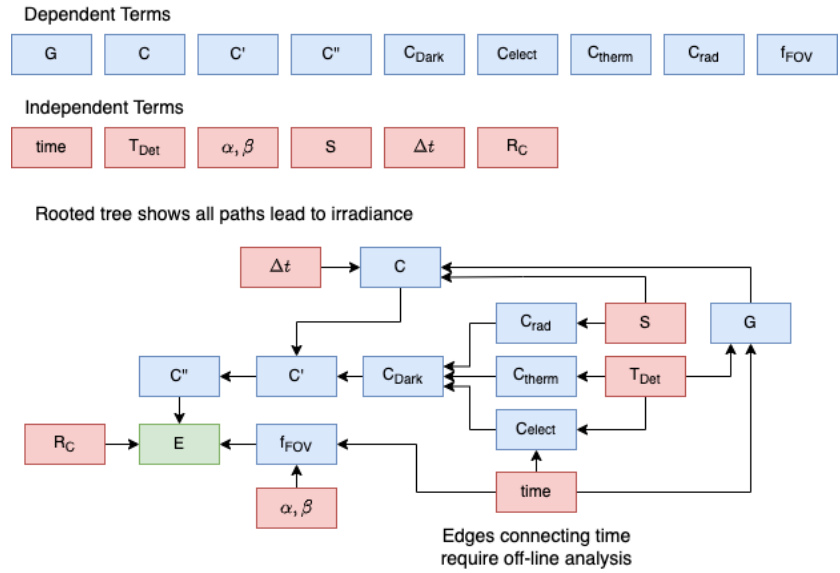


**Figure 4 XRS rooted dependency tree**

Note that the arrows that emanate from “time” require periodic off-line analysis. Here “time” represents a long-term analysis is needed, whereas  $\Delta t$  represents a dependence on the integration time. Some items may need to be updated more often than others. For example, the field of view correction only needs to be updated after the field of view calibration is performed, but historical data needs to be available in order to perform the analysis. We recommend at least 3 months of historical data should be available to the off-line analysis procedures, however, the gain requires the results of calibration analysis for the full mission (one file with one result set per quarter).

## 4.4 XRS Algorithm Steps

This section describes the steps performed in the XRS Ground Processing Algorithm. Each subsection is ordered according to the evaluation in the measurement equations. Some steps may be executed in parallel due to the associative property of multiplication (for example, the responsivity and FOV may be determined in parallel).

An overview is presented in Figure 5.

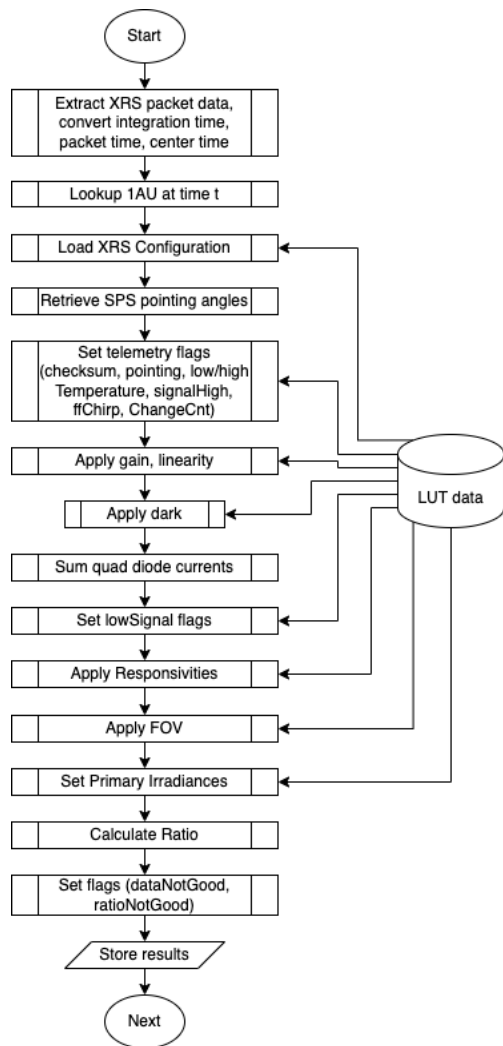


Figure 5. XRS GPA Overview

This is described in more detail in the following pseudocode where the 1-AU correction is possibly calculated well in advance. The SUVI guide telescope pointing angles closest to the packet time shall be included in the data product.

```

#Main thread
xrs.extractPacket(packet)
lookupOneAu(time)

#XRS thread
xrs.loadConfigurationFiles() // calibration files and config files load
only at start of UT day
set telemetry flags //checksum, pointingBad (needs pointing angles),
lowTemperature, highTemperature, signalHigh, flatfieldChirpWarning,
detChangeCountNotValid
xrs.applyGain() // also applies the integration time
xrs.applyDarkDiodeCorrections()
    
```

```

set lowSignal flags
xrs.sumQuadDiodeCurrents()
xrs.applyResponsivities()
xrs.applyFovCorrections() //averaged pointing angles during integration
xrs.setPrimaryBandParameters()
xrs.calculateRatio()
set dataNotGood flags and ratioNotGood flag
xrs.createOutput()
}
    
```

The loadConfigurationFiles method is included to provide a convenient mechanism for maintaining and refreshing updated calibration information. This method reloads the gain coefficients from calibration files, the dark tables, and all other corrections from off-line analysis.

The following diagram shows the functions involved in XRS processing.

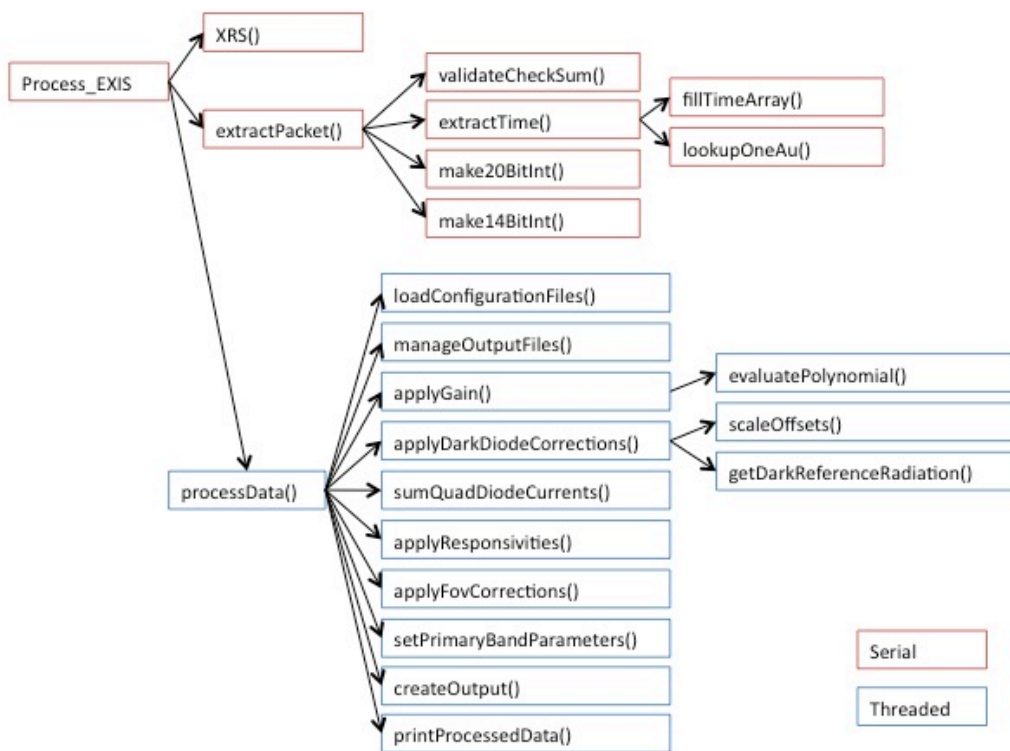


Figure 6. XRS functions

#### 4.4.1 Packet Decomposition

The format of the packet is described in EXIS CDRL 43. The XRS packet contains the following information: flight model number (8-bits), configuration ID (16-bits), timestamp (CCSDS header day segmented time), power status for the EXIS power board (exs\_px\_pb\_stat described in CDRL 43), integration time (0-255), calibration state (0=science, 1=calibration), six 20-bit diode DN values for XRS-

A, six 20-bit DN values for XRS-B, corresponding 14-bit commanded offset values for all diodes, a set of calibration parameter values (Vstep, Tstep, Cal\_cycles, Vmin, Vmax), various temperatures, and 2 sets of flatfield parameters (power control bits and 12-bit level). All of the standard CCSDS header information should also be extracted into variables. This is useful for debugging and identifying missing telemetry packets.

All of these values will be extracted to variables for use in the processing algorithm. We have chosen to use an object-oriented design, but a procedural approach (without objects) is also possible. In the demonstration software, the variables are contained within an object, where each XRS packet will be copied into an XRS object. We further choose to implement a dedicated thread for XRS processing.

Use the field entitled xrs\_det\_chg to disregard all packets whose value is less than 20. After power up, the detector and associated electronics need to stabilize, so this data should be disregarded. Note that flight software resets xrs\_det\_chg to indicate that something significant on the detector has changed that affects data quality for a short period. A persistent zero count rate effect is observed for up to 5 integrations after exiting the internal gain calibration circuit. These are easily discarded using this counter.

Data should also be disregarded when the xrs\_inval flags are any values other than 0 or 4. The value of zero indicates no detectable errors. The value of 4 corresponds to a single bit error that was detected and corrected in the electronics, so this data should be valid as marked. This may be of interest to future hardware designers. Other fields in the invalid flag indicate bad data was received for the following reasons: multibit error (uncorrectable), integration time change warning, or flatfield chirp warning. The flatfield chirp warning indicates that an LED was turned on that may cause spurious current in one or more LEDs for a brief instant. The integration time change warning indicates that flight software detects a state change and the data may not correspond to the exposure indicated. The multibit error indicates that the hardware has detected more than one bit flip in the data and cannot correct it.

#### 4.4.1.1 Temperature Conversions

The two temperatures contained within the XRS packet are converted from DN to degrees Celsius using a lookup table of pre-flight converted values. This is classified as table of Static Parameters. The tables contain 65535 (or  $2^{16}$ ) rows where the row number corresponds to the DN value, and each value is the corresponding floating point temperature. All temperatures from EXIS are converted the same way.

Snippets from the calibration file are provided below.

```
;Created: Mon Jul 23 11:27:10 2012
;Author: Don Woodraska
;Identifier: exis_temperature
;NumberOfDataColumns: 1
;NumberOfRows: 65536
;Comment-
;Comment- Data_file: exis_temperature.cal
;Comment- Last_Update: 2012 Jul 23 1127 UTC
;Comment-
```

```

;Comment- Usage: Use read_goes_10b_file to read the array, use the raw 16-bit DN value
;Comment- as the subscript into the array for conversion to degrees Celsius.
;Comment- Units: Degrees Celsius
;Comment-
;record={data:dblarr(1) }
;format=(e14.7)
;end_of_header
-1.4251690e+02
-1.3697193e+02
-1.3359133e+02
...
7.3309841e+02
9.3317316e+02
9.3317316e+02
    
```

Different thermistors may have slightly different offsets depending on subtleties of the wiring. This is particularly true when comparing A-side to B-side thermistors. Corrections that depend on temperature are measured on both sides during instrument calibration. Separate lookup tables will be provided for those items in CDRL 79.

#### 4.4.2 Lookup\_1-AU

The result will not have the 1-AU correction applied, but it will be provided as specified in CCR1382. The 1-AU correction tables are classified as Static Parameters. Refer to the section Appendix D - Astronomical Unit Correction. The 1-AU correction is based solely on time, so this could be calculated for each timestamp for each packet. It may be faster to calculate the 1-AU correction for each second of the day and interpolate to the specific fractional second. The mean 1-AU distance is approximately  $1.49 \times 10^8$  km, so a 1-second lookup table could introduce additional uncertainty no larger than about 200 parts per million, since the spacecraft translates about 3 km in one second.

#### 4.4.3 Signal, S

The extracted photometer measurements from the XRS packet are called  $D_1, D_2, A_1, B_1, A_{21}, A_{22}, A_{23}, A_{24}, B_{21}, B_{22}, B_{23},$  and  $B_{24}$ , representing the dark diodes, the solar minimum diodes, and the 4 diodes comprising the solar maximum quadrant diodes in each band. These data are 20-bit unsigned integers from 0-1,048,575 (note that the individual electrometer offsets should always be greater than 0). These are the  $S_{ij}$  used in Eq. 4.10.

#### 4.4.4 Integration time, $\Delta t$ (and application of time stamp)

The next step is to extract the integration time. For the default case this is 1 second, but could be changed operationally to other values (not recommended). The integration duration,  $dt_{DN}$ , that was commanded by the flight software is encoded in the CCSDS telemetry packet as a single byte-value (8-bits) which represents the number of quarter seconds for the exposure minus 1. The calculation of the integration time (in seconds) is shown in Eq. 4.19.

**Eq. 4.19** 
$$\Delta t = 0.25 \cdot (dt_{DN} + 1) - 0.011$$



Specifically, a  $dt_{DN}$  of zero corresponds to 0.239 seconds, and a  $dt_{DN}$  value of 255 corresponds to 63.989 seconds. The 11-millisecond subtraction is a feature of the ASIC hardware where the counters are disabled while the data are being shifted out. For nomenclature, we usually disregard the 11 ms offset, thus a 1 (or 0.989) second integration time corresponds to 3 DN. Additional detail is contained in the FPGA Design Specification.

The time reported in the packet secondary header refers to the end time ( $t_{Packet}$ ) for the integration cycle when the data is finished being shifted out. In the level 1b product, we report the center time of the exposure ( $t_{Center}$ ). The calculation of the center time uses only the packet time and the integration duration ( $dt_{DN}$ ) as shown in Eq. 4.20.

**Eq. 4.20** 
$$t_{Center} = t_{Packet} - \frac{1}{2}[0.250 \cdot (dt_{DN} + 1) - 0.011]$$

The center time accounts for the 11 ms offset after the exposure has ended while data is being shifted out. For an integration time of one second, the  $dt_{DN}$  value is 3, and the adjustment to the packet time becomes -0.4945 seconds. This is common behavior for SPS, EUVS-A, and EUVS-B as well. The 11 ms inactive period occurs at the start of the integration. Previous CDRL 80 documents erroneously had this at the end of the integration.

#### 4.4.4.1 Timing Details

The EXIS instrument time is divided into quarter second ticks and all ASIC detector exposures end at the tick. The detector integration begins with a transfer of the data from the previous integration. This readout time takes 11 milliseconds (ms). The exposures begin 11 ms after the quarter second tick. The time stamp in the CCSDS secondary header (packet time) is the tick time at the end of the integration and flight software packetizes the data using the end of the integration time (the previous tick). Flight software uses the time at the tick so the uncertainty is on the order of 1 microsecond.

All ASIC channels operate in this way. All XRS diodes are integrated together with identical timing controlled by the hardware. The EUVS-A and EUVS-B detectors share some control electronics so they are linked together with identical hardware timing. The science packets can only have time differences as integer number of quarter seconds.

The accuracy of the spacecraft time delivered to EXIS relative to the NIST atomic clock is ignored here. EXIS flight software sets the EXIS clock based on the spacecraft timing packet every second. Since the spacecraft clock can be adjusted and demonstrates on-orbit drift, the timestamps will appear to not be separated by exactly the correct time. This is demonstrated in comparing timestamps from consecutive packets. They should always be exactly an integer number of seconds apart, but there is jitter and drift in the absolute clock of several microseconds each second.

#### 4.4.5 Gain, G

The gain correction, G, shown in Eq. 4.11, converts instrument data numbers into the physical units of current, or charge per second. This is primarily an electronics effect due to the mixture of circuitry (Ohmic and non-Ohmic) involved in converting on-board diode current values into digital numbers for telemetry. The physical units of G are [Coulombs / DN]. This correction has an absolute, temperature-dependent component,  $G_{preflight,ij}$ , a time-dependent, relative component,  $f_{G,ij}$ , for each diode, and a signal-dependent linearity component,  $f_{Lin}$ . The absolute (static) calibration value is determined from the pre-flight calibration activities at NIST-SURF. The time-dependent gain change starts at 1.0 (at the reference temperature) and is expected to change with time due to the in-flight radiation environment. This is tracked in-flight with the special gain calibration / voltage-reference-substitution measurements (see 9.1.3 for more details).

##### 4.4.5.1 Inputs & Dependencies

The XRS object contains the data and temperatures needed for the calculation. An additional pre-flight calibration table is also needed.

###### 4.4.5.1.1 Preflight Gain Temperature Dependence, $G_{preflight}$

The diode gain calibration data will be stored in a two dimensional table in an ASCII text file. The rows correspond to each temperature DN (0-65535), and the columns correspond to the preflight gain for each of the diodes (telemetry order). The temperature dependence is linear with temperature, but the thermistor has a complicated logarithmic response. We approximate the thermistor response with a Steinhart-Hart equation, so a lookup table is easier and provides better performance. The preflight gain is classified as a table of Static Parameters and should not be changed in-flight. The file will be provided in CDRL 79.

The telemetry mnemonics for the two ASIC temperatures are `xrs_1_bd_tmp_dn` and `xrs_2_bd_tmp_dn` as specified in CDRL 43. Use `xrs_1_bd_tmp_dn` as the row number in the lookup table. The other thermistor is a backup and could be used if the recommended thermistor becomes suspect (but a different table may be needed). The top of the gain calibration file for flight model 1 is provided here for reference.

```
;Created: Mon Jul 23 11:55:35 2012
;Author: Don Woodraska
;Identifier: exis_fm1_xrs_gain
;NumberOfDataColumns: 13
;NumberOfRows: 65536
;Comment-
;Comment- Data_file: exis_fm1_xrs_gain.cal
;Comment- Last_Update: 2012 Jul 23 1155 UTC
;Comment-
;Comment- Usage: Use read_goes_10b_file to read the array, use the raw 16-bit Temperature DN
value
;Comment- from ASIC1 Temp as the subscript into the array.
;Comment- Order is Temperature_C, XRS-Dark1, B21, B22, B23, B24, A1, A21, A22, A23, A24, B1,
Dark2
;Comment- Units = Coulombs/DN
;record={data:dblarr(13)}
;format=(e14.7,12(x,e14.7))
```

```
;end_of_header
-1.4251690e+02  9.8280636e-15  1.2436908e-14  1.2348660e-14  1.0816563e-14  8.4293273e-15
1.1383497e-14  1.1051696e-14  1.2562892e-14  1.1421888e-14  1.0591007e-14  1.0141740e-14
8.8225875e-15
-1.3697193e+02  9.8300299e-15  1.2345393e-14  1.2257017e-14  1.0785029e-14  8.4227187e-15
1.1357859e-14  1.0960689e-14  1.2441887e-14  1.1351057e-14  1.0528775e-14  1.0118235e-14
8.8246462e-15
```

#### 4.4.5.1.2 Calibration Table for Time Dependence, $f_G$

The time dependent diode gain calibration data will be stored in an ASCII text file containing the columns for Julian Date and each diodes relative correction factor. Initially all values shall be 1.0. Based on radiation testing measurements (A Jones et al, "Radiation Testing a Very Low-Noise RHBD ASIC Electrometer", IEEE proceedings), the relative gain change for these detectors is 0.04% / krd, so no measureable change is expected for XRS. The expected radiation dose at the radiation-hardened ASICs is 2.3 krd over 15 years (which includes a factor of two margin). The in-flight gain calibration accuracy is only about 2% for each observation, so it is possible that no trend may be detectable over the life of the instrument. The corrections are always based on previous measurements. The correction will likely return 1.0 for the first two years regardless of the analysis results in order to obtain good statistics.

An off-line analysis procedure updates this file periodically (run daily, but changes are based on available data). The file contains the values produced by analysis as  $(G/Cap)/(G_0/Cap_0)$ . The ratio  $(G_0/Cap_0)$  is reported in CDRL 79, the calibration data books. The internal in-flight gain calibration analysis reports the ratio of the gain to the capacitance. Off line analysis is described in section 9.1.3. This is classified as a table of Dynamic Parameters. An example gain file follows with fictitious entries.

```
;Created: Wed Sep 26 17:24:03 2012
;Author: Don Woodraska
;Identifier: exis_fm1_xrs_gain_relative
;NumberOfDataColumns: 13
;NumberOfRows: 4
;Comment-
;Comment- Data_file: exis_fm1_xrs_gain_relative.cal
;Comment- Last_Update: 2012 Sep 26 1724 UTC
;Comment-
;Comment- Usage: Use read_goes_l0b_file to read the array, col number+1 is the diode number in
telemetry.
;Comment- Contains a julian date and XRS relative gain factors used in CDRL 80 eq 4.2 and 4.11.
;Comment- Data contained represents f_sub_G
;Comment- Order is JD, then relative gain factors in telemetry order
;Comment- Each line represents the value to use after and including that day.
;Comment- The concept is that new results can be added with a date to affect a change.
;Comment- This could be updated as frequently as once per quarter.
;Comment- Units = NA
;record={data:dblarr(13)}
;format=(e14.7,12(x,e14.7))
;end_of_header
2.4515445e+06  0.0000000e+00  0.0000000e+00  0.0000000e+00  0.0000000e+00  0.0000000e+00
0.0000000e+00  0.0000000e+00  0.0000000e+00  0.0000000e+00  0.0000000e+00  0.0000000e+00
0.0000000e+00
2.4515455e+06  1.0000000e+00  1.0000000e+00  1.0000000e+00  1.0000000e+00  1.0000000e+00
1.0000000e+00  1.0000000e+00  1.0000000e+00  1.0000000e+00  1.0000000e+00  1.0000000e+00
1.0000000e+00
2.4533695e+06  1.0000000e+00  1.0000000e+00  1.0000000e+00  1.0000000e+00  1.0000000e+00
1.0000000e+00  1.0000000e+00  1.0000000e+00  1.0000000e+00  1.0000000e+00  1.0000000e+00
1.0000000e+00
```

```
2.4533705e+06 1.0000000e+00 1.0000000e+00 1.0000000e+00 1.0000000e+00 1.0000000e+00  
1.0000000e+00 1.0000000e+00 1.0000000e+00 1.0000000e+00 1.0000000e+00 1.0000000e+00  
1.0000000e+00
```

...

#### 4.4.5.1.3 Calibration Table for Linearity, $f_{Lin}$

The initial test results for linearity indicate that the detectors are extremely linear. The GPDS system will implement a linearity function that returns 1.0. In principle, the diodes could exhibit non-linear behavior at very high currents, but this was not observed during the tests performed at NIST using flight model 1 (GOES-R). The concept behind the correction is to convert non-linear inputs into linear outputs. This could be applied as a lookup table that is resampled from a coarsely sampled calibration data set, and really only affects the highest currents. This is classified as a table of Static Parameters.

##### 4.4.5.1.4 Table Details

At the request of the ground system contractor, we have created a lookup table with 21 rows and 13 columns called `exis_fm1_xrs_linearity.cal` to remove ambiguity in the definition of the table structure and contents. The first column is the raw DN value, and the other 12 columns are the linearity factors in telemetry order for each of the XRS diodes. All linearity factors are set to 1.0. The raw DN spacing is reversed power of 2 differences from the saturation value of 989,000 DN. A zero DN value is in the first row. The last row is the saturation value so no extrapolation beyond these ranges is possible.

Explicitly, the values of raw DN from column 1 in the file are listed here.

```
0, 464713, 726857, 857929, 923465, 956233, 972617, 980809, 984905, 986953, 987977, 988489,  
988745, 988873, 988937, 988969, 988985, 988993, 988997, 988999, 989000
```

Recall that the linearity effect could not be measured. The detectors respond linearly up to the saturation value.

##### 4.4.5.1.5 Maintenance

The calibration table will be updated based on in-flight data collection. This could be daily or weekly. After each in-flight calibration measurement, the associated `analyze_xrs_gain` procedure should be executed to create the most up-to-date calibration (see section 9.1.3). Failure to update the calibration tables in a timely manner could result in steps that are observable in the irradiance data.

#### 4.4.5.2 Output

Gain is a function that returns the updated intermediate calculation and a status indicator. The total gain returned should be retained since it is needed to convert the thermal dark from data numbers into current units.

### 4.4.5.3 Implementation Recommendations

The gain function requires the temperature to be known for the XRS-A channel. The gain function pseudocode is provided below.

```

applyGain()
{
    loop over each diode
    {
        if temperature is outside the good science range then
        {
            set lo/hi bad temperature flag
        }
        calculate the preflight temperature-dependent gain Gpreflight
        calculate the time dependent gain change term fg
        get the linearity correction flin
        multiply 3 components to create the total gain G
        multiply G to create modified data and update the xrs structure
    }

    return good_status;
}
    
```

### 4.4.6 Evaluate C'

We now have all of the pieces needed to evaluate C', the diode signal current shown in Eq. 4.12.

#### 4.4.6.1 C<sub>Dark</sub>

The dark term is the result of a sophisticated calculation involving temperature, the commanded offset, and the reference dark diode averaged over the previous 60 seconds.

##### 4.4.6.1.1 Electrometer Offset, C<sub>elect</sub>

The electrometer offsets have default values determined during ground testing (to be provided in CDRL 79). The IDAC setting is the value that was commanded to the detector. The offset is the value from the diode in DN and is different for each diode. The same IDAC setting will give a different offset for another diode. For example, an IDAC setting of 300 may correspond to one particular diode offset of 49 DN, but could give 198 DN on another diode.

Since the IDAC settings are changed via a ground command to EXIS, these commanded values are embedded with the science measurements in the telemetry packet definitions. This electronic functionality provides a way to avoid zero values during dark measurement periods. The offset may change over time due to radiation damage (while the setting remains constant). Since the commanded setting does not correspond directly to the offset, it needs to be measured. This will be tracked in-flight using the dark measurements that are collected during off-point maneuvers and the extreme ends of the cruciform scans. Dark measurements for XRS can only be obtained by pointing the EXIS far enough away from the

sun such that no solar signal reaches the detectors. This is one of the items described in the routine calibration analysis section 9.1.2.

#### 4.4.6.1.2 Thermal Contribution to Dark, $C_{therm}$

The temperature dependence of each diode will be calibrated on the ground. The signal contributed by thermal sources is a fairly simple function, but we choose to implement a lookup table for speed and simplicity. The lookup table uses temperature DN and shall be provided in CDRL 79. Temperatures that are far outside the operationally achievable range will be pegged at the last achievable value.

In practice, the two thermal and electronic contributions to the dark current are not directly measurable in isolation. The calibration file containing the sum of the electrometer offset and thermal dark contributions is provided as an example for flight model 1. Note that this is provided in units of DN, and needs to be converted into the units of current using the same gain factor applied in Eq. 4.2 and Eq. 4.11.

```
;Created: Mon Jul 23 11:53:39 2012
;Author: Don Woodraska
;Identifier: exis_fm1_xrs_dark_asic1temp_aside
;NumberOfDataColumns: 13
;NumberOfRows: 65536
;Comment-
;Comment- Data_file: exis_fm1_xrs_dark_asic1temp_aside.cal
;Comment- Last_Update: 2012 Jul 23 1153 UTC
;Comment-
;Comment- Usage: Use read_goes_l0b_file to read the array, use the raw 16-bit Temperature DN
value
;Comment- from ASIC1 Temp (TS3 U2 XRSA) as the subscript into the array.
;Comment- Order is Temperature_C, XRS-Dark1, B21, B22, B23, B24, A1, A21, A22, A23, A24, B1,
Dark2
;Comment- Units = DN
;Comment- For use with ASIC1Temp on SIDE A ONLY
;record={data:dblarr(13)}
;format=(e14.7,12(x,e14.7))
;end_of_header
-1.4251690e+02 1.6151051e-07 9.9999997e-10 9.9999997e-10 9.9999997e-10 9.9999997e-10
8.4598148e-09 9.9999997e-10 9.9999997e-10 9.9999997e-10 9.9999997e-10 3.2492200e-07
6.8043345e-07
-1.3697193e+02 3.3071176e-07 9.9999997e-10 9.9999997e-10 9.9999997e-10 9.9999997e-10
1.9816626e-08 9.9999997e-10 9.9999997e-10 9.9999997e-10 9.9999997e-10 6.6600059e-07
1.3404038e-06
```

#### 4.4.6.1.3 Background, $C_{rad}$

The reference diode provides in-situ radiation background measurements. With the appropriate temperature and offset corrections, the variable radiation environment will be measured by the dark photometers. The radiation background for each diode that observes solar signals is determined from a correlation to the dark diode behavior (Eq. 4.14).

This term uses a scale factor,  $k$ , for each diode to estimate the contribution from the measured background from the dark diode averages. These coefficients must be updated in flight since the radiation background is difficult to measure in preflight. We set all  $k$ 's to 1.0 until more information is available during PLT. The expected contribution to the currents for XRS is 90-100 fA, which is on the order of 10 DN.

#### 4.4.7 Responsivity, $R_c$

The responsivity will be determined from pre-flight calibration. This will not change during flight. The values will be provided in the calibration data books (CDRL 79).

The Instrument Response,  $\epsilon$ , and assumed spectral shape,  $\Phi(\lambda)$ , will be calculated from pre-flight analysis.

#### 4.4.8 Field of View (FOV)

The detector field of view correction will be a table lookup involving the pointing angles. The reference pointing provided by SPS is sufficient to determine the pointing angles (see section 8.0). SPS pointing angles are maintained in the EXIS superclass, and are available to XRS and all other processing threads. Pointing angles,  $a$  and  $b$ , are calculated for each SPS integration, and then averaged over the integration period of XRS to obtain the effective pointing angles over the exposure. The FOV will be updated in flight based on analysis procedures documented in Appendix C - Calibration Coefficients and Lookup Tables. SUVI guide telescope angles could be used instead of SPS after the relative offset is determined during PLT, but this is less desirable than using SPS angles due to higher uncertainties associated with the transfer.

The FOV correction factors are provided as a 5x5 table for each XRS diode, based on ground calibration analysis. Bilinear interpolation should be used to evaluate the correction factors using the averaged pointing angles,  $a$  and  $b$ , for each XRS integration. While lookup tables are provided for all diodes, only the light sensitive diodes need the FOV correction applied.

Note that for XRS the relative FOV can only be measured accurately with an isolated X-ray point source during ground testing. The FOV correction applied in the GPA is a relative correction that is normalized to one at the center pointing angles. The relative FOV is intended to capture the relative change from center pointing as a function of pointing angles. However, for solar X-rays there is almost never an isolated bright point source (limb brightening and multiple bright points). The FOV measurements capture baffle edges, not pure relative response changes to a point source. The solar distribution of X-rays is dominated by active regions and limb brightening in the east and west edges that are about 0.25 degrees from the center. In practice, the FOV correction is always 1 since pointing is well-controlled to keep the sun at disk center. Furthermore, the measured FOV from ground measurements are very close to flat (within a few percent) everywhere. Also, the best correction would require science analysis to determine the relative contribution from all the bright spots with a weighted FOV contributions. Detailed X-ray locations and relative absolute brightness would be needed for each bright spot for each 1-Hz integration to determine the net relative FOV contribution to make the best correction. In practice, they would all be very close to 1.

#### 4.4.9 XRS Ratio

The ratio of XRS is defined as the primary XRS-A (short wavelength) irradiance divided by the primary XRS-B (long wavelength) irradiance. This ratio has been shown (S. White, et al., *Solar Physics*, 2005, vol. 227, p. 231-248) to be scientifically, and operationally useful for estimating temperatures and other phenomena associated of flaring plasma. The ratio adds significant value to the level 1b data product.

The ratio should be a fill value (say -99999) unless the irradiances are known to be normal solar measurements.

#### 4.5 XRS Output

The XRS will store all irradiances from both bands covered by XRS-A and XRS-B. A flag will be used to indicate which band is the primary irradiance measurement. For solar minimum diode irradiances below some threshold ( $1e-6 \text{ W/m}^2$  for XRS B,  $1e-6 \text{ W/m}^2$  for XRS-A, possibly readjusted during PLT), the solar minimum diodes ( $A_1$  or  $B_1$ ) will be flagged as primary, and above that threshold the solar maximum channels ( $A_2$  or  $B_2$ ) will be chosen instead. The primary irradiance for both channels will be used to calculate the proxies for the spectral model described in section 6.0. Explicitly, one flag shall be provided in the level 1b product to indicate whether  $A_1$  or  $A_2$  is the primary short wavelength irradiance, and another flag shall be provided to indicate whether  $B_1$  or  $B_2$  is the primary long wavelength irradiance.

Quality bit-flags shall also be provided. These flags contain the information needed to properly interpret the measurements. Most users will likely use the A Primary Channel, B Primary Channel, Data Good A, and Data Good B flags. A value of zero is used to indicate that the state is good. These flags are summarized in Table 7.

Flag Name	Bit Value (1/0)	Description/Explanation
PointingBad	Bad/Good	The pointing of EXIS (a,b) is both known (exs_tl_fov_stat) and either angle is more than 0.8 deg (48 arcmin) from center (0,0).
PointingDegraded	Bad/Good	Pointing is outside the calibrated range between 0.4 and 0.8 deg (24-48 acmin). The FOV correction is truncated to the map edge.
PointingWarning	Bad/Good	Pointing angles are in the calibrated FOV range between 0.11667 and 0.4 deg (7-24 arcmin). The spacecraft is not meeting ICD pointing requirements (+/-7 arcmin).
Checksum	Mismatch/Match	The checksum in the XRS packet matches the calculated 0xFF seeded XOR checksum starting after the checksum byte in the packet.
LowTemperature	Low/Good	The temperatures (ASIC1Temperature and ASIC2Temperature) are either low or within the valid range to make measurements. If either temperature is low, the flag is set to 1.



HighTemperature	High/Good	The temperatures (ASIC1Temperature and ASIC2Temperature) are either high or within the valid range to make measurements. If either temperature is high, the flag is set to 1.
SignalLowA1	Low/Not Low	The diode signal is distinguishable from zero current (above dark).
SignalLowAquad	Low/Not Low	The diode signals are all distinguishable from zero current (above dark).
SignalLowB1	Low/Not Low	The diode signal is distinguishable from zero current (above dark)..
SignalLowBquad	Low/Not Low	The diode signals are all distinguishable from zero current (above dark).
SignalHighA1	High/Not high	The diode signal is below the saturation value (989,000 DN for 1 second integration rate).
SignalHighAquad	High/Not high	The diode signals are all below the saturation value.
SignalHighB1	High/Not high	The diode signal is below the saturation value.
SignalHighBquad	High/Not high	The diode signals are all below the saturation value.
FlatfieldChirpWarning	Bad/Good	This integration may contain a flatfield flash (flatfield chirp from InvalidFlags)
DetChangeCountNotValid	Bad/Good	Flight software counts the integrations in xrs_det_chg. For values lower than 60 after power on, set the detector change count valid flag to bad, otherwise it is good. After exiting the XRS internal gain calibration, the counter is reset, and for values of xrs_det_chg less than 20 this flag shall be set to bad.
DataNotGoodA	Bad/Good	0 = Primary A channel data is a normal solar measurement 1 = Primary A channel data is NOT a normal solar measurement The definition of a good normal solar measurement is derived using all other flags, and telemetry indicators, some of which are defined in Table 8. <b>Good is defined as:</b> not Calibration (xrsCal=1, runctrlmd=1), checksum is good, not Flatfield (LED_power=0), good Pointing (PointingBad=0, PointingDegraded=0, and PointingWarning=0), not Low Temperature, not High Temperature, not Low Signal (primary only), not High Signal (primary only), DetChangeCnt is good, not Integration Time Warning, not Flatfield Chirp Warning, not EDAC Multibit Error, not Offpoint Maneuver, not Lunar transit, not Eclipse, not FOV flags unknown, intTime=3, and DetChangeCount ge 20.
DataNotGoodB	Bad/Good	0 = Primary B channel data is a normal solar measurement 1 = Primary B channel data is NOT a normal solar measurement
RatioNotGood	Bad/Good	Good mean DataNotGoodA=Good AND DataNotGoodB=Good

Table 7 XRS measurement flags

Note that the quality flags described in Table 7 are derived quantities.

The instrument modes and component status information bits are just passed from the XRS packet along to the product, and are listed in Table 8. The instrument calibration mode (XRSMODE="Cal") indicates that the XRS has been commanded to the calibration mode, but this does not affect science collection. Results may still contain good solar measurements. The diagnostic or "Diag" bit indicates that the instrument is in a diagnostic mode. Usually, this indicates that a diagnostic packet is being generated that does not affect science production. Most of the time, the diagnostic mode data is useable for producing high quality science results, but it is possible to perform diagnostics on the detectors that will cause erroneous processed results (for example, IDAC setting changes directly affect the dark subtraction in a non-trivial way). The "Safe" bit indicates that the XRS has entered a safe state and no further commands to XRS will be accepted, except for the power off command. The safe configuration for XRS is to point at the sun. High quality science data is possible in safe mode, however, if the safing event is caused by a spacecraft anomaly, then there may be less accurate pointing, or thermal control. The "Norm" flag indicates that XRS is configured for normal science operation. The Cal, Diag, Norm, and Safe bits are mutually exclusive, however, after boot the state may be unknown and none of the flags are set. Additional details on instrument mode and status are captured in the EXIS Operations Handbook.

The time stamp and integration time shall be stored. The timestamp from the packet corresponds to the end of the integration, but we recommend storing the center time of the exposure. This is the timestamp minus half of the actual integration time reported in Eq. 4.19. The day number and seconds of day (not milliseconds) are expected.

Additionally, the dark corrected signal currents for the quadrant diodes from Eq. 4.12 shall be provided in the XRS data product along with the averaged pointing angles calculated from SPS processing, and the roll angle. The roll angle cannot be determined from EXIS data, and therefore, must be determined from the spacecraft telemetry (see section 8.4). These shall be provided in order to support the flare location determination at a later processing level. The roll angle is also likely needed for SUVI level 1b processing. Properly calculating the flare location requires using higher-level products to indicate flare times and pre-flare times, and a long time-history of the orientation angle (obtained elsewhere) and dark corrected signal currents. The SUVI guide telescope angles could be used as a backup in the event that SPS stops functioning. The SUVI guide telescope angles will need to be calibrated to the SPS angles during PLT (during FOV maps and cruciform scans). All extracted values from the XRS packet shall be included in the product, and the non-redundant information from the last SPS packet available shall also be reported. This supports the necessary certification activities, plus debugging, and off-line analysis activities.

A very rough set of mutually exclusive bit flags related to roll orientation is detailed in the EXIS ICD. If this is all that is possible to obtain, then this will limit the accuracy of flare location calculations.

EXISICD164:

Spacecraft will include in telemetry a three state status item, at a rate of at least once every 5.0 seconds to indicate the orientation of the spacecraft as one of the following conditions:

- Within 5 degrees of upright yaw attitude
- Within 5 degrees of inverted yaw attitude
- Greater than 5 degrees off upright or inverted yaw attitude

The XRS product output variables are listed in Table 8.

Variable	Units	Data type	Needed for	Description
E <sub>A1</sub>	W/m <sup>2</sup>	32-bit float	L1b product	Irradiance from XRS-A solar minimum diode
E <sub>A2</sub>	W/m <sup>2</sup>	32-bit float	L1b product	Irradiance from XRS-A solar maximum diode (quad sum)
E <sub>A_Primary</sub>	NA	bit	L1b product	1 = channel A2 (quad) is primary 0 = channel A1 (solar min) is primary
E <sub>B1</sub>	W/m <sup>2</sup>	32-bit float	L1b product	Irradiance from XRS-B solar minimum diode
E <sub>B2</sub>	W/m <sup>2</sup>	32-bit float	L1b product	Irradiance from XRS-B solar maximum diode (quad sum)
E <sub>B_Primary</sub>	NA	bit	L1b product	1 = channel B2 (quad) is primary 0 = channel B1 (solar min) is primary
XRS Ratio	NA	32-bit float	L1b product	The primary XRS-A irradiance divided by the primary XRS-B irradiance.
C <sub>A1</sub>	Amps	32-bit float	L1b product	XRS-A quad 1 corrected current
C <sub>A2</sub>	Amps	32-bit float	L1b product	XRS-A quad 2 corrected current
C <sub>A3</sub>	Amps	32-bit float	L1b product	XRS-A quad 3 corrected current
C <sub>A4</sub>	Amps	32-bit float	L1b product	XRS-A quad 4 corrected current
C <sub>B1</sub>	Amps	32-bit float	L1b product	XRS-B quad 1 corrected current
C <sub>B2</sub>	Amps	32-bit float	L1b product	XRS-B quad 2 corrected current
C <sub>B3</sub>	Amps	32-bit float	L1b product	XRS-B quad 3 corrected current
C <sub>B4</sub>	Amps	32-bit float	L1b product	XRS-B quad 4 corrected current
a	degrees	32-bit float	L1b product & diagnostics	Averaged dispersion direction pointing angle from SPS
b	degrees	32-bit float	L1b product & diagnostics	Averaged cross-dispersion direction pointing angle from SPS

a_GT	degrees	32-bit float	L1b product & diagnostics	Averaged SUVI Guide Telescope angle along SPS alpha direction (yaw)
b_GT	degrees	32-bit float	L1b product & diagnostics	Averaged SUVI Guide Telescope angle along SPS beta direction (pitch)
g_SC	degrees	32-bit float	L1b product & diagnostics	Spacecraft derived roll angle along the line of sight to the sun (roll).
Yaw Flip flag	NA	3-bits	L1b product & diagnostics	The coarse orientation of the spacecraft, up or down.
AuFactor	AU	32-bit float	L1b product	The 1-AU correction factor that could be multiplied by the irradiances to remove the earth orbit effect.
QualityFlags	NA	32-bit int	L1b product & diagnostics	All flags defined in Table 7
days_since_jan1_2000	Days	16-bit int	L1b product	Days since the epoch at the end of the integration
centerTime	Seconds	32-bit float	L1b product	Seconds of the UT day at the center of the exposure using the secondary header <code>exs_px_tm_ms</code> (microseconds are unnecessary) and <code>intTime</code> shifted to the center. This corresponds to the CENTER time defined in Eq. 4.20.
scPowerSide	NA	bit	diagnostics	0=B, 1=A ( <code>exs_px_pb_stat</code> )
exisMode	NA	4-bits	diagnostics	0=failsafe, 1=normal, 2=diag, 3=safe ( <code>exs_px_exs_md</code> )
exisFlightModel	NA	8-bits	L1b product	1=FM1, 2=FM2, 3=FM3, 4=FM4 ( <code>exs_px_md1_num</code> )
exisConfigId	NA	16-bits	L1b product	Configuration ID ( <code>exs_px_exs_cfg</code> )
checksum	NA	8-bits	diagnostics	Checksum ( <code>exs_px_pkt_cksm</code> )
xrsDiodeCounts	DN	12 x 32-bit int	L1b product & diagnostics	12 raw diodes measurements ( <code>xrs_1_cnt_ch0-5</code> and <code>xrs_2_cnt_ch0-5</code> )
xrsIdacSettings	NA	12 x 16-bit	diagnostics	IDAC register settings ( <code>xrs_1_idac_ch0-5</code> and <code>xrs_2_idac_ch0-5</code> )
xrsCal	NA	2-bits	diagnostics	Internal gain calibration circuit indicator, 1=science, 2=cal ( <code>xrs_runctrlmd</code> )
asic2Power	NA	bit	diagnostics	0=off, 1=on ( <code>xrs_2_pwr</code> )
asic1Power	NA	bit	diagnostics	0=off, 1=on ( <code>xrs_1_pwr</code> )
intTime	NA	8-bits	L1b product	Integration time in quarter second increments, 0=0.25 sec, 1=0.5 sec, 2=0.75 sec, 3=1.0 sec, ... ( <code>xrs_integ_tm</code> )

LED_select	NA	4-bits	diagnostics	LED selection, 0=EUVSC-Backup, 1=EUVSB-Backup, 2=EUVSA-Backup, 3=XRS-Backup, 4=EUVSC-Pri, 5=EUVSB-Pri, 6=EUVSA-Pri, 7=XRS-Pri (exs_sl_sel)
LED_power	NA	bit	diagnostics	LED power, 0=off, 1=on (exs_sl_pwr_ena)
LED_level	NA	16-bits	diagnostics	LED level setting, 12 bits used, (exs_sl_lvl)
IfBoardTemp	DN	16-bits	diagnostics	Interface board temperature (exs_ifb_tmp_dn)
ProcFpgaTemp	DN	16-bits	diagnostics	Microprocessor board FPGA temperature (Exs_mb_fp_tmp_dn)
PowerSupplyTemp	DN	16-bits	diagnostics	Power board temperature (exs_pb_tmp_dn)
CaseHeaterTemp	DN	16-bits	diagnostics	Case heater temperature (exs_cs_oh_tmp_dn)
ASIC1Temperature	Deg C	32-bits	L1b product & diagnostics	ASIC 1 temperature (converted xrs_1_bd_tmp_dn)
ASIC2Temperature	Deg C	32-bits	L1b product & diagnostics	ASIC 2 temperature (converted xrs_2_bd_tmp_dn)
FilterTemp	DN	16-bits	diagnostics	Filter holder temperature (xrsflt_tmp_dn)
MagnetTemp	DN	16-bits	diagnostics	Magnet assembly temperature (xrs_mag_tmp_dn)
InvalidFlags	NA	8-bits	L1b product	Invalid flags, 0=good, 1=integration time warning, 2=flatfield chirp, 4=EDAC single bit error (corrected), 8=EDAC multiple bit errors (not corrected) (xrs_inval)
DetChangeCount	NA	16-bits	L1b product	Detector change counter, counts from 0 to 65535 whenever cal circuit is enabled or disabled, or xrs is powered on, sticks at 65535 (xrs_det_chg)
LEDChangeCount	NA	16-bits	diagnostics	Counts quarter seconds elapsed since LED was powered on or off, sticks at 65535 (exs_sl_chg)
asicSciVDAC	NA	16-bits	diagnostics	Science voltage DAC last input (xrs_sci_v_lst)
asicCalVmin	NA	16-bits	diagnostics	Min voltage for the cal ramp (xrs_cal_v_min)
asicCalVmax	NA	16-bits	diagnostics	Max voltage for the cal ramp (xrs_cal_v_max)
asicCalVstepUp	NA	8-bits	diagnostics	Voltage step size during ramp up (xrs_cal_v_sup)

asicCalTstepUp	NA	8-bits	diagnostics	Time step size during ramp up (10 microsec), (xrs_cal_t_sup)
asicCalVstepDown	NA	8-bits	diagnostics	Voltage step size during ramp down (xrs_cal_v_sdn)
asicCalTstepDown	NA	8-bits	diagnostics	Time step size during ramp down (10 microsec), (xrs_cal_t_sdn)
XrsMode	NA	2-bits	L1b product & diagnostics	XRS detector mode, 0=normal, 1=cal, 2=diagnostic, 3=safe, these do not affect XRS and normal should not be used to filter any science data, XRS can generate good measurements for all values of XrsMode (xrs_md)
fovFlagsKnown	NA	1-bit	L1b product	FOV flags are known by flight software, 0=known, 1=unknown (exs_tl_fov_stat)
Eclipse	NA	1-bit	L1b product	Earth eclipse imminent or in progress, set by ground command, 0=no eclipse, 1=eclipse (exs_tl_fov_eclip)
LunarTransit	NA	1-bit	L1b product	Lunar transit imminent or in progress, set by ground command, 0=no transit, 1=transit (exs_tl_fov_lunar)
PlanetTransit	NA	1-bit	L1b product	Planetary transit imminent or in progress, set by ground command, 0=no transit, 1=transit (exs_tl_fov_plnt)
OffPoint	NA	1-bit	L1b product	Off-pointing calibration maneuver is imminent or in progress, set by ground command, 0=no maneuver (or sun pointed), 1=off-point maneuver (exs_tl_fov_offpt)
Gain_corrections	C/DN	12 x 32-bit floats	diagnostics	The total gain correction applied (preflight, relative, and linearity) to the 12 diodes.
Dark_corrections	Amps	10 x 32-bit floats	diagnostics	Total dark correction applied to the 8 quad diodes and the 2 solar minimum diodes.
FOV_corrections	NA	4 x 32-bit floats	diagnostics	The FOV corrections applied to the 2 quad diodes and the 2 solar minimum diodes.
spsTime	Seconds	32-bit float	diagnostics	Seconds of UT day converted from the secondary header exs_ps_tm_ms of the last SPS packet used to determine pointing angles

spsDiodeCounts	DN	6 x 32-bit ints	diagnostics	SPS diode data numbers for the diodes and precision resistors (sps_cnt_ch0-5)
spsIdacOffsets	DN	6 x 16-bit ints	diagnostics	SPS IDAC offsets commanded (sps_idac_ch0-5)
spsCal	NA	2-bits	diagnostics	Internal gain calibration circuit indicator, 1=science, 2=cal (sps_runctrlmd)
spsPower	NA	1-bit	diagnostics	SPS power good indicator, 0=off, 1=on (sps_pwr)
spsIntTime	DN	8-bits	diagnostics	SPS integration time in quarter seconds, 0=0.25 sec, (sps_integ_tm)
spsTemperature	DN	16-bits	diagnostics	SPS detector temperature (sps_dt_tmp_dn)
spsDetChangeCount	NA	16-bits	diagnostics	SPS detector change counter (sps_det_chg)
spsAsicSciVDAC	NA	16-bits	diagnostics	Science voltage DAC last input (sps_sci_v_lst)
spsAsicCalVmin	NA	16-bits	diagnostics	Min voltage for the cal ramp (sps_cal_v_min)
spsAsicCalVmax	NA	16-bits	diagnostics	Max voltage for the cal ramp (sps_cal_v_max)
spsAsicCalVstepUp	NA	8-bits	diagnostics	Voltage step size during ramp up (sps_cal_v_sup)
spsAsicCalTstepUp	NA	8-bits	diagnostics	Time step size during ramp up (10 microsec), (sps_cal_t_sup)
spsAsicCalVstepDown	NA	8-bits	diagnostics	Voltage step size during ramp down (sps_cal_v_sdn)
spsAsicCalTstepDown	NA	8-bits	diagnostics	Time step size during ramp down (10 microsec), (sps_cal_t_sdn)

**Table 8 XRS data product variables**

## 4.6 XRS Measurement Flag Details

Many of the XRS flags listed in CDRL 80 Rev F Table 7 (XRS measurement flags) can be populated during the telemetry decomposition step. These include Checksum, LowTemperature, HighTemperature, SignalHighA1, SignalHighAquad, SignalHighB1, SignalHighBquad FlatfieldChirpWarning, and DetChangeCountNotValid.

### 4.6.1 Flags Set in Telemetry Decomposition

Any checksum (exs\_px\_pkt\_cksm) that fails to match the calculated checksum result will set the Checksum flag. This is described in section 3.2 of CDRL 80. A failed checksum should cause this packet to be disregarded. The checksum flag is provided to PM (or similar group). It does not need to be provided in the product.

Any value of `xrs_1_bd_tmp` below -20 deg C (less than 16,706 DN) will set the LowTemperature flag. If `xrs_1_bd_tmp` fails, then `xrs_2_bd_tmp` will be used. This value is different than what was reported in 109620RevFTechnicalMemo-1, and now corresponds to the Operating Mission Allowable Temperature Range. If this flag is set, the data quality will likely be reduced, but it can still be processed to create irradiances.

Any value of `xrs_1_bd_tmp` above 20 deg C (greater than 45,069 DN) will set the HighTemperature flag. If this flag is set, the data quality will likely be reduced, but it can still be processed to create irradiances.

Any value greater than or equal to 989,000 DN for A1 will set the SignalHighA1 flag. This channel cannot provide useful irradiances. Process into an irradiance anyway.

Any value greater than or equal to 989,000 DN for B1 will set the SignalHighB1 flag. This channel cannot provide useful irradiances. Process into an irradiance anyway.

Any value greater than or equal to 989,000 DN for any of the A21, A22, A23, or A24 diodes will set the SignalHighAquad flag. This channel cannot provide quality irradiances. Process anyway.

Any value greater than or equal to 989,000 DN for any of the B21, B22, B23, or B24 diodes will set the SignalHighBquad flag. This channel cannot provide quality irradiances. Process anyway. The instrument is designed such that this should never happen under normal operation of the instrument.

Copy the `xrs_tl_ivsl` value into the FlatfieldChirpWarning flag. If set this packet may produce low quality results. Until the chirp is measured, we recommend processing anyway whether the flag is set or not set.

If the `xrs_det_chg` value is less than the number reported in Table 7 then set the DetChangeCountNotValid flag, and process into an irradiance anyway.

#### 4.6.1.1 Special Note about Pointing Flags

These flags can only be set after the SPS pointing angles are averaged over the XRS integration period. Only one pointing flag is set for any integration based on the mean of the 4 Hz pointing angles. Pointing flags are mutually exclusive.

We define 4 ranges with 3 pointing-related flags. We call these the good range, the warning range, the degraded range, and the bad range. When the 3 flags are zero, the pointing is within the good range.

The good range is the innermost central region in the FOV. This is the best region and is defined by the spacecraft pointing requirements for the EXIS reference boresight. The spacecraft is required to point EXIS within 7 arcminutes of sun center (3-sigma). Values of SPS alpha and beta that are within +/- 7 arcminutes are good. None of the pointing flags are set here.

If either of the SPS angles is outside of the central +/- 7-arcminute box, the PointingWarning flag is set. This is the warning region. This is just a warning that the spacecraft is not pointing EXIS within the



required range. Processing continues as normal, and the FOV calibration table provides the proper corrections to produce irradiances. This extends up to 0.4 degrees. Accuracy requirements can be met in this region.

If either of the SPS angles is outside of +/- 0.4 degrees calibrated FOV region, then the PointingDegraded flag is set. This region is beyond the FOV map region, but can still be useful for tracking relative irradiance changes. Processing continues as normal in this region, but the FOV corrections are truncated to the edge of the measured map with no extrapolation. This extends up to 0.8 degrees. Accuracy requirements cannot be met in this region.

If either of the SPS angles is outside of +/- 0.8 degrees, or if the `exs_tl_fov_stat` value is set, then the PointingBad flag is set. If the `exs_tl_fov_stat` value is set, this indicates that the FOV flags are unknown. The PointingBad flag means the science quality of the measurement is compromised, and the sun may be partially or totally outside of the view factor of the detectors. This data is only useful for calibration purposes such as cruciform maneuvers.

The ranges are defined programmatically in `xrs.config` through 12 variables (low and high for alpha and beta indicating warning, degraded, and bad ranges) delivered with CDRL 82 rev G. The variable names have the form of `POINTING_ANGLE_ALPHA/BETA_WARNING/DEGRADED/BAD_MAX/MIN_DEG`. Refer to a pictorial representation in Figure 7. The boundaries will need to be updated on-orbit during PLT.

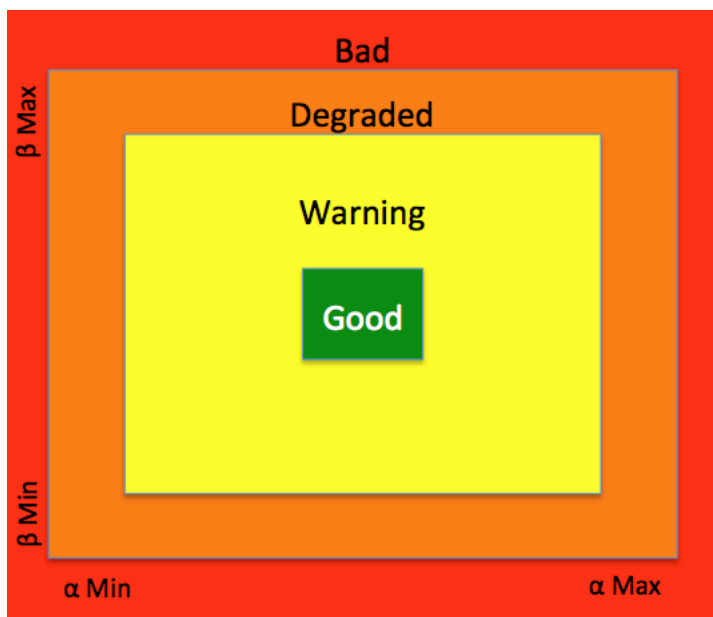


**Figure 7. The pointing flag mutually exclusive nested regions represented as rectangles. The good flag is 0-7 arcmin from center. Warning is 7 arcmin to 0.4 degrees away from center. Degraded is 0.4 degrees to 0.8 degrees from center. Bad is anything larger than 0.8 degrees from center. The largest pointing angle defines the region.**

#### 4.6.1.2 Special Note about DataNotGood Flags

The DataNotGood flags can be partially set during telemetry decomposition. These derived flags use many of the above flags, and other flags calculated later, and other telemetry values that are not flags themselves. Here we present only those flags that have already been set or are included in the telemetry packet.

The DataNotGoodA and DataNotGoodB flags are set if the `xrs_runctrlmd` is not equal to 1 (not science). The flags are set if `exs_sl_pwr_ena` is set (Flatfield power is on) and `exs_sl_sel` is either `XRS_PRI` or `XRS_RED` (7 or 3). The flags are set if any of these conditions are met.

PointingBad is set, LowTemperature is set, HighTemperature is set, FlatfieldChirpWarning is set, DetChangeCountNotValid is set, `xrs_tl_ivtm` (Integration Time Warning) is set, `xrs_tl_ivmbe` is set (EDAC multibit error), `exs_tl_fov_offpt` (Offpoint Maneuver) is set, `exs_tl_fov_lunar` (lunar transit) is set, `exs_tl_fov_eclip` (eclipse) is set, `xrs_integ_tm` is not equal to 3.

We have opted to not include the planetaryTransit flag in the DataNotGood flags, since the measurements are not affected significantly enough by the tiny partial blockage of Venus or Mercury. This is a departure from 109620RevFTechnicalMemo-1.

The rest of the specific contributions to DataNotGoodA and DataNotGoodB are in subsequent sections.

#### 4.6.2 Flags Set After Evaluation of Eq. 4.3

Recall the result of equation 4.3 is a current. Specifically, this is the real signal current above the dark subtracted background. This is where SignalLow flags for the solar minimum diodes can be set.

Any value of  $C'_{A1}$  less than or equal to zero will set the SignalLowA1 flag. Processing into irradiance should continue.

Any value of  $C'_{B1}$  less than or equal to zero will set the SignalLowB1 flag. Processing into irradiance should continue.

#### 4.6.3 Flags Set After Evaluation of Eq. 4.12

Any value of  $C'_{A21}$ ,  $C'_{A22}$ ,  $C'_{A23}$ , or  $C'_{A24}$  that is less than or equal to zero will set the SignalLowAquad flag. Processing into irradiance should continue.

Any value of  $C'_{B21}$ ,  $C'_{B22}$ ,  $C'_{B23}$ , or  $C'_{B24}$  that is less than or equal to zero will set the SignalLowBquad flag. Processing into irradiance should continue.

#### 4.6.4 Flags Set After Evaluation of Eq. 4.9 and Eq. 4.18

After the irradiance is calculated and the primary channels are identified, the rest of the DataNotGood flags can be set.

##### 4.6.4.1 DataNotGoodA

If the primary XRS-A channel is A1, then DataNotGoodA is set if SignalLowA1 is set, or if SignalHighA1 is set.

If the primary XRS-A channel is A2, then DataNotGoodA is set if SignalLowAquad is set, or if SignalHighAquad is set.

##### 4.6.4.2 DataNotGoodB

If the primary XRS-B channel is B1, then DataNotGoodB is set if SignalLowB1 is set, or if SignalHighB1 is set.

If the primary XRS-B channel is B2, then DataNotGoodB is set if SignalLowBquad is set, or if SignalHighBquad is set.

##### 4.6.4.3 RatioNotGood

If DataNotGoodA is set or if DataNotGoodB is set, then RatioNotGood is set.

## 5.0 EUVS Algorithm Description

The EUVS has three channels, A, B, and C. EUVS-A has 24 diodes, and so does EUVS-B. The diodes are non-uniformly arranged in the grating dispersion direction, clustered around specific solar lines. Channel C is a uniform, linearly arranged array of 512 diodes that span the wavelength range of about 275-285 nm, around the Mg II h and k lines.

The primary data product of the EUVS processing is a low-resolution spectrum. This spectrum is created after calculating the solar irradiances for the XRS-A, XRS-B (long channel), the EUVS-A and B lines, and extracting the Mg II core-to-wing ratio from EUVS-C. These are averaged, then converted to proxies for use in the spectral model. All measurements (proxies) are measured by EXIS. The model spectrum is calculated over 30 seconds in order to meet the requirements for model accuracy. The algorithm may be used with less than 30 seconds of data, but will result in a lower accuracy spectrum.

EUVS-A, B, and XRS have a nominal integration rate of 1 Hz. EUVS-C will be adjusted on orbit during PLT to achieve the desired signals (faster than 10 seconds).

## 5.1 Detector Measurement Input

EUVS-A measures these 3 EUV lines: He II 25.6 nm, Fe XV 28.4 nm, and He II 30.4 nm. These wavelengths are only approximate. Some of the diodes contain solar spectral information beyond the intended line, and those diodes will be masked out to prevent biasing the intended measurement.

EUVS-B measures these 4 EUV-FUV lines: C III 117.5 nm, H I 121.6 nm, C II 133.6 nm, Si IV/O IV 140.5 nm. Similar to EUVS-A, a diode mask will be used to filter contributions from outside of the intended measurement lines.

EUVS-C measures the entire MUV spectrum from approximately 275 to 285 nm. In this wavelength region are 2 Mg II lines (h & k) at 279.6 and 280.3 nm. The ratio of these lines to the surrounding spectral region is the Mg II index.

All of these measurements are summarized in Figure 8.

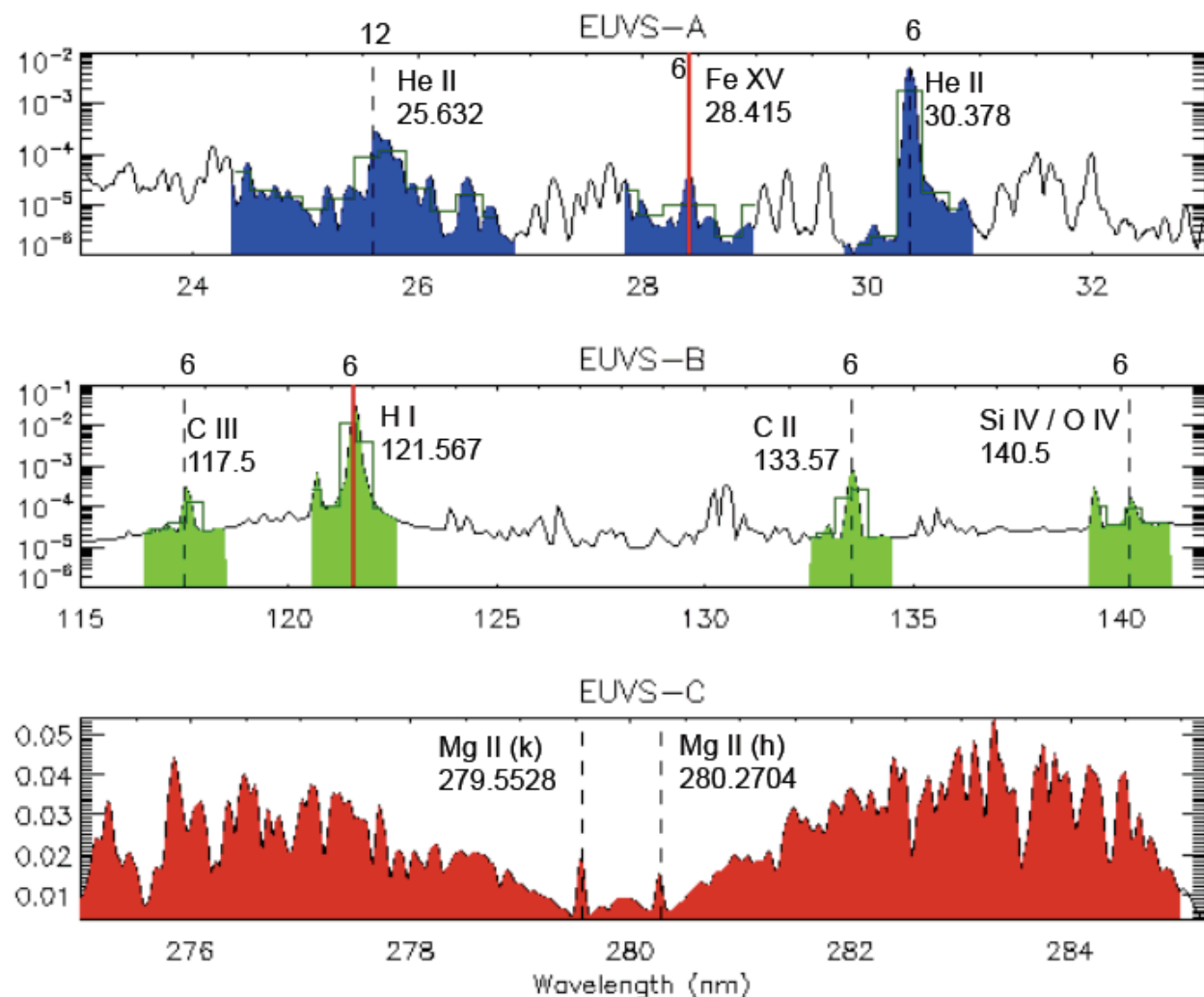


Figure 8. EUVS-A, EUVS-B, & EUVS-C spectral measurements

## 5.2 Mathematical Description and Algorithm Design

The complete measurement equation for EUVS-A and EUVS-B is represented in a series of equations. Each of the diode groups around the seven solar emission lines is processed separately (serial loop). The seven groups of diodes are: He II 25.6, Fe XV 28.4, He II 30.4, CIII 117.5, H I 121.6, C II 133.6, Si IV/O IV 140. Each diode group has its own electrical circuitry with different properties.

$$\text{Eq. 5.1} \quad C_j = \frac{S_j}{\Delta t} \cdot G_j \cdot f_{FF,j}$$

$$\text{Eq. 5.2} \quad C'_j = C_j - C_{SL,j} - C_{OS,j} - C_{Dark,j}$$

$$C_{Dark,j} = C_{\Delta T,j} + C_{Rad,j} + C_{time,j}$$

$$\text{where } C_{time,j} = \tau_j \cdot \frac{G_j}{\Delta t}$$

$$\text{Eq. 5.3} \quad \text{and } C_{\Delta T,j} = \Delta T \cdot \theta_j \cdot \frac{G_j}{\Delta t} \text{ and } \Delta T \equiv T_{detector} - T_{Ref}$$

The  $C_{time}$  and  $C_{\Delta T}$  capture dark drift over long times and delta temperature terms. The  $\tau$  and  $\theta$  terms are calculated using LUT coefficients for equation 9.1.

$$\text{Eq. 5.4} \quad C_{Rad,j} = k_j \cdot \langle C_{rad,Dark} \rangle$$

$$\begin{aligned} \text{a) } C_{rad,Dark_1} &= \frac{G_{Dark_1}}{\Delta t} \cdot [\langle S_{Dark_1} \rangle_{60} - \tau_{Dark_1} - (\Delta T \cdot \theta_{Dark_1})] \\ &= \frac{\langle S_{Dark_1} \rangle_{60} \cdot G_{Dark_1}}{\Delta t} - C_{time,Dark_1} - C_{\Delta T,Dark_1} \end{aligned}$$

$$\begin{aligned} \text{b) } C_{rad,Dark_2} &= \frac{G_{Dark_2}}{\Delta t} \cdot [\langle S_{Dark_2} \rangle_{60} - \tau_{Dark_2} - (\Delta T \cdot \theta_{Dark_2})] \\ \text{Eq. 5.5} \quad &= \frac{G_{Dark_2}}{\Delta t} \cdot \langle S_{Dark_2} \rangle_{60} - C_{time,Dark_2} - C_{\Delta T,Dark_2} \end{aligned}$$

$$\text{c) } \langle C_{rad,Dark} \rangle = (W_{Dark_1} \cdot C_{rad,Dark_1}) + (W_{Dark_2} \cdot C_{rad,Dark_2}) \text{ and always } \geq 0$$

$$\text{Eq. 5.6} \quad \text{The } W \text{ terms represent darkweights specified in the EUVS LUTs. Since the } W \text{ terms are both set to } 0.5, \text{ then eq 5.5c reduces to a mean.}$$

$$C''_k = C'_j$$

except for the split diodes where  $C''_k = C'_{split1} + C'_{split2}$

Eq. 5.7

$$E_i = \sum_k \frac{Mask_{ik} \cdot C''_k}{R_{C,k} \cdot f_{FOV,k} \cdot f_{Degrad,k}}$$

The split diode currents ( $C'$ ) need to be added prior to conversion to irradiance. This is necessary because the responsivity and FOV corrections can only be properly calibrated over the sum.

The irradiance is expressed in Eq. 5.7. The responsivity has been formulated to include the static constants (Planck's constant, the speed of light, and the wavelength) necessary for conversion from current to irradiance. This simplifies the appearance of the equations.

Variable descriptions with units are listed in Table 9.

Variable	Description	Units
i	Solar line	NA
j	Diode number in telemetry	NA
k	Same as j except that the split diode is added to form one measurement	NA
S	Raw signal from a diode	DN / integration
$\Delta t$	Integration time	Seconds / integration
G	Detector gain (includes linearity)	Coulombs / DN
$f_{FF}$	Flatfield correction	Dimensionless
C	Diode current	Amperes
$C_{SL}$	Scattered light correction	Amperes
$C_{OS}$	Order sorting correction	Amperes
$C_{Dark}$	Dark correction	Amperes
$C'$	Corrected current	Amperes
$C_{time}$	Temperature dependent dark drift, slow changes	Amperes
$C_{\Delta t}$	Thermal contribution to dark, uses temperature difference from reference	Amperes
$C_{rad}$	Radiation background	Amperes
$C''$	Measurement current	Amperes
$W_{Dark}$	The weight for dark diode 1 and 2	Dimensionless
Mask	Mask (0 and 1 only) to filter only the relevant diodes for each line	NA
$R_C$	Responsivity	Amperes / (W/m <sup>2</sup> )
$f_{FOV}$	Field of view correction	Dimensionless
$f_{Degrad}$	Degradation correction	Dimensionless

E	Irradiance	$W/m^2$
---	------------	---------

**Table 9 EUVS-A and EUVS-B Measurement Equation Variables**

### 5.2.1 Dependency Analysis

The terms in the measurement equations for EUVS-A (and B) are inter-related. The dependency is shown graphically in Figure 9.

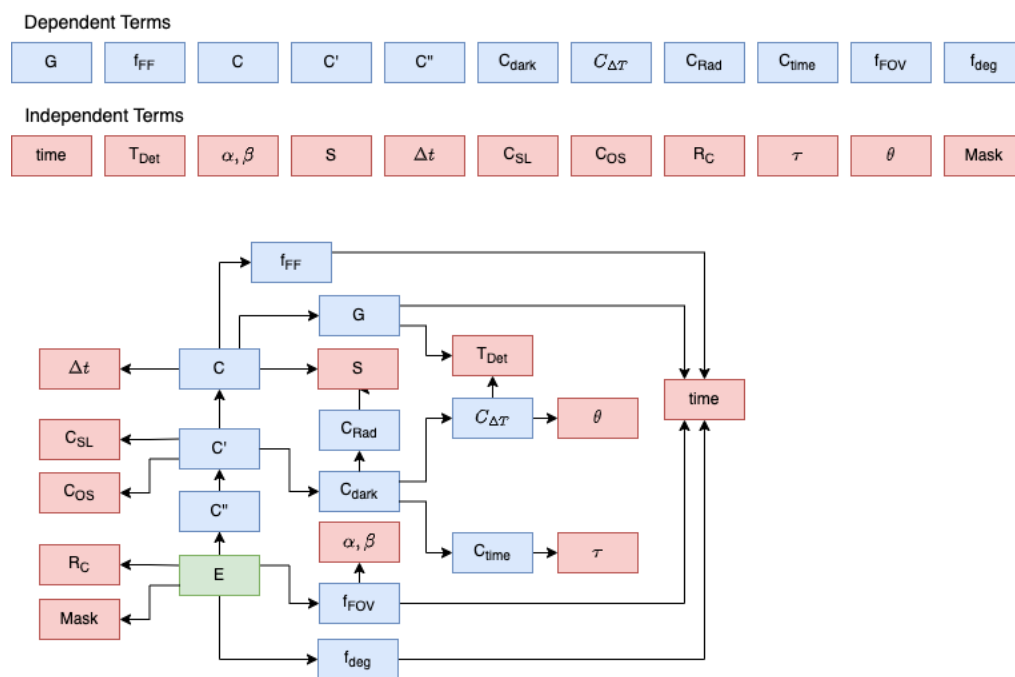


**Figure 9 EUVS-A, B dependency graph**

The dependency graph is useful for identifying the connectedness of the terms in the measurement equations. The acyclic property of the graph ensures that no terms are dependent in a way that would cause an infinite loop.

Reversing the arrows of Figure 9 creates a rooted-tree as shown in Figure 10. This elucidates the acyclic property and shows that all paths will eventually terminate with the irradiance.

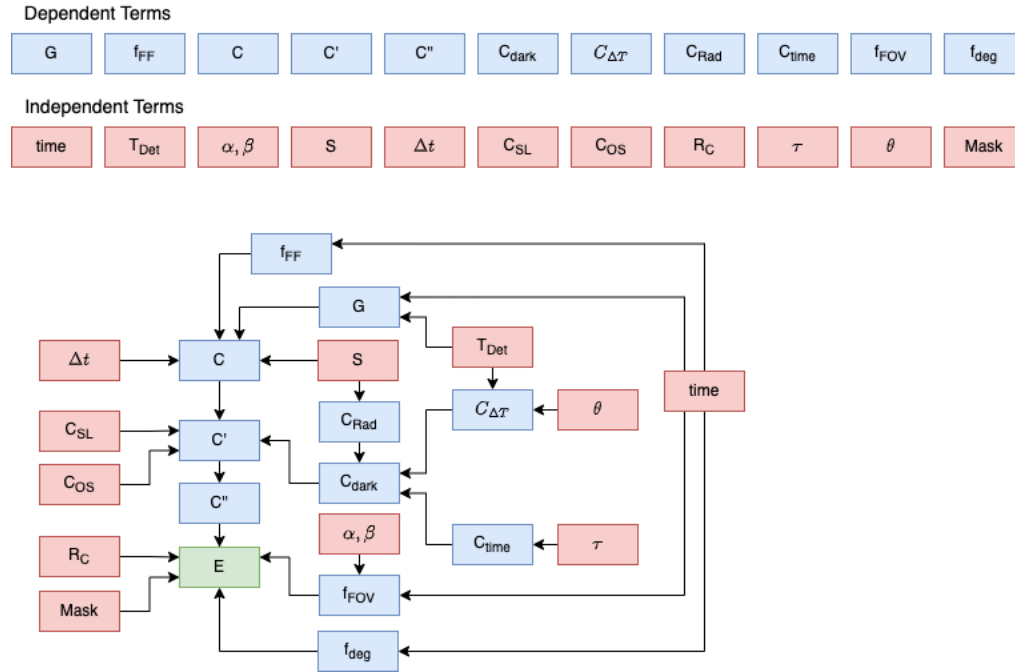
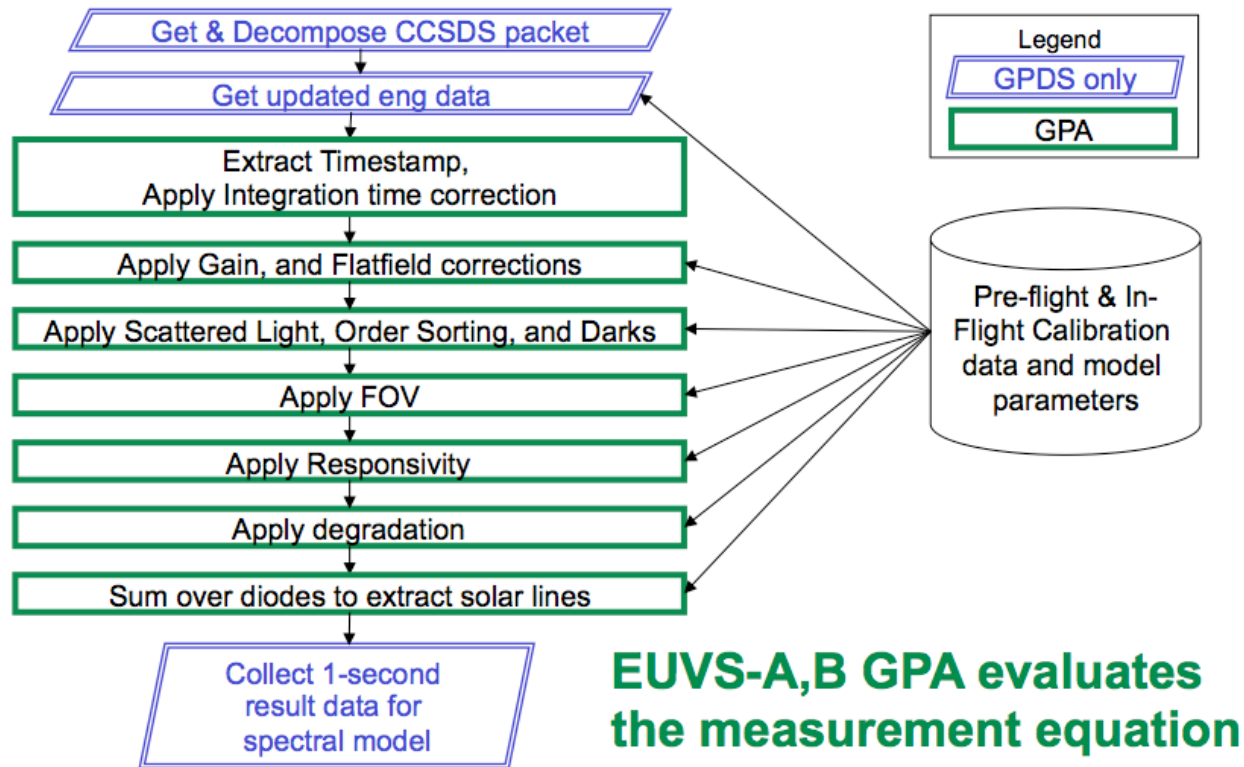


Figure 10 EUVS-A, B Rooted dependency tree

### 5.3 EUVS-A Algorithm Steps

A high-level graphical representation of the processing flow is shown in Figure 11.





**Figure 11. EUVS-A and EUVS-B Algorithm Overview**

A more detailed overview is provided in this pseudocode.

```

#Main thread
euvs_ab.extract_pkt(packet)
lookup_lau(time)

#EUVS-A thread
euvs_ab.loadConfigurationFiles()
divide by integration time
euvs_ab.applyGain()
euvs_ab.applyFlatfieldCorrections()
euvs_ab.applyScatteredLightCorrections()
euvs_ab.applyOrderSortingCorrections()
euvs_ab.applyDarkDiodeCorrections()
euvs_ab.applyFovCorrections()
euvs_ab.applyResponsivities()
euvs_ab.applyDegradationCorrections()
euvs_ab.sumDiodes()
euvs_ab.createOutput()
euvs_ab.printProcessedData()
    
```

EUVS-A and B tasks are similar enough that the objects could share a class. This is further illustrated in the following figure.

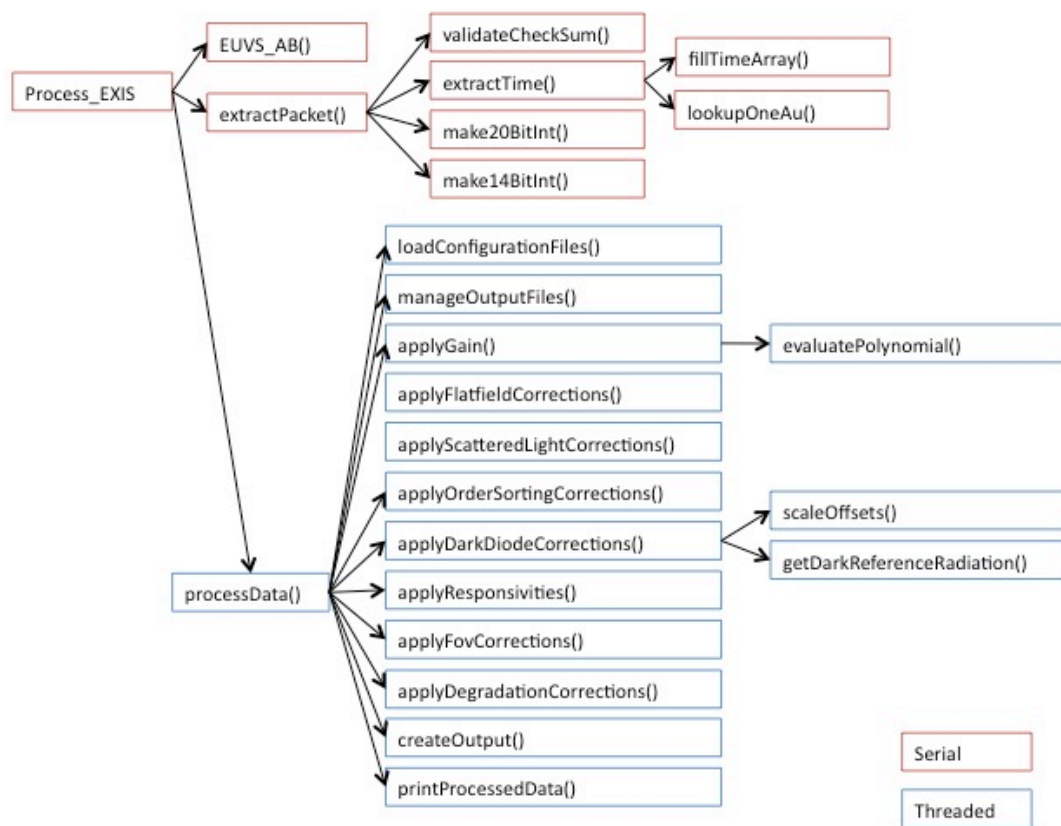


**Figure 12. EUVS-A (and EUVS-B) functions**

However, we have decided to use the singleton pattern, and we have split EUVS-A and EUVS-B into separate classes for the GPDS. This somewhat simplifies the bookkeeping and reduces the number of special cases in the code, at the expense of extra test code.

Note that for the He II 30.4 line, the diodes are arranged with the center diode split in the cross-dispersion direction as shown in Figure 13. Two diode currents (number 3 and 4 in Figure 13) contain information about relative pointing in the cross-dispersion direction. This is useful for alignment verification, but for the irradiance calculation the two irradiances must be added.



**Figure 13. EUVS-A 30.4 diode layout**

The physical diode layout of light-sensitive diodes is shown in Figure 14. Two dark diodes (not shown) are farther left and farther right of the diodes shown. Note that the telemetry order is not a straightforward linear readout of the diodes. It is rather a seemingly jumbled and non-intuitive sequence that warrants significant care when mapping the diodes to the intended solar emissions. This is the result of physical packaging plus the FPGA and ASIC order interplay. In Table 10, the diode description column uses subscripts to indicate increasing wavelength order. The left-most and right-most diodes (not shown) are dark, and 2 through 23 follow the left-to-right order shown in Figure 14. The 30.4 nm line split is in subscripts 20 and 21, which is equivalent to telemetry order 15 and 16.

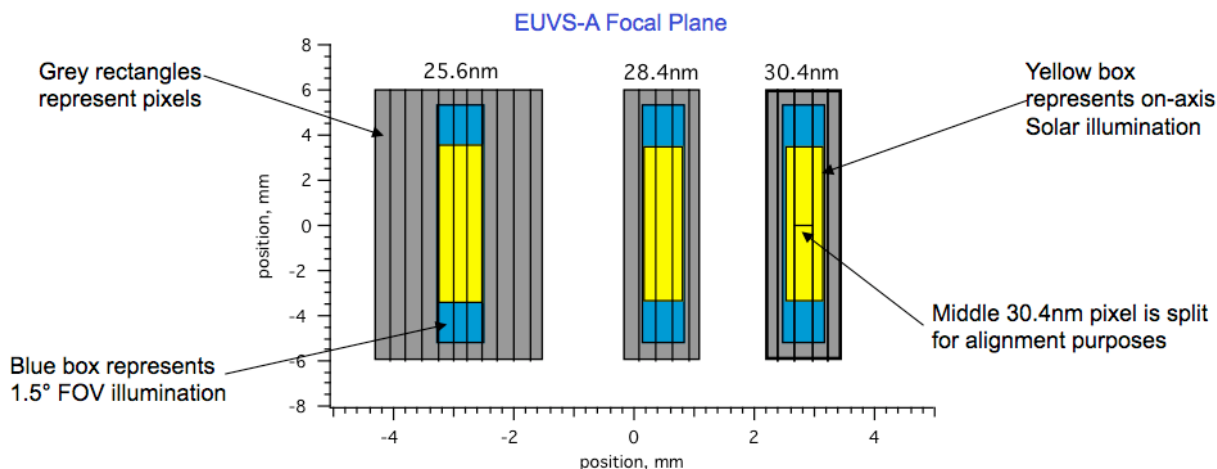


**Figure 14. EUVS-A diode layout**

Telemetry Order	Diode Description/Cathode subscript	ASIC	Band
1	A <sub>1</sub> – Dark diode on ASIC 1	1	NA
2	A <sub>2</sub>	1	25.6
3	A <sub>3</sub>	1	25.6
4	A <sub>4</sub>	1	25.6
5	A <sub>5</sub>	1	25.6
6	A <sub>6</sub> – Expected peak	1	25.6

7	A <sub>13</sub>	2	28.4
8	A <sub>14</sub>	2	28.4
9	A <sub>15</sub> – Expected peak	2	28.4
10	A <sub>16</sub>	2	28.4
11	A <sub>17</sub>	2	28.4
12	A <sub>24</sub> – Dark diode on ASIC 2	2	NA
13	A <sub>23</sub>	3	30.4
14	A <sub>22</sub>	3	30.4
15	A <sub>21</sub> – top of 30.4	3	30.4
16	A <sub>20</sub> – bottom of 30.4	3	30.4
17	A <sub>19</sub>	3	30.4
18	A <sub>18</sub>	3	30.4
19	A <sub>12</sub>	4	25.6
20	A <sub>11</sub>	4	25.6
21	A <sub>10</sub>	4	25.6
22	A <sub>9</sub>	4	25.6
23	A <sub>8</sub>	4	25.6
24	A <sub>7</sub>	4	25.6

**Table 10 EUVS-A diode telemetry order and ASIC relationship**

A cartoon of the diodes in the detector is shown in Figure 15. The black triangles correspond to pins with the lower left pin designated number 1. The telemetry order cannot be completely determined from the black triangles in Figure 15. Pins are accessed by the FPGA in largely a counterclockwise direction with 2 exceptions being pins 21 and 24. The first 6 pins (1-6) connect to ASIC 1. Pins 13-17 plus 24 connect to ASIC 2. Pins 23 down to 18 are connected to ASIC 3 and the order is reversed from wavelength order following the counter-clockwise convention. Pins 12 down to 7 are connected to ASIC 4 and are also reversed from the wavelength order sense. It should be clear that Table 10 is far more useful. However the reason why telemetry order 6 and telemetry order 24 are physically adjacent diodes is now explained.

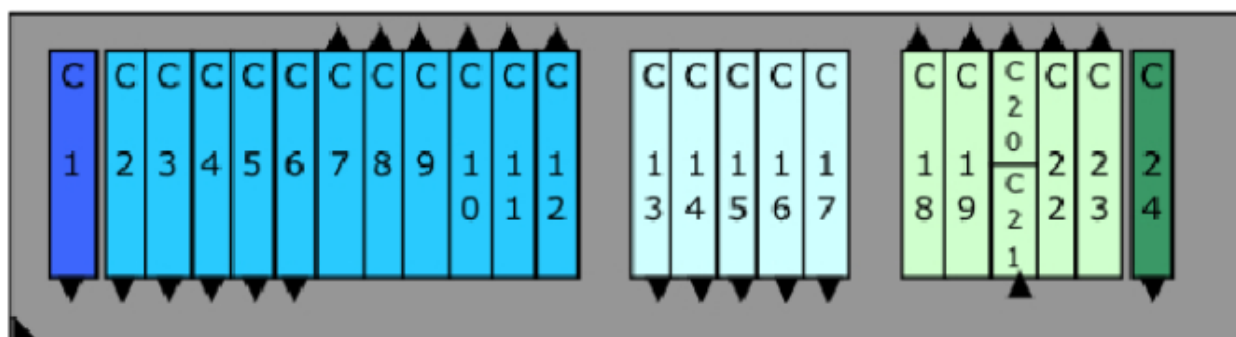


**Figure 15. EUVS-A cathode numbers are fortuitously in wavelength order**

### 5.3.1 Packet Decomposition

The format of the packet is described in EXIS CDRL 43. All fields in the CCSDS packet are extracted and stored in variables within the EUVS-A object.

Use the field entitled `euv_a_det_chg` to disregard all packets whose value is less than 10. After power up, the detector and associated electronics need to stabilize, so this data should be disregarded. Note that flight software resets `euv_a_det_chg` to indicate that something significant on the detector has changed that affects data quality for a short period. A persistent zero count rate effect is observed for up to 5 integrations after exiting the internal gain calibration circuit. These are easily discarded using this counter.

For EUVS-B, the time lag is longer, so values of `euv_b_det_chg` should be disregarded where they are less than 20. Up to 18 integrations have been observed to retain zero values after exiting the gain calibration on EUVS-B. This behavior may be different for each flight model.

### 5.3.2 Lookup\_1au

The result will not have the 1-AU correction applied, but it will be provided. Refer to the section Appendix D - Astronomical Unit Correction.

### 5.3.3 Signal, S

The extracted photometer measurements are encoded as 20-bit integers in units of DN.

### 5.3.4 Integration time, $\Delta t$

The integration time is encoded the same way it is for XRS. For more details, see Eq. 4.19. For EUVS-A, the default integration time is 1.0 seconds, which corresponds to 3 DN.

### 5.3.5 Gain

The gain correction is the same as it is for XRS. Refer to section 4.4.5 for more details.

### 5.3.6 Flatfield

The flatfield correction is a relative pixel-to-pixel adjustment to compensate for small differences in the diodes in response to the on-board LEDs. Periodically (we assume weekly) in normal operations the LEDs will be used to illuminate the diode array. This provides a direct measure of the relative changes when divided by the reference flatfield values. The reference will be provided in CDRL 79. An analysis procedure (see 9.1.1) will be used to generate a recent (6 months) trend in the flatfield changes to allow for adjustments. The flatfield correction evaluates the curve fits for the current date.

The flatfield correction file will contain a Julian date for each row when a new set of correction functions are needed. Each row then contains 121 columns from the date and 5 function parameters for each diode. The flatfield corrections take effect at the Julian date provided. This allows for historical data to be reprocessed if necessary.

### 5.3.7 Scattered Light

The scattered light correction should remove the unwanted signal contributions from stray light. This is determined in pre-flight calibration. Scattered light is a Static Parameter and will be provided in CDRL 79.

The scattered light correction for each will be provided in an ASCII file.

### 5.3.8 Order Sorting

The order sorting correction is zero for all diodes in EUVS-A. No higher order light is expected to arrive at the EUVS-A detectors because the primary science filter transmission is nearly zero for wavelengths shorter than 17 nm (aluminum edge). The order sorting contribution is included to allow for the flexibility if it becomes necessary. The order sorting correction file is provided in CDRL 79.

The order sorting correction is a constant for each diode. The values are written in an ASCII file.

### 5.3.9 Dark

The dark correction is the same as what was described in the XRS. See section 4.4.6.1 for more details. Although there are 4 ASICs, there are only 2 dark diodes. As in XRS, a 60-second trailing average of the dark diodes is used to decrease noise. These 60-second averages are then averaged together to obtain a single representative estimate of the effective radiation background contribution, and that result is used (with the scale factors) to approximate the radiation contribution the other diodes are experiencing. The scale factors basically attempt to compensate for discrepancies in radiation shielding and net particle sensitivity.

### 5.3.10 Mask

A mask will be provided that prevents unwanted diodes from being included in the irradiance. It is likely that only 3 or 4 diodes from each region around the line cores will be used, since the other have significant contributions from possibly different solar temperature plasmas/emission lines. The mask is either 0 or 1 for each diode. The mask is a Semi-Static Parameter that may be changed in PLT. The best estimate will be provided in CDRL 79. The mask is needed during focus and alignment testing, prior to the final analysis of pre-flight calibration data.

### 5.3.11 Responsivity

The responsivity is calculated similarly to the XRS. The responsivity includes the physical constants required to properly convert the summed line currents into irradiances. Responsivities are Static Parameters and will be provided in CDRL 79.

For EUVS-A, the responsivity changes for each filter position. Responsivities will be provided for each filter in CDRL 79, and care must be used to apply the correct responsivity for the filter position. One filter position is designated the primary position, and will be reported in CDRL 79.

### 5.3.12 Field of View

The field of view correction will be a table lookup based on the pointing angles. The SPS processing results for the pointing angles are used to determine the value from the lookup table.

If the SPS angles are not available, then the SUVI Guide Telescope angles shall be used. This requires calibration of the guide telescope to EXIS angles prior to implementation operationally.

### 5.3.13 Degradation

The degradation correction is calculated from evaluating a function that has the same form as Eq. 9.1, similar to the way the flatfield time dependence is determined. The curve fit coefficients are stored in an ASCII file.

### 5.3.14 Sum over Lines

The measurement currents for each of the lines are summed to obtain a total irradiance over a band that contains the line. The specific diodes to sum are unique for each line, and the mask filters out undesired contributions.

This step is the final step in calculating the irradiance for a line.

## 5.4 EUVS-A Output

The EUVS-A processing creates the fully calibrated irradiance for the 3 measured solar emission lines. All 3 lines may be used to create the model spectrum.

Quality flags shall be tracked for each packet indicating measurement valid / status and shall be provided in the EUVS product. The individual packets are needed for diagnostics and are necessary for determining updates to correction factors, like the flatfield, gain, etc. The flags are summarized in Table 11.

Flag Name	Bit Value (1/0)	Description / Explanation
PointingBad	Bad/Good	The pointing of EXIS is both known and within the valid calibration range of the EUVS-A.
PointingDegraded	Bad/Good	Pointing is outside the calibrated range (+/- 0.4deg) and FOV correction is truncated to the map edge.
PointingWarning	Bad/Good	Pointing angles are in the calibrated FOV range, but spacecraft is not meeting pointing requirements (+/-7 arcmin).
Checksum	Mismatch/Match	The checksum matches
SignalLow256 (per integrated line)	Low/Not low	All diode signals in the good part of the mask are distinguishable from zero.
SignalHigh256 (per integrated line)	High/Not high	All diode signals in the good part of the mask are below the saturation value (989,000 at 1 sec).
SignalLow284 (per integrated line)	Low/Not low	All diode signals in the good part of the mask are distinguishable from zero.
SignalHigh284 (per integrated line)	High/Not high	All diode signals in the good part of the mask are below the saturation value.
SignalLow304 (per integrated line)	Low/Not low	All diode signals in the good part of the mask are distinguishable from zero.
SignalHigh304 (per integrated line)	High/Not high	All diode signals in the good part of the mask are below the saturation value.
LowTemperature	Low/Good	The EUVS-A temperature is either low or within the valid range to make measurements.
HighTemperature	High/Good	The EUVS-A temperature is either high or within the valid range to make measurements.
FlatfieldChirpWarning	Bad/Good	This integration may contain a flatfield flash (flatfield chirp from InvalidFlags)
FilterPositionNotSolar	Not Solar/Solar	The filter wheel is not moving, the filter wheel position is known, and the filter position is one that allows sun light to the EUVS-A detector.
DoorPositionNotOpen	Not Open/Open	The door is not moving, the door position is known, and the door absolute step number is 31.
DataNotGood256	Bad/Good	The irradiance is good. Here good means: pointing is good, checksum is good, signal is not low, signal is not high, temperature is not low, temperature is not high, flatfield is off, integration time warning is good, flatfield chirp warning is good, no multibit EDAC errors, no offpoint maneuver in progress, no lunar transit, no eclipse, intTime=3, and detChangeCount is greater than 10 and FilterPositionNotSolar is Solar for EUVS-A and DoorPositionNotOpen is Open.
DataNotGood284	Bad/Good	The irradiance is good (as above).
DataNotGood304	Bad/Good	The irradiance is good (as above).

**Table 11 EUVS-A measurement flags**



The primary filter position is a Static Parameter and will be determined through ground calibration, and will be reported in CDRL 79. The open position for the door mechanism is 31. The value of 31 is only valid if the door position known status (euv\_dr\_pos\_stat) is set. After power up, the door position known bit is zero and the door absolute step number (euv\_dr\_step\_num) is also zero. An operator must take action so that the values related to door telemetry are correct. This can be done without moving the door if it was previously in the open position and is described in the Operations Handbook. There is only one door on EXIS, and it covers EUVS-A, EUVS-B, and EUVS-C.

The proxies will use the solar minimum reference values provided in CDRL 79.

The time stamp and integration time shall also be provided. The time stamp follows the convention defined for the XRS.

The following table describes some of the variables in the EUVS level 1b data product. For 1 second integrations, there will be 30 sets of these variables that are needed for the model to create the product. For diagnostics and analysis, all of these data would be needed.

Variable	Units	Data type	Description
E256	W/m <sup>2</sup>	32-bit float	Irradiance from EUVS-A 25.6 nm line
E284	W/m <sup>2</sup>	32-bit float	Irradiance from EUVS-A 28.4 nm line
E304	W/m <sup>2</sup>	32-bit float	Irradiance from EUVS-A 30.4 nm line
a	degrees	32-bit float	Averaged dispersion direction pointing angle from SPS
b	degrees	32-bit float	Averaged cross-dispersion direction pointing angle from SPS
a_GT	degrees	32-bit float	Averaged SUVI Guide Telescope angle along SPS alpha direction (yaw)
b_GT	degrees	32-bit float	Averaged SUVI Guide Telescope angle along SPS beta direction (pitch)
AuFactor	AU	32-bit float	The 1-AU correction factor that could be multiplied by the irradiances to remove the earth orbit effect.
QualityFlags	NA	32-bit int	All flags defined in Table 11
days_since_jan1_2000	Days	16-bit int	Days since the epoch at the end of the integration
centerTime	Seconds	32-bit float	Seconds of the UT day at the center of the exposure using the secondary header exs_pea_tm_ms (microseconds are unnecessary) and intTime shifted to the center. This corresponds to the CENTER time defined in Eq. 4.20.
scPowerSide	NA	bit	0=B, 1=A (exs_pea_pb_stat)

exisMode	NA	4-bits	0=failsafe, 1=normal, 2=diag, 3=safe (exs_pea_exs_md)
exisFlightModel	NA	8-bits	1=FM1, 2=FM2, 3=FM3, 4=FM4 (exs_pea_md1_num)
exisConfigId	NA	16-bits	Configuration ID (exs_pea_exs_cfg)
checksum	NA	8-bits	Checksum (exs_pea_pkt_cksm)
euvsADiodeCounts	DN	24 x 32-bit int	24 raw diodes measurements (euv_a_cnt_ch0-23)
euvsAIdacOffsets	NA	24 x 16-bit	IDAC offset registers (euv_a_idac_ch0-23)
euvsABCal	NA	2-bits	Internal gain calibration circuit indicator, 1=science, 2=cal (euv_ab_runctrlmd)
euvsBPower	NA	bit	0=off, 1=on (euv_b_pwr)
euvsAPower	NA	bit	0=off, 1=on (euv_a_pwr)
intTime	NA	8-bits	Integration time in quarter second increments, 0=0.25 sec, 1=0.5 sec, 2=0.75 sec, 3=1.0 sec, ... (euv_ab_integ_tm)
LED_select	NA	4-bits	LED selection, 0=EUVSC-Backup, 1=EUVSB- Backup, 2=EUVSA-Backup, 3=XRS-Backup, 4=EUVSC-Pri, 5=EUVSB-Pri, 6=EUVSA-Pri, 7=XRS-Pri (exs_sl_sel)
LED_power	NA	1-bit	LED power, 0=off, 1=on (exs_sl_pwr_ena)
LED_level	NA	16-bits	LED level setting, 12 bits used, (exs_sl_lvl)
IfBoardTemp	DN	16-bits	Interface board temperature (exs_ifb_tmp_dn)
ProcFpgaTemp	DN	16-bits	Microprocessor board FPGA temperature (exs_mb_fp_tmp_dn)
PowerSupplyTemp	DN	16-bits	Power board temperature (exs_pb_tmp_dn)
CaseHeaterTemp	DN	16-bits	Case heater temperature (exs_cs_oh_tmp_dn)
euvsATemp	Deg C	32-bits	EUVS-A detector board temperature (converted euv_a_dt_tmp_dn)
euvsBTemp	Deg C	32-bits	EUVS-B detector board temperature (converted euv_b_dt_tmp_dn)
slitTemp	DN	16-bits	Entrance slit temperature (euv_slit_tmp_dn)
InvalidFlags	NA	8-bits	Invalid flags, 0=good, 1=integration time warning, 2=flatfield chirp, 4=EDAC single bit error (corrected), 8=EDAC multiple bit errors (not corrected) (euv_ab_inval) Either 0 or 4 is good.
DetChangeCount	NA	16-bits	Detector change counter, counts from 0 to 65535 whenever cal circuit is enabled or disabled, or EUVS-A is powered on, sticks at 65535 (euv_ab_det_chg)
LEDChangeCount	NA	16-bits	Counts quarter seconds elapsed since LED was powered on or off, sticks at 65535 (exs_sl_chg)
asicSciVDAC	NA	16-bits	Science voltage DAC last input (euv_ab_sci_v_lst)
asicCalVmin	NA	16-bits	Min voltage for the cal ramp (euv_ab_cal_v_min)
asicCalVmax	NA	16-bits	Max voltage for the cal ramp (euv_ab_cal_v_max)
asicCalVstepUp	NA	8-bits	Voltage step size during ramp up (euv_ab_cal_v_sup)

asicCalTstepUp	NA	8-bits	Time step size during ramp up (10 microsec), (euv_ab_cal_t_sup)
asicCalVstepDown	NA	8-bits	Voltage step size during ramp down (euv_ab_cal_v_sdn)
asicCalTstepDown	NA	8-bits	Time step size during ramp down (10 microsec), (euv_ab_cal_t_sdn)
DoorPositionKnown	NA	1-bit	The EUVS door position is known by flight software (resets after power up) 0=unknown, 1=known (euv_dr_pos_stat)
FilterWheelMoving	NA	1-bit	The EUVS filter wheel mechanism is moving, 0=not moving, 1=moving (euv_fw_mv_stat)
FilterWheelPositionKnown	NA	1-bit	The EUVS filter wheel mechanism position is known by flight software, 0=unknown, 1=known (euv_fw_pos_stat)
DoorPositionStepNumber	NA	8-bits	The EUVS door absolute position step number from 0-107. 0=closed, 31=open. (euv_dr_step_num)
FilterWheelStepNumber	NA	8-bits	The EUVS filter wheel mechanism absolute step number 0-107. (euv_fw_step_num)
EuvsMode	NA	2-bits	EUVS detector mode with same states as XRS, also has no effect on data collection (euvs_md)
fovFlagsKnown	NA	1-bit	FOV flags are known by flight software, 0=known, 1=unknown (exs_tl_fov_stat)
Eclipse	NA	1-bit	Earth eclipse imminent or in progress, set by ground command, 0=no eclipse, 1=eclipse (exs_tl_fov_eclip)
LunarTransit	NA	1-bit	Lunar transit imminent or in progress, set by ground command, 0=no transit, 1=transit (exs_tl_fov_lunar)
PlanetTransit	NA	1-bit	Planetary transit imminent or in progress, set by ground command, 0=no transit, 1=transit (exs_tl_fov_plnt)
OffPoint	NA	1-bit	Off-pointing calibration maneuver is imminent or in progress, set by ground command, 0=no maneuver (or sun pointed), 1=off-point maneuver (exs_tl_fov_offpt)

**Table 12 EUVS-A data product variables**

## 5.5 EUVS-A Measurement Flag Details

Many of the EUVS-A flags listed in Table 11 can be populated during the telemetry decomposition step. These include Checksum, LowTemperature, HighTemperature, SignalHigh256, SignalHigh284, SignalHigh304, FlatfieldChirpWarning, and DetChangeCountNotValid.

### 5.5.1 Flags Set in Telemetry Decomposition

Any checksum that fails to match the calculated checksum result will set the Checksum flag. A failed checksum should cause this packet to be disregarded. The checksum flag is provided to PM (or similar group). It does not need to be provided in the product.

Any value of `euv_a_dt_tmp_dn` below -20 deg C (less than 16,706 DN) will set the LowTemperature flag. If this flag is set, the data quality will likely be reduced, but it can still be processed to create irradiances.

Any value of `euv_a_dt_tmp_dn` above 20 deg C (greater than 45,069 DN) will set the HighTemperature flag. If this flag is set, the data quality will likely be reduced, but it can still be processed to create irradiances.

Any value greater than or equal to 989,000 DN for any diode in the 25.6 nm line masked pixels will set the SignalHigh256 flag. This channel cannot provide useful irradiances. Process into an irradiance anyway. The same is true for the other lines, that is, process into irradiance anyway. The instrument is designed such that this should not happen under normal operations of the detector.

The value of the FlatfieldChirpWarning flag is in the telemetry. If set this packet may produce low quality results. Until the chirp is measured, we recommend processing anyway whether the flag is set or not set.

If the `euv_ab_det_chg` value is less than the number reported in Table 11 then set the DetChangeCountNotValid flag, and process into an irradiance anyway.

#### 5.5.1.1 Special Note about Pointing Flags

These flags can only be set after the SPS pointing angles are averaged over the EUVS-A integration period. Only one pointing flag is set at any instant based on the mean of the 4 Hz pointing angles. Pointing flags are mutually exclusive.

The 3 pointing-related flags are defined in the XRS flags section 4.6.1.1. Recall these are the good range, the warning range, the degraded range, and the bad range. When the 3 flags are zero, the pointing is within the good range.

The good range is the innermost region, the central region in the FOV. This is the best region and is defined by the spacecraft pointing requirements for the EXIS reference boresight. The spacecraft is required to point EXIS within 7 arcminutes of sun center (3-sigma). Values of SPS alpha and beta that are within +/- 7 arcminutes are good. None of the pointing flags are set here.

If either of the SPS angles is outside of the central +/- 7-arcminute box, the PointingWarning flag is set. This is the warning region. This is just a warning that the spacecraft is not pointing EXIS within the required range. Processing continues as normal, and the FOV calibration table provides the proper

corrections to produce irradiances. This extends up to 0.4 degrees. Accuracy requirements can be met in this region.

If either of the SPS angles is outside of +/- 0.4 degrees calibrated FOV region, then the PointingDegraded flag is set. This region is beyond the FOV map region, but can still be useful for tracking relative irradiance changes. Processing continues as normal in this region, but the FOV corrections are truncated to the edge of the measured map with no extrapolation. This extends up to 0.8 degrees. Accuracy requirements cannot be met in this region.

If either of the SPS angles is outside of +/- 0.8 degrees, or if the `exs_tl_fov_stat` value is set, then the PointingBad flag is set. If the `exs_tl_fov_stat` value is set, this indicates that the FOV flags are unknown. The PointingBad flag means the science quality of the measurement is compromised, and the sun may be partially or totally outside of the view factor of the detectors. This data is only useful for calibration purposes such as cruciform maneuvers.

The ranges are defined programmatically in `euvs_a.config` through 12 variables (low and high for alpha and beta indicating warning, degraded, and bad ranges) delivered with CDRL 82 rev G. The variable names have the form of

`POINTING_ANGLE_ALPHA/BETA_WARNING/DEGRADED/BAD_MAX/MIN_DEG`. Refer to a pictorial representation in Figure 7. The boundaries will need to be updated on-orbit during PLT.

### 5.5.1.2 Special Note about DataNotGood Flags

The DataNotGood flags can be partially set during telemetry decomposition. These derived flags use many of the above flags, and other flags calculated later, and other telemetry values that are not flags themselves. Here we present only those flags that have already been set or are included in the telemetry packet.

The DataNotGood256 and similar flags for the other lines are set if the `euvs_ab_runctrlmd` is not equal to 1 (not science). The flags are set if `exs_sl_pwr_ena` is set (Flatfield power is on) and `exs_sl_sel` is either `EUVSA_PRI` or `EUVSA_RED` (6 or 2). The flags are set if any of these conditions are met.

PointingBad is set, LowTemperature is set, HighTemperature is set, FlatfieldChirpWarning is set, DetChangeCountNotValid is set, `euvs_ab_tl_ivtm` (Integration Time Warning) is set, `euvs_ab_tl_ivmbe` is set (EDAC multibit error), `exs_tl_fov_offpt` (Offpoint Maneuver) is set, `exs_tl_fov_lunar` (lunar transit) is set, `exs_tl_fov_eclip` (eclipse) is set, `euvs_ab_integ_tm` is not equal to 3, DetChangeCountNotValid is set, FilterPositionNotSolar is set, DoorPositionNotOpen is set.

We have opted to not include the planetaryTransit flag in the DataNotGood flags, since the measurements are not affected significantly enough by the tiny partial blockage of Venus or Mercury.

The rest of the specific contributions to DataNotGood flags are in the next section.

### 5.5.2 Flags Set After Evaluation of Eq. 5.2

Recall the result of Eq. 5.2 is a current. Specifically, this is the real signal current above the dark subtracted background. This is where SignalLow flags for the lines can be set.

Any value of diodes from the mask for the 25.6 nm line that are less than or equal to zero will set the SignalLow256 flag. Processing into irradiance should continue. Set the SignalLow flags for the other lines.

The line-specific DataNotGood flags can then be determined.

## 5.6 EUVS-B Algorithm Steps

Same as EUVS-A algorithm, except there is no order sorting correction due to the window. Shorter wavelength light that could create higher orders cannot penetrate the filter. The next figure shows the EUVS-B diode layout. Note that some diodes are wider than others.

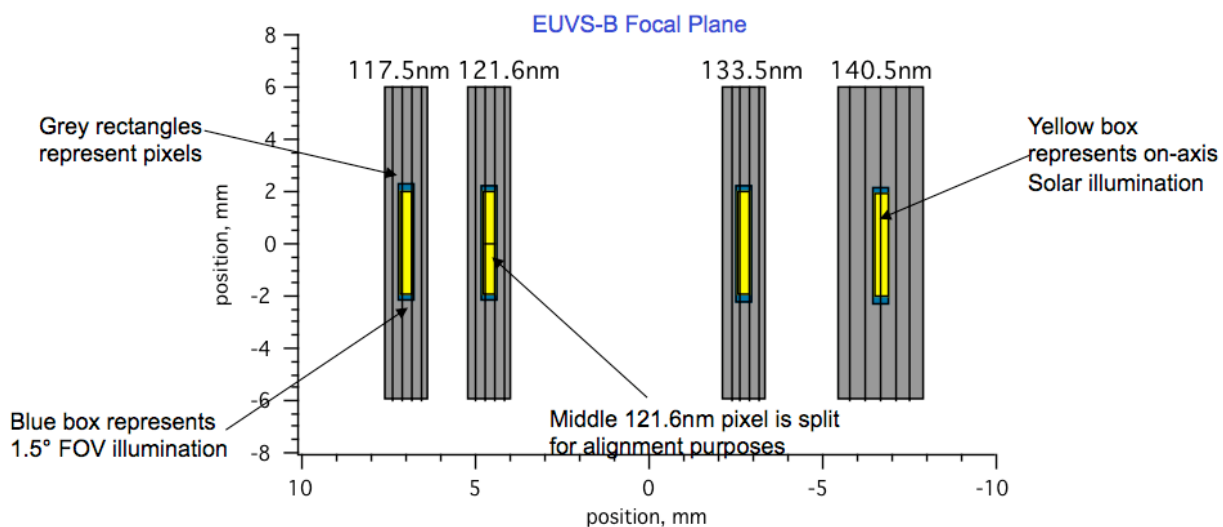


**Figure 16. EUVS-B diode layout**

Telemetry Order	Diode Description	ASIC	Band
1	B <sub>2</sub>	1	140.5
2	B <sub>3</sub>	1	140.5
3	B <sub>4</sub>	1	140.5
4	B <sub>5</sub>	1	140.5
5	B <sub>6</sub>	1	140.5
6	B <sub>7</sub>	1	140.5
7	B <sub>13</sub>	2	121.6
8	B <sub>14</sub>	2	121.6

9	B <sub>15</sub> – top of 121.6	2	121.6
10	B <sub>16</sub> – bottom of 121.6	2	121.6
11	B <sub>17</sub>	2	121.6
12	B <sub>18</sub>	2	121.6
13	B <sub>24</sub> – Dark diode on ASIC 3	3	NA
14	B <sub>23</sub>	3	117.5
15	B <sub>22</sub>	3	117.5
16	B <sub>21</sub>	3	117.5
17	B <sub>20</sub>	3	117.5
18	B <sub>19</sub>	3	117.5
19	B <sub>12</sub>	4	133.6
20	B <sub>11</sub>	4	133.6
21	B <sub>10</sub>	4	133.6
22	B <sub>9</sub>	4	133.6
23	B <sub>8</sub>	4	133.6
24	B <sub>1</sub> – Dark diode on ASIC 4	4	NA

**Table 13 EUVS-B diode telemetry order and ASIC relationship**

Note that for the H I (Lyman-alpha) line, the diodes are arranged as shown in Figure 16. The two center diodes (3 and 4) contain information that is useful for the relative cross-dispersion alignment verification. The irradiance should be added for these diodes, analogous to the 30.4 diodes for EUVS-A.

As in EUVS-A, the sampling of ASICs and pin direction is complicated. To make it worse, the EUVS-B detector was numbered backwards relative to wavelength order. This makes it harder since a 180 degree rotation is needed to view the pins in wavelength order. This puts pin 1 in the opposite corner. A picture would not necessarily clarify the relationship to wavelength. As with EUVS-A, the pin order is not followed rigorously since the split diode and one of the darks do not follow the convention.

### 5.6.1 Hydrogen Lyman-alpha and Geocorona

The near-earth environment contains a diffuse hydrogen gas cloud (geocorona) with varying density and extent. During periods (daily) when the earth is roughly between the sun and the spacecraft, this cloud absorbs photons that would otherwise be detected. This interferes only with the direct measurement of the H1 Lyman-alpha line, since the absorption is greatly diminished for other wavelengths. The GOES-15 EUV-E detector shows that this effect can be measurable for about 5 hours and decreases the irradiance by over 2%. The decrease is dependent on solar activity, and the line of sight through the geocorona, but the GOES-R EXIS instrumentation will show a very similar behavior to GOES-15 EUV-E. Conceptually, this effect is similar to an earth-grazing eclipse every day.

The peak of the effect is predicable (in concept), and a flag could be provided by the planning system to incorporate into the product to indicate when the measurement is suspect. When this flag is set, the Lyman-alpha line should not be used to create the model EUVS spectrum.

Without the benefit of detailed analysis of in-flight data over at least one year, we propose a more general rule. Define a time window 6 hours wide centered at local solar midnight and set the geocorona flag during that window. This is a reasonable estimate to prevent corrupted output from the proxy model for the EUVS product. The 6-hour period was chosen based on analysis of GOES-15 EUV-E data from November 2-10, 2010, so the window may be longer or shorter based on solar activity (11-year period) and earth's orbit (annual period).

## 5.7 EUVS-B Output

The EUVS-B processing creates the fully calibrated irradiance for the 4 measured solar emission lines. The H I line is the primary proxy used to create the model spectrum. The flags for EUVS-B are listed in Table 14. These are largely the same as the flags identified in EUVS-A (see Table 11), with a few exceptions. The line-related flags are provided for 4 lines (instead of 3). There is an extra geocorona flag, which is 0 when no absorption is occurring, and 1 when it is suspect. For all flags in the table, the value of 0 is good.

Flag Name	Bit Value (1/0)	Description / Explanation
PointingBad	Bad/Good	The pointing of EXIS is both known and within the valid calibration range of EUVS-B.
PointingDegraded	Bad/Good	Pointing is outside the calibrated range ( $\pm 0.4$ deg) and FOV correction is truncated to the map edge.
PointingWarning	Bad/Good	Pointing angles are in the calibrated FOV range, but spacecraft is not meeting pointing requirements ( $\pm 7$ arcmin).
Checksum	Mismatch/Match	The checksum matches
SignalLow1175 (per integrated line)	Low/Not low	All diode signals in the good part of the mask are distinguishable from zero.
SignalHigh1175 (per integrated line)	High/Not high	All diode signals in the good part of the mask are below the saturation value (989,000 at 1 sec).
SignalLow1216 (per integrated line)	Low/Not low	All diode signals in the good part of the mask are distinguishable from zero.
SignalHigh1216 (per integrated line)	High/Not high	All diode signals in the good part of the mask are below the saturation value.
SignalLow1335 (per integrated line)	Low/Not low	All diode signals in the good part of the mask are distinguishable from zero.
SignalHigh1335 (per integrated line)	High/Not high	All diode signals in the good part of the mask are below the saturation value.
SignalLow1405 (per integrated line)	Low/Not low	All diode signals in the good part of the mask are distinguishable from zero.
SignalHigh1405 (per integrated line)	High/Not high	All diode signals in the good part of the mask are below the saturation value.
LowTemperature	Low/Good	The EUVS-B temperature is either low or within the valid range to make measurements.
HighTemperature	High/Good	The EUVS-B temperature is either high or within the valid range to make measurements.



FlatfieldChirpWarning	Bad/Good	This integration may contain a flatfield flash (flatfield chirp from InvalidFlags)
FilterPositionNotSolar	Bad/Good	The filter wheel is not moving, the filter wheel position is known, and the filter position is one that allows sun light to the EUVS-B detector.
DoorPositionNotOpen	Bad/Good	The door is not moving, the door position is known, and the door absolute step number is 31.
DataNotGood1175	Bad/Good	The irradiance is good. Here good means: pointing is good, checksum is good, signal is not low, signal is not high, temperature is not low, temperature is not high, flatfield is off, integration time warning is good, flatfield chirp warning is good, no multibit EDAC errors, no offpoint maneuver in progress, no lunar transit, no eclipse, intTime=3, and detChangeCount is greater than 20 and FilterPositionNotSolar is good for EUVS-B, DoorPositionNotOpen is good and irradiance is greater than the solar minimum reference provided in CDRL 79.
DataNotGood1216	Bad/Good	The irradiance is good (as above).
DataNotGood1335	Bad/Good	The irradiance is good.
DataNotGood1405	Bad/Good	The irradiance is good.
Geocorona	Present/Not Present	The geocorona flag indicates that the Lyman-alpha emission may have absorption, and the proxy should not be used in creation of the spectrum.

**Table 14 EUVS-B measurement flags**

There are many open positions for EUVS-B. These are Static Parameters and will be reported in CDRL 79. Refer to the EUVS-A section for details related to the door position.

Variable	Units	Data type	Description
E1175	W/m <sup>2</sup>	32-bit float	Irradiance from EUVS-B 117.5 nm line
E1216	W/m <sup>2</sup>	32-bit float	Irradiance from EUVS-B 121.6 nm line
E1335	W/m <sup>2</sup>	32-bit float	Irradiance from EUVS-B 133.5 nm line
E1405	W/m <sup>2</sup>	32-bit float	Irradiance from EUVS-B 140.5 nm line
a	degrees	32-bit float	Averaged dispersion direction pointing angle from SPS
b	degrees	32-bit float	Averaged cross-dispersion direction pointing angle from SPS
a_GT	degrees	32-bit float	Averaged SUVI Guide Telescope angle along SPS alpha direction (yaw)
b_GT	degrees	32-bit float	Averaged SUVI Guide Telescope angle along SPS beta direction (pitch)

AuFactor	AU	32-bit float	The 1-AU correction factor that could be multiplied by the irradiances to remove the earth orbit effect.
QualityFlags	NA	32-bit int	All flags defined in Table 14
days_since_jan1_2000	Days	16-bit int	Days since the epoch at the end of the integration
centerTime	Seconds	32-bit float	Seconds of the UT day at the center of the exposure using the secondary header <code>exs_peb_tm_ms</code> (microseconds are unnecessary) and <code>intTime</code> shifted to the center. This corresponds to the CENTER time defined in Eq. 4.20.
scPowerSide	NA	bit	0=B, 1=A ( <code>exs_peb_pb_stat</code> )
exisMode	NA	4-bits	0=failsafe, 1=normal, 2=diag, 3=safe ( <code>exs_peb_exs_md</code> )
exisFlightModel	NA	8-bits	1=FM1, 2=FM2, 3=FM3, 4=FM4 ( <code>exs_peb_mdl_num</code> )
exisConfigId	NA	16-bits	Configuration ID ( <code>exs_peb_exs_cfg</code> )
checksum	NA	8-bits	Checksum ( <code>exs_peb_pkt_cksm</code> )
euvSBdiodeCounts	DN	24 x 32-bit int	24 raw diodes measurements ( <code>euv_b_cnt_ch0-23</code> )
euvSBIdacOffsets	NA	24 x 16-bit	IDAC offset registers ( <code>euv_b_idac_ch0-23</code> )
euvSABCAL	NA	2-bits	Internal gain calibration circuit indicator, 1=science, 2=cal ( <code>euv_ab_runcntrlmd</code> )
euvSBPower	NA	bit	0=off, 1=on ( <code>euv_b_pwr</code> )
euvSAPower	NA	bit	0=off, 1=on ( <code>euv_a_pwr</code> )
intTime	NA	8-bits	Integration time in quarter second increments, 0=0.25 sec, 1=0.5 sec, 2=0.75 sec, 3=1.0 sec, ... ( <code>euv_ab_integ_tm</code> )
LED_select	NA	4-bits	LED selection, 0=EUVSC-Backup, 1=EUVSB-Backup, 2=EUVSA-Backup, 3=XRS-Backup, 4=EUVSC-Pri, 5=EUVSB-Pri, 6=EUVSA-Pri, 7=XRS-Pri ( <code>exs_sl_sel</code> )
LED_power	NA	1-bit	LED power, 0=off, 1=on ( <code>exs_sl_pwr_ena</code> )
LED_level	NA	16-bits	LED level setting, 12 bits used, ( <code>exs_sl_lvl</code> )
IfBoardTemp	DN	16-bits	Interface board temperature ( <code>exs_ifb_tmp_dn</code> )
ProcFpgaTemp	DN	16-bits	Microprocessor board FPGA temperature ( <code>exs_mb_fp_tmp_dn</code> )
PowerSupplyTemp	DN	16-bits	Power board temperature ( <code>exs_pb_tmp_dn</code> )
CaseHeaterTemp	DN	16-bits	Case heater temperature ( <code>exs_cs_oh_tmp_dn</code> )
euvSATemp	Deg C	32-bits	EUVS-A detector board temperature (converted <code>euv_a_dt_tmp_dn</code> )
euvSBTemp	Deg C	32-bits	EUVS-B detector board temperature (converted <code>euv_b_dt_tmp_dn</code> )
slitTemp	DN	16-bits	Entrance slit temperature ( <code>euv_slit_tmp_dn</code> )
InvalidFlags	NA	8-bits	Invalid flags, 0=good, 1=integration time warning, 2=flatfield chirp, 4=EDAC single bit error (corrected), 8=EDAC multiple bit errors (not corrected), ( <code>euv_ab_inval</code> ) Either 0 or 4 is good.

DetChangeCount	NA	16-bits	Detector change counter, counts from 0 to 65535 whenever cal circuit is enabled or disabled, or EUVS-B is powered on, sticks at 65535 (euv_ab_det_chg)
LEDChangeCount	NA	16-bits	Counts quarter seconds elapsed since LED was powered on or off, sticks at 65535 (exs_sl_chg)
asicSciVDAC	NA	16-bits	Science voltage DAC last input (euv_ab_sci_v_lst)
asicCalVmin	NA	16-bits	Min voltage for the cal ramp (euv_ab_cal_v_min)
asicCalVmax	NA	16-bits	Max voltage for the cal ramp (euv_ab_cal_v_max)
asicCalVstepUp	NA	8-bits	Voltage step size during ramp up (euv_ab_cal_v_sup)
asicCalTstepUp	NA	8-bits	Time step size during ramp up (10 microsec), (euv_ab_cal_t_sup)
asicCalVstepDown	NA	8-bits	Voltage step size during ramp down (euv_ab_cal_v_sdn)
asicCalTstepDown	NA	8-bits	Time step size during ramp down (10 microsec), (euv_ab_cal_t_sdn)
DoorPositionKnown	NA	1-bit	The EUVS door position is known by flight software (resets after power up) 0=unknown, 1=known (euv_dr_pos_stat)
FilterWheelMoving	NA	1-bit	The EUVS filter wheel mechanism is moving, 0=not moving, 1=moving (euv_fw_mv_stat)
FilterWheelPositionKnown	NA	1-bit	The EUVS filter wheel mechanism position is known by flight software, 0=unknown, 1=known (euv_fw_pos_stat)
DoorPositionStepNumber	NA	8-bits	The EUVS door absolute position step number from 0-107. 0=closed, 31=open. (euv_dr_step_num)
FilterWheelStepNumber	NA	8-bits	The EUVS filter wheel mechanism absolute step number 0-107. (euv_fw_step_num)
EuvsMode	NA	2-bits	EUVS detector mode with same states as XRS, also has no effect on data collection (euvs_md)
fovFlagsKnown	NA	1-bit	FOV flags are known by flight software, 0=known, 1=unknown (exs_tl_fov_stat)
Eclipse	NA	1-bit	Earth eclipse imminent or in progress, set by ground command, 0=no eclipse, 1=eclipse (exs_tl_fov_eclip)
LunarTransit	NA	1-bit	Lunar transit imminent or in progress, set by ground command, 0=no transit, 1=transit (exs_tl_fov_lunar)
PlanetTransit	NA	1-bit	Planetary transit imminent or in progress, set by ground command, 0=no transit, 1=transit (exs_tl_fov_plnt)
OffPoint	NA	1-bit	Off-pointing calibration maneuver is imminent or in progress, set by ground command, 0=no maneuver (or sun pointed), 1=off-point maneuver (exs_tl_fov_offpt)

**Table 15 EUVS-B data product variables**

## 5.8 EUVS-C Mathematical Description and Algorithm Design

This section describes the complete set of measurement equations for EUVS-C.

### 5.8.1 Data Encoding

The EUVS-C data that is decomposed from the telemetry packets may be encoded. If it is encoded, it needs to be converted to detector raw signed signals prior to processing. We implement this functionality in the `extractPacket` function for EUVS-C. Three options exist that control the hardware encoding scheme, and the value of `euv_c_pixel_md` (EUVS-C pixel mode) dictates which is being used.

#### 5.8.1.1 EUVS-C Pixel Mode 0 and 1, Data Minus Reference

A value of 0 or 1 indicates the normal operation of the detector where the data represents the detector value minus a reference value determined from the integrator circuit at the time just prior to the readout of each pixel. The value of 0 and 1 are identical. The FPGA treats these register values the same.

For each pixel value two samples are taken. The first sample is after the integrator pre-amplifier is reset (prior to data collection), and the second sample is taken at the end of the pixel read process. This differencing is performed in hardware and is needed to compensate for the noise in the output value of the pre-amplifier circuit after each reset. When pixel mode is 0 or 1, the difference is stored.

This difference value corresponds to the amount of charge that was contained within the photodiode plus an offset. The offset is caused by the zero-charge read value being a non-zero number, but an equivalent signal is added into the signal path to compensate for this. Due to detector differences, and thermal differences in the circuit behavior, negative numbers are possible in the final result. This will probably happen for some of the masked pixels. Negative numbers are encoded in telemetry by wrapping the low values to the highest in the 16-bit value range, so a value of -1 is 65,535, -2 is 65,534, etc.

To convert the telemetry data into signed signal values, follow these steps.

- 1) convert the 16-bit values to 32-bit signed integers
- 2) add a temporary offset value (refer to CDRL 79 for values for each detector)
- 3) modular divide by  $2^{16}$
- 4) subtract the same temporary offset value.

The result is a signed signal value,  $S$ , that is related to the measured charge. The temporary value will be approximately 2048.

### 5.8.1.2 EUVS-C Pixel Mode 2, Data Only

When `euv_c_pixel_md` is set to 2, the packet contains just the detector values without the reference value subtracted. This is an undesirable mode since it has higher noise contributions. However, this data is simpler to process since the signal in telemetry becomes  $S$  directly.

### 5.8.1.3 EUVS-C Pixel Mode 3, Reference Only

The final `euv_c_pixel_md` is 3. When this is received, the packet contains only the reference values, and has no science content. This should be considered a diagnostic mode could be used for anomaly investigation or possibly for tracking drifts in the reference value.

## 5.8.2 Algorithm Concept

The detector signed signals,  $S_i$ , at time  $t$  are first compared to the one previous integration at time  $t-dt$ . Where  $S_i(t)$  is greater than  $(S_i(t-1) + P_{ThresholdLimit})$ , the pixel  $i$  is known to be contaminated with particles. The value of  $P_{ThresholdLimit}$  is initially set to 1000 DN (LUT variable name is `filter_threshold`), but a final value will be provided in CDRL 79, and needs to be updated during PLT. We use this knowledge to create a particle-filtered detector signed signal  $S'(t)$ . This requires keeping track of the present  $S(t)$  and previous integration  $S(t-dt)$ . At startup, or when switching EUVS-C channels, there will be no previous integration, so the particle filtering step should be skipped. This will not remove successive particle hits from the second integration, which is expected only during large particle storms. An alternative particle-filtering scheme could be devised on orbit after real data is available for analysis. Differencing the packet sequence numbers (modulo  $2^{14}-1$ ) can be used to ensure filtering is performed only on consecutive integrations. All EUVS-C packets for the same integration possess the same CCSDS packet source sequence counter (e.g. `exs_pc0_seq_ct`).

**Eq. 5.8**

$$\begin{aligned} &\text{If } S_i(t) < [S_i(t-1) + P_{ThresholdLimit}] \\ &\quad \text{Then } S'_i(t) = S_i(t) \\ &\quad \text{Else } S'_i(t) = S_i(t-1) \end{aligned}$$

The particle filtering only removes large particles. The particle filtered signed signals are corrected for background ( $D_{BG}$ ) to produce a quantity  $D$ , representing signal above background. This is then corrected for flatfield non-uniformities, linearity, and scattered light which results in a corrected, floating-point quantity,  $D'$ , in units of DN (data numbers). The filtering described is only valid for normal sun pointing, and must be disabled for non-routine observing times such as eclipse entry/exit, lunar transit, or any maneuver that changes pointing. When pointing changes the spectrum moves on the detector. The assumption of similarity between consecutive measurements is violated during any motion or blockage of sunlight. The most obvious difference from the other instruments is that there is no gain correction. The primary purpose of EUVS-C is to provide the Mg II core to wing ratio, so such absolute corrections

(including integration time) that affect the entire measurement would divide out of the ratio. This simplifies the measurement equations.

$$\text{Eq. 5.9} \quad D_i = S'_i - D_{BG,i}$$

$$\text{Eq. 5.10} \quad D_{BG,i} = (\langle D_{Therm} \rangle_{Mast} \cdot d_{Flatfield,i}) + D_{Offset,i}$$

$$\text{Eq. 5.11} \quad \langle D_{Therm} \rangle_{Mask} = \frac{\sum_i (S'_i - D_{Offset,i}) \cdot W_{Mask,i}}{\sum_i W_{Mask,i}}$$

$$\text{Eq. 5.12} \quad D'_i = (D_i \cdot f_{FF,i} \cdot f_{Lin,i}) - D_{SL,i}$$

$$\text{Eq. 5.13} \quad D''_{RedWing} = \frac{\sum_i D'_i \cdot W_{Red,i}}{\sum_i W_{Red,i}}$$

$$D''_{BlueWing} = \frac{\sum_i D'_i \cdot W_{Blue,i}}{\sum_i W_{Blue,i}}$$

The red and blue wings are determined using a weighted average. The general shape of the weighting functions is trapezoidal which is optimized to reduce the effects of possible wavelength shifting. The initial weights are provided in CDRL 79 (LUTs). These must be adjusted when the instrument is in the post-launch-test phase.

$$\text{Eq. 5.14} \quad D''_h = \frac{\sum_i D'_i \cdot W_{h,i}}{\sum_i W_{h,i}}$$

$$D''_k = \frac{\sum_i D'_i \cdot W_{k,i}}{\sum_i W_{k,i}}$$

The Mg II h and k lines are determined using the weighted averages given in Eq. 5.14.

$$\text{Eq. 5.15} \quad \text{Reserved}$$

$$\text{Eq. 5.16} \quad R_{MgII,EXIS} = \frac{D''_h + D''_k}{D''_{BlueWing} + D''_{RedWing}}$$

$$\text{Eq. 5.17} \quad R_{MgII,NOAA} = (M_{NOAA} \cdot R_{MgII,EXIS}) + B_{NOAA}$$

The variable descriptions are summarized in Table 16.

Variable	Description	Units
i	Pixel number (0-511) in the detector array	NA
S	Detector signed signal (decoded)	DN/integration
S'	Particle filtered detector signed signal (decoded)	DN/integration
f <sub>FF</sub>	Flatfield correction normalized to preflight values to correct pixel-to-pixel changes	Dimensionless
f <sub>Lin</sub>	Linearity correction	Dimensionless
D <sub>SL</sub>	Scattered light correction	DN/integration
D <sub>BG</sub>	Total background correction	DN/integration
D <sub>Rad</sub>	Radiation background correction	DN/integration
D <sub>offset</sub>	Electronics dark contribution, determined using multiple integration times	DN/integration
D <sub>Therm</sub>	Pixel dark contribution for temperature determined using masked pixels	DN/integration
d <sub>Flatfield</sub>	The relative dark shape over the detector determined in preflight calibration	Dimensionless
D'	Pixel signal above dark. This is proportional to irradiance, but needs a gain, and responsivity applied to get proper units.	DN/integration
W	Weights for averaging the wings or masked pixels	Dimensionless
D''	Red wing, blue wing, Mg II h line, or Mg II k line measurement	DN/integration
R <sub>MgII,EXIS</sub>	EXIS Mg II core to wing ratio	Dimensionless
M <sub>MgII,NOAA</sub>	Slope of correlation	Dimensionless
B <sub>MgII,NOAA</sub>	Offset of correlation	Dimensionless
R <sub>MgII,NOAA</sub>	NOAA Mg II core to wing ratio	Dimensionless

**Table 16 EUVS-C Measurement Equation Variables**

It is important to note that there are two physically distinct EUVS-C detectors on EXIS, C1 and C2, but only one is powered at a time. Do not confuse the redundant electrical power with the dual detectors. Either side of the electronics bus may provide power to either detector. In the telemetry packet definition, there is a byte value that indicates the channel 1 or 2 (euv\_c\_pwr\_sel), and a separate byte value that indicates which side is providing electrical power (evs\_pc0\_pb\_stat). This is an important distinction, since all corrections/calibrations are distinct unless otherwise noted. To be explicit, two parallel sets of lookup tables and corrections are necessary. All functions that depend on physical properties of the detector or electronics should have a parameter to indicate which EUVS-C is being used.

### 5.8.3 Dependency Analysis

The terms in the measurement equations for EUVS-C are inter-related. The dependency is shown graphically in Figure 17.

## EUVS-C Dependency Graph

Dependent Terms



Independent terms



Dependency hierarchy is a planar directed acyclic graph

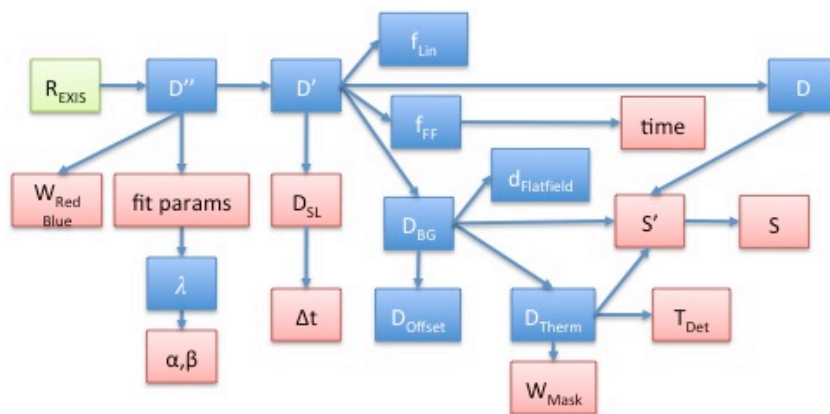


**Figure 17 EUVS-C dependency graph**

The dependency graph is useful for identifying the connectedness of the terms in the measurement equations. The acyclic property of the graph ensures that no terms are dependent in a way that would cause an infinite loop.

Reversing the arrows of Figure 17 creates a rooted-tree as shown in Figure 18. This elucidates the acyclic property and shows that all paths will eventually terminate with the Mg II ratio.

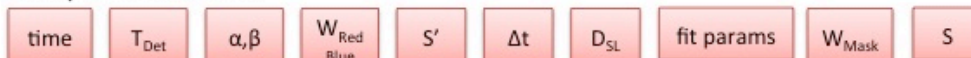


# EUVS-C Rooted Tree

Dependent Terms



Independent terms



Rooted-tree shows all paths terminate in the Mg II ratio

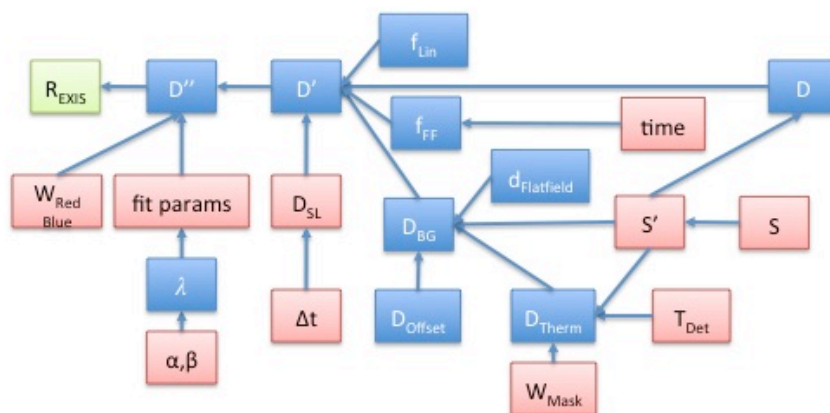


Figure 18 EUVS-C rooted dependency tree

## 5.9 EUVS-C Algorithm Steps

A high level graphical representation of the processing flow for EUVS-C is provided in Figure 19.

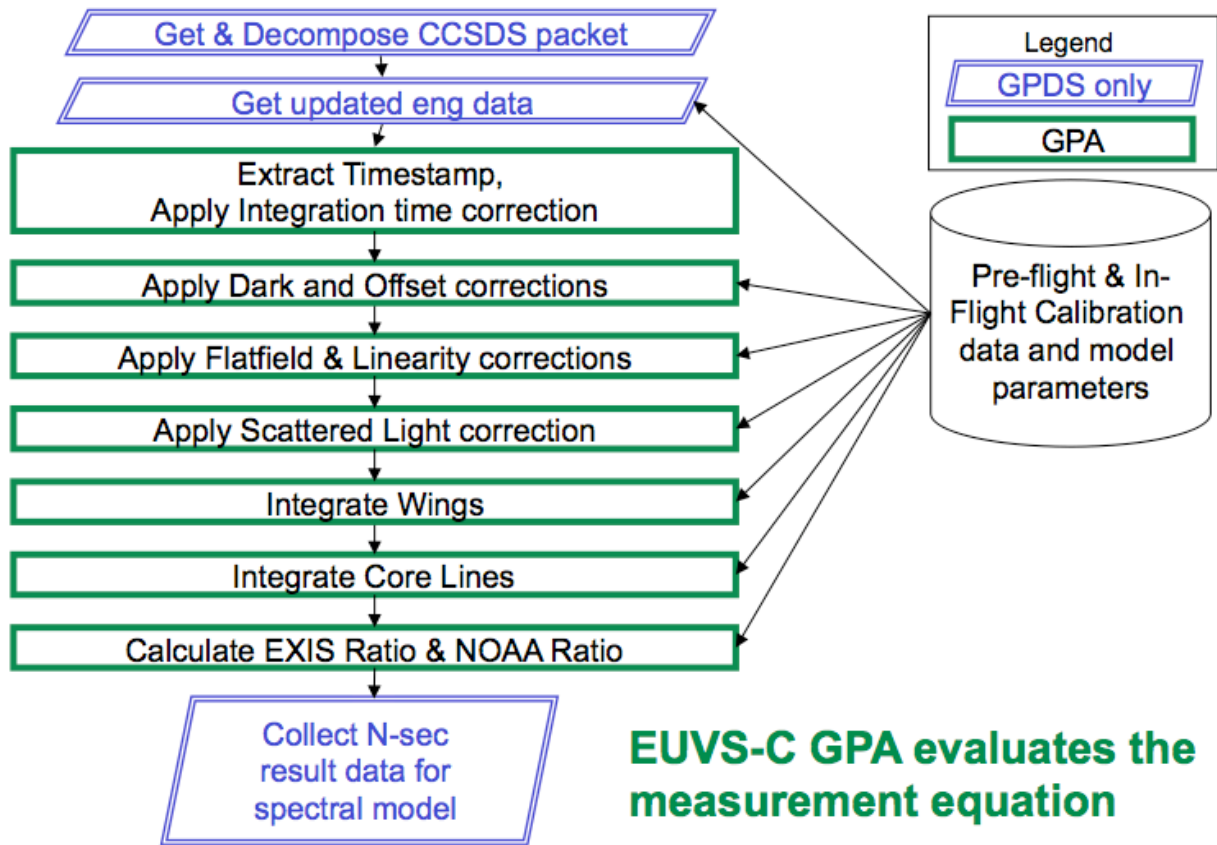


Figure 19 EUVS-C algorithm flow

This section describes the steps performed in the EUVS-C Ground Processing Algorithm. Each subsection is ordered according to the evaluation in the measurement equations.

An overview of the process is shown in the following pseudocode.

```

#Main thread
    evvs_c.extractPacket(packet)
    lookupOneAu(time)

#EUVS-C thread (process_data())
    evvs_c.loadConfigurationFiles()
    evvs_c.applyBackgroundCorrections()
    evvs_c.applyFlatfieldCorrections()
    evvs_c.applyLinearityCorrections()
    evvs_c.applyScatteredLightCorrections()
    evvs_c.lookupWavelength()
    evvs_c.integrateCore()
    evvs_c.integrateWings()
    evvs_c.calculateCoreWingRatio()
    evvs_c.createOutput()
    evvs_c.printProcessedData()
    
```

The following diagram shows the functions involved in EUVS-C processing to create the Mg II core to wing ratio.

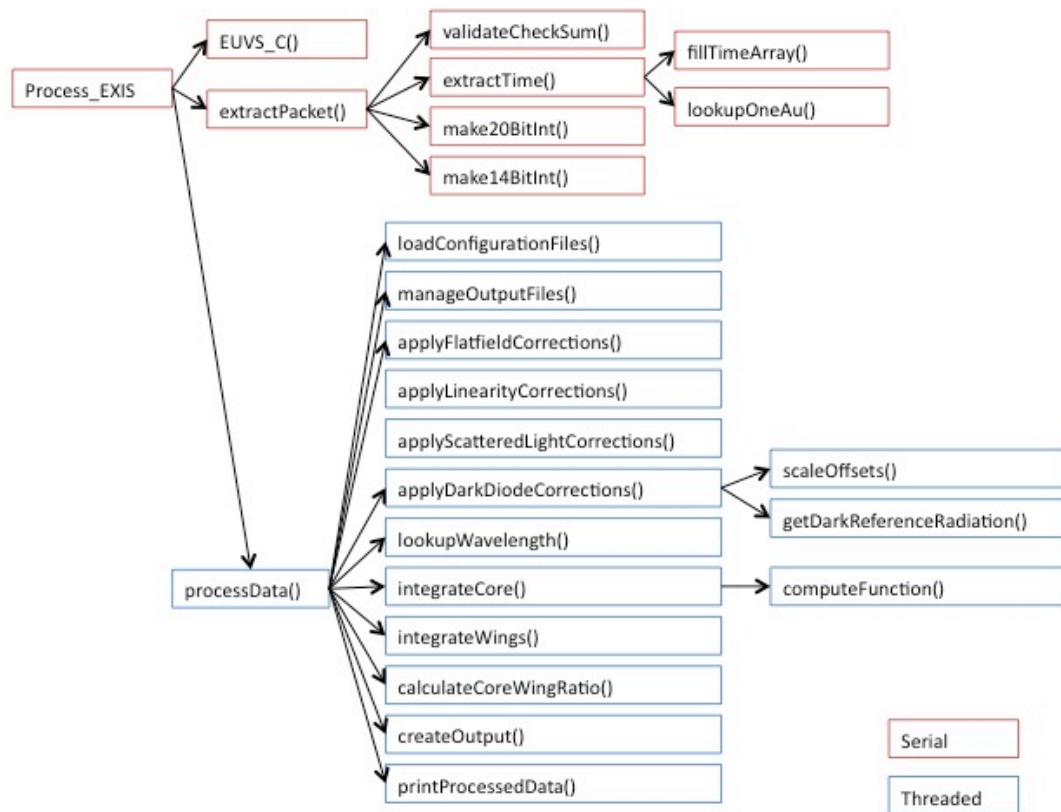


Figure 20. EUVS-C functions

### 5.9.1 Packet Decomposition

The format of the packets is described in CDRL 43. The EUVS-C data spans 8 packets with each packet containing 64 consecutive pixel values. It is similar to having 8 different detectors. Each of these packet types is a separate APID. Integrations from the same instant have the same packet sequence number, and the same time stamp in the secondary header. Each packet will have the same values for pixel mode, ADC mode, flush count, run control, power, integration time, dead count, LED select, LED power, LED level, interface board temperature, FPGA temperature, power board temperature, case op heater temperature, EUVS-C operational heater temperature, C1 temperature, C2 temperature, EUVS-C ADC board temperature, invalid flags, detector change counter, LED change counter, door status, filter status, door position, filter position, XRS mode, EUVS mode, and FOV flags. Since EUVS-C is a commercially available detector it does not have an ASIC, so there are no ASIC offsets to downlink. Pixel values must be decoded as described in section 5.8.1.

A single integration is created by joining the data from the 8 packets together into an array of 512 pixels. The remainder of the packet contents after the diode data is repeated in all 8 packets (non-unique).

Use the field entitled `euv_c_det_chg` to disregard all packets whose value is less than 5. After power up, the detector and associated electronics need to stabilize, so this data should be disregarded. Note that flight software resets `euv_c_det_chg` to indicate that something significant on the detector has changed that affects data quality for a short period.

### 5.9.2 Signal, S

Unlike all of the other channels, EUVS-C pixels are 16-bits (not 20-bits). Assembling the packet data into the EUVS-C measurement spectrum simplifies the masking process. APID 0x3B0 contains pixel numbers 0-63, and 0x3B1 contains pixel numbers 64-127, etc.

Under most circumstances, the particle filtered value  $S'$  is the same as  $S$ . To determine  $S'$ , the values in  $S$  are compared against the previous integration. For diodes where the present integration is greater than the previous integration by some threshold (provided in CDRL 79), the previous values are used to replace the spuriously high values in the present integration. This should only be performed when the two integrations are the same integration time, filter position, and channel.

### 5.9.3 Integration time, Dt

The integration time is not directly used in the algorithm, provided the integration time is not changed. The integration time does affect the scattered light contribution, but after PLT it may be not need to change during normal solar observations. The EUVS-C detector electronics is much more flexible in changing parameters associated with exposure.

One significant difference with EUVS-C and all other detectors is the integration time. The integration time is calculated using 3 different telemetry points contained in each of the EUVS-C packets. These telemetry points are: integration count (IC), dead count (DC), and flush count (FC). Using these values, the integration time is calculated according to Eq. 5.18.

$$\text{Eq. 5.18} \quad \Delta t = \frac{[250 \cdot (IC + 1)] - [25 \cdot (DC + 1)] - [20.48 \cdot (FC - 1)]}{1000}$$

There is one exception. If FC is 3 and DC is 7 then the integration time has an extra quarter second. Normally the dead count register is zero. It represents the number of 25 ms intervals between the read and flush, so this allows for very short exposures. This is described in Eq. 5.19.

$$\text{Eq. 5.19} \quad \Delta t = 0.25 + \frac{[250 \cdot (IC + 1)] - [25 \cdot (DC + 1)] - [20.48 \cdot (FC - 1)]}{1000}$$

This sophisticated behavior is a result of the engineering capability to integrate faster than telemetry can be downlinked (4 Hz). Recall that the default integration rate is about 10 seconds. It is important to realize that the IC contribution is about 10 times larger than the DC or FC contribution, and is clearly the most important part in the calculation of the integration time when IC is greater than 1. A set of DC and FC will be chosen during ground calibration and testing. These are not expected to be changed during routine observing, but could be used during diagnostic testing.

The timestamp reported in the packet secondary header corresponds to the end of the integration interval, and we wish to report the center time of the interval. Similar to the method used in Eq. 4.20, the center time is calculable from the packet information.

**Eq. 5.20**

$$Pixel_{hkCenter} = \text{mean}[\text{median}(h_{maskPixels}) + \text{median}(k_{maskPixels})]$$

$$t_{Center} = t_{Packet} - \frac{\Delta t}{2} + (Pixel_{hkcenter} \cdot 0.00004)$$

Since this is not an ASIC, the hardware behavior differs from all other EXIS detectors. First the readout starts at a quarter second tick, then the dead count occurs (default is none), then the flushes, and then the next integration begins. The readout takes 20.48 ms with each pixel taking 40 microseconds to be read. The cumulative time to read all 512 pixels is then 20,480 microseconds. The flushes are reads that are discarded and each flush takes the same time as a read. The “end” of the integration is spread out for each pixel with 20.48 ms elapsing between the start of reading the first pixel and the end of reading the last pixel. The flush and read take the same time so each pixel is exposed for the exact same duration, just with a shift in time from pixel to pixel. We will estimate the center time using the end of the center pixel between the h and k line mask centers. The line mask centers are the median of the line mask indices (somewhere around pixel index 278 on GOES-16 EUVS-C C2 channel). The Mg II line centers are separated by about 35 pixels, so they are about +/-350 microseconds from their center. The center time of the integration becomes a fixed offset. For the case where the center is at pixel 278, the center moves by 278\*40 microseconds = 11.120 ms. The Mg II line center time is shifted by that amount.

#### 5.9.4 Dark Background, $D_{BG}$

The dark term is a straightforward calculation involving the masked pixels on the short wavelength end, an effective dark flatfield, and an electronic offset.

##### 5.9.4.1 Electronic Offset, $D_{Offset}$

The electronic offset is set to a default value. Unlike the ASICs, this value cannot be changed. This is a set of static parameters (one value per diode) provided in CDRL 79.

#### 5.9.4.2 Thermal Dark, $D_{\text{Therm}}$

The thermal dark will be determined from in situ measurements of the diodes under the mechanical mask. This scalar term is the mean of the diodes under the mask after particle filtering. A mask identifying which diodes to use will be delivered with CDRL 79.

The thermal dark term is multiplied by an effective dark flatfield,  $d_{\text{Flatfield}}$ , to allow for long-term changes that could differ over the detector. Currently, the dark flatfield is 1.0 for every diode. The dark flatfield is a semi-static parameter that must be revisited during PLT.

#### 5.9.5 Flatfield

The flatfield correction is a relative pixel-to-pixel adjustment to compensate for small differences in the pixels in response to the on-board LEDs. Periodically in normal operations the LEDs will be used to illuminate the pixel array. This provides a direct measure of the relative changes. An analysis procedure (see 9.1.1) will be used to generate a recent (6 month) trend in the flatfield changes to allow for adjustments. The flatfield correction evaluates the curve fits for the current date.

#### 5.9.6 Linearity

The purpose of the linearity function is to account for the non-linear response of the detector. This value has a lower limit of 1.0 and can be higher. Most of the solar spectrum in this wavelength range does not vary by large amounts compared to the other channels, and the filter used in the optical design will keep the signals largely out of the non-linear regime. For higher count-rates, the detector response falls off. This non-linear behavior will be measured in preflight via ground calibration.

Linearity is provided in a lookup table, since there are a maximum of 65,535 possible integer values, which takes about 130 kB of memory. In the table provided in CDRL 79, the decoded values that are less than 0 should use the value that corresponds to 0.

#### 5.9.7 Scattered Light

The scattered light contribution includes stray light and will be a constant at one integration rate. The value will be reported in CDRL 79. The result may be different for all diodes, and is likely different for each channel. This must be tuned during PLT after the final integration rate is determined.

#### 5.9.8 Lookup Wavelength

The wavelength scale is measured in preflight calibration for each EUVS-C detector. A preliminary lookup table will be provided in CDRL 79. Based on ray-trace analysis, there is little change expected in the wavelength scale as a function of pointing angle. Errors in the wavelength scale could cause problems when integrating over the features, so a final wavelength table needs to be determined during PLT. The solar spectrum itself provides the wavelength scale to eliminate these errors. Some analysis is needed

during PLT to determine the final wavelength scale on-orbit for center pointing. Once determined, this will become a static parameter table. The wavelength scale is useful for physical interpretation.

### 5.9.9 Integrate Features

The core line emissions are treated the same the wings. These are described in the next two subsections.

#### 5.9.9.1 Lines, h, k

The h and k lines are separately summed according to equation 5.14 using the line masks in the LUT.

The initial guesses at the initial fit parameters are shown in Table 17 for reference but are not used in the GPA.

Parameter	Line k, 279.6352 nm	Line h, 280.3530 nm
p <sub>0</sub>	9878.	8255.
p <sub>1</sub>	279.6352	280.3530
p <sub>2</sub>	0.047	0.048
p <sub>3</sub>	0.0	0.0

**Table 17 Mg II h and k fit parameter initial guesses**

These values will be adjusted after preflight calibration, and should be tuned in-flight to reduce the number of iterations to obtain convergence. Convergence criteria could be estimated using data from a ray trace model prior during ground calibration, and may need to be adjusted during PLT to ensure good fits results with real solar data. If either of the fits fails to converge a missing value shall be returned, and the Mg II proxy good flags should be set to invalid to prevent it from being used in the proxy model.

Experimentation shows that fit quality improves with using values of zero for the diodes outside of the line masks provided in CDRL 79.

#### 5.9.9.2 Wings, red and blue

The red and blue wings are defined by the weights. Each wing will have a separate trapezoidal weight function that has a maximum value of 1.0 and a minimum value of 0.0. The weight will be broad enough that any shifting of the wavelength scale with pointing angle will be negligible. The trapezoid pixel numbers are defined in Table 18. In this representation, the four pixel locations define the corners of the trapezoid (where the slope changes). Pixel weights prior to the pixel number listed in the first row are all zero. Between the pixels in the first two rows, the values are linearly increasing from 0.0 to 1.0. Between the second and third row, all pixel weights are 1.0. The weights decrease from 1.0 back to 0.0 between the third and fourth rows, and pixel weights beyond the fourth row are all zero. The integrated wing signals should be trended over long time periods (years), since the solar signal in the wings is not supposed to change very much over a solar cycle.

Point on trapezoid	Blue wing, ~276-278 nm	Red wing, ~282-284 nm
Low 0.0 edge	65	330
Low 1.0 edge	105	370
High 1.0 edge	140	440
High 0.0 edge	180	480

**Table 18 Wing weights around the Mg II lines**

These final numbers for the wing weights are updated in CDRL 79, and different for each flight model, so they are updated during PLT.

### 5.9.10 Calculate Ratio

The EXIS Mg II core to wing ratio for EXIS involves summing the h and k line measurements and dividing by the sum of the wing measurements. The NOAA Mg II core to wing ratio uses the EXIS value and the two scaling parameters, M, and B. These parameters must be determined using in-flight solar measurements. A broad range of solar activity levels will help determine those parameters with greater accuracy. The parameters are updated during PLT and provided in CDRL 79.

### 5.10 EUVS-C Output

The EUVS-C will produce the Mg II core to wing ratio with status flags indicating validity. These are listed in Table 24. The threshold for distinguishing decoded 32-bit signed diode signals from zero shall be reported in CDRL 79. The threshold for distinguishing the decoded 32-bit signed diodes signals from saturation will also be reported in CDRL 79.

Flag Name	Bit Value (1/0)	Description / Explanation
PointingBad	Bad/Good	The pointing of EXIS is both known and within the valid calibration range of the EUVS-C. See section 5.11.1.1
Checksum	Mismatch/Match	The 8 checksums match (from the 8 packets)
SignalLowBlueWing	Low/Not low	All decoded signed diode signals under the blue wing mask are distinguishable from zero.
SignalHighBlueWing	High/Not high	All decoded signed diode signals in the blue wing mask are below the saturation value.
SignalLowRedWing	Low/Not low	All decoded signed diode signals under the red wing mask are distinguishable from zero.
SignalHighRedWing	High/Not high	All decoded signed diode signals in the red wing mask are below the saturation value.
SignalLowHLine	Low/Not low	All decoded signed diode signals in the Mg II h line region are distinguishable from zero.
SignalHighHLine	High/Not high	All decoded signed diode signals in the Mg II h line region are below the saturation value.
SignalLowKLine	Low/Not low	All decoded signed diode signals in the Mg II k line region are distinguishable from zero.
SignalHighKLine	High/Not high	All decoded signed diode signals in the Mg II k line region are below the saturation value.



LowTemperature	Low/Good	The lowest of EUVS-C1 and EUVS-C2 temperatures is either low or within the valid range to make measurements.
HighTemperature	High/Good	The highest of EUVS-C1 and EUVS-C2 temperatures is either high or within the valid range to make measurements.
FlatfieldChirpWarning	Bad/Good	This integration may contain a flatfield flash (flatfield chirp from InvalidFlags)
DetChangeCountNotValid	Bad/Good	The detector change count needs to be greater than or equal to 5 to be valid.
FilterPositionNotSolar	Bad/Good	The filter wheel is not moving, the filter wheel position is known, and the filter position is one that allows sun light to the EUVS-C detector.
DoorPositionNotOpen	Bad/Good	The door is not moving, the door position is known, and the door absolute step number is 31.
DataNotGoodHLine	Bad/Good	The area for the h lines is good. Here good means: pointing is good, checksum is good, EUVS-C is in data minus reference, Door position is open, filter positions is solar, signal is not low, signal is not high, lowest temperature is not low, highest temperature is not high, flatfield is off, integration time warning is good, flatfield chirp warning is good, no multibit EDAC errors, no offpoint maneuver in progress, no lunar transit, no eclipse, euvsCPixelMode is data minus reference, and detChangeCount is greater than or equal to 5.
DataNotGoodKLine	Bad/Good	Same as DataNotGoodHLine, except low and high signals are for the k line masked pixels.
DataNotGoodBlueWing	Bad/Good	Same as DataNotGoodHLine, except low and high signals are for the blue wing masked pixels.
DataNotGoodRedWing	Bad/Good	Same as DataNotGoodHLine, except low and high signals are for the red wing masked pixels.
RatioNotGoodMg	Bad/Good	DataNotGoodHLine and DataNotGoodKLine and DataNotGoodBlueWing and DataNotGoodRedWing are good, and FilterPositionNotSolar is good and DoorPositionNotOpen is good.

**Table 19 EUVS-C measurement flags**

The proxy is calculated based on the solar minimum reference value and will be provided in CDRL 79.

Variable	Units	Data type	Description
RatioMgEXIS	NA	32-bit float	Mg II core to wing ratio at EXIS instrument resolution.
RatioMgNOAA	NA	32-bit float	Mg II core to wing ratio from EXIS scaled to match historical values at lower resolution.
FitParametersH	Varied	4 x 32-bit floats	Gaussian fit parameters for the Mg II h line near 280.3530 nm.
FitParametersK	Varied	4 x 32-bit floats	Gaussian fit parameters for the Mg II k line near 279.6352 nm.
AreaH	DN / integration	32-bit float	Area under the Gaussian for the Mg II h line.
AreaK	DN / integration	32-bit float	Area under the Gaussian for the Mg II k line.
AreaBlueWing	DN / integration	32-bit float	Area under the blue wing of the photospheric continuum.
AreaRedWing	DN / integration	32-bit float	Area under the red wing of the photospheric continuum.
a	degrees	32-bit float	Averaged dispersion direction pointing angle from SPS
b	degrees	32-bit float	Averaged cross-dispersion direction pointing angle from SPS
a_GT	degrees	32-bit float	Averaged SUVI Guide Telescope angle along SPS alpha direction (yaw)
b_GT	degrees	32-bit float	Averaged SUVI Guide Telescope angle along SPS beta direction (pitch)
AuFactor	AU	32-bit float	The 1-AU correction factor that could be multiplied by the irradiances to remove the earth orbit effect.
QualityFlags	NA	32-bit int	All flags defined in Table 14
days_since_jan1_2000	Days	16-bit int	Days since the epoch at the CENTER of the integration
centerTime	Seconds	32-bit float	Seconds of the UT day converted from the secondary header <code>exs_pc0_tm_ms</code> (microseconds are unnecessary) minus half the actual integration time. This corresponds to the CENTER time of the exposure.
scPowerSide	NA	bit	0=B, 1=A ( <code>exs_pc0_pb_stat</code> )
exisMode	NA	4-bits	0=failsafe, 1=normal, 2=diag, 3=safe ( <code>exs_pc0_exs_md</code> )
exisFlightModel	NA	8-bits	1=FM1, 2=FM2, 3=FM3, 4=FM4 ( <code>exs_pc0_md1_num</code> )
exisConfigId	NA	16-bits	Configuration ID ( <code>exs_pc0_exs_cfg</code> )
checksum	NA	8-bits	Checksum ( <code>exs_pc0_pkt_cksm</code> )
euvsCDiodeCounts	DN	512 x 16-bit int	512 raw diodes measurements ( <code>euvs_c_pix0-511</code> )

euvsCPixelMode	NA	2-bits	Type of data being produced from EUVS-C. 0=Data minus reference, 1=Data minus reference, 2=Raw detector data (extremely noisy), 3=Reference values (euv_c_pixel_md)
FlushCount	NA	2-bits	0 to 3 20.48 ms flushes prior to integration start. (euv_c_flush_cnt)
euvsCChannelPower	NA	bit	0=C1, 1=C2 (euv_c_pwr_sel)
intTime	NA	8-bits	Integration time in quarter second increments, 0=0.25 sec, 1=0.5 sec, 2=0.75 sec, 3=1.0 sec, ... (euv_c_integ_tm)
DeadTime	NA	3-bits	Controls the dead time between readout and the first flush. Non zero value indicate a readout noise measurement. (euv_c_wait_tm)
LED_select	NA	4-bits	LED selection, 0=EUVSC-Backup, 1=EUVSB-Backup, 2=EUVSA-Backup, 3=XRS-Backup, 4=EUVSC-Pri, 5=EUVSB-Pri, 6=EUVSA-Pri, 7=XRS-Pri (exs_sl_sel)
LED_power	NA	1-bit	LED power, 0=off, 1=on (exs_sl_pwr_ena)
LED_level	NA	16-bits	LED level setting, 12 bits used, (exs_sl_lvl)
IfBoardTemp	DN	16-bits	Interface board temperature (exs_ifb_tmp_dn)
ProcFpgaTemp	DN	16-bits	Microprocessor board FPGA temperature (exs_mb_fp_tmp_dn)
PowerSupplyTemp	DN	16-bits	Power board temperature (exs_pb_tmp_dn)
CaseHeaterTemp	DN	16-bits	Case heater temperature (exs_cs_oh_tmp_dn)
euvsC1Temp	Deg C	32-bits	EUVS-C channel 1 detector board temperature (euv_c1_dt_tmp_dn converted to degrees C)
euvsC2Temp	Deg C	32-bits	EUVS-C channel 2 detector board temperature (euv_c2_dt_tmp_dn converted to degrees C)
euvsCAdcTemp	DN	16-bits	EUVS-C analog to digital convertor board temperature (euv_c_adc_tmp_dn)
slitTemp	DN	16-bits	Entrance slit temperature (euv_slit_tmp_dn)
InvalidFlags	NA	8-bits	Invalid flags, 0=good, 1=integration time warning, 2=flatfield chirp, 4=EDAC single bit error (corrected), 8=EDAC multiple bit errors (not corrected) (euv_c_inval) Either 0 or 4 is good.
DetChangeCount	NA	16-bits	Detector change counter, counts from 0 to 65535 whenever cal circuit is enabled or disabled, or EUVS-C is powered on, sticks at 65535 (euv_c_det_chg)
LEDChangeCount	NA	16-bits	Counts quarter seconds elapsed since LED was powered on or off, sticks at 65535 (exs_sl_chg)
DoorPositionKnown	NA	1-bit	The EUVS door position is known by flight software (resets after power up) 0=unknown, 1=known (euv_dr_pos_stat)
FilterWheelMoving	NA	1-bit	The EUVS filter wheel mechanism is moving, 0=not moving, 1=moving (euv_fw_mv_stat)
FilterWheelPositionKnown	NA	1-bit	The EUVS filter wheel mechanism position is known by flight software, 0=unknown, 1=known (euv_fw_pos_stat)

DoorPositionStepNumber	NA	8-bits	The EUVS door absolute position step number from 0-107. 0=closed, 31=open. (euv_dr_step_num)
FilterWheelStepNumber	NA	8-bits	The EUVS filter wheel mechanism absolute step number 0-107. (euv_fw_step_num)
XrsMode	NA	2-bits	XRS detector mode, 0=normal, 1=cal, 2=diagnostic, 3=safe, these do not affect XRS and normal should not be used to filter any science data, XRS can generate good measurements for all values of XrsMode (xrs_md)
EuvsMode	NA	2-bits	EUVS detector mode with same states as XRS, also has no effect on data collection (euvs_md)
fovFlagsKnown	NA	1-bit	FOV flags are known by flight software, 0=known, 1=unknown (exs_tl_fov_stat)
Eclipse	NA	1-bit	Earth eclipse imminent or in progress, set by ground command, 0=no eclipse, 1=eclipse (exs_tl_fov_eclip)
LunarTransit	NA	1-bit	Lunar transit imminent or in progress, set by ground command, 0=no transit, 1=transit (exs_tl_fov_lunar)
PlanetTransit	NA	1-bit	Planetary transit imminent or in progress, set by ground command, 0=no transit, 1=transit (exs_tl_fov_plnt)
OffPoint	NA	1-bit	Off-pointing calibration maneuver is imminent or in progress, set by ground command, 0=no maneuver (or sun pointed), 1=off-point maneuver (exs_tl_fov_offpt)

**Table 20 EUVS-C data product variables**

## 5.11 EUVS-C Measurement Flags

Many of the EUVS-C flags listed in Table 19 can be populated during the telemetry decomposition step. These include Checksum, LowTemperature, HighTemperature, SignalHighBlueWing, SignalHighRedWing, SignalHighHLine, SignalHighKLine, FilterPositionNotSolar, DoorPositionNotOpen, FlatfieldChirpWarning, and DetChangeCountNotValid. This also includes the flags in Table 20 such as: exisFlightModel, euvsCChannelPower, intTime, InvalidFlags, FilterWheelStepNumber, Eclipse, LunarTransit, and Offpoint.

Note that the SignalHighRedWing flag is set if any of the diodes it contains exceed the saturation value calibration file provided in CDRL 82. The saturation values are around 50,000-60,000 DN. The other SignalHigh flags are set similarly.

### 5.11.1 Flags Set in Telemetry Decomposition

Any checksum that fails to match the calculated checksum result will set the Checksum flag. A failed checksum should cause this packet to be disregarded. The checksum flag is provided to PM (or similar group). It does not need to be provided in the product.

Any value of `euv_c1_dt_tmp_dn` below -20 deg C (less than 16,706 DN) will set the LowTemperature flag. If this flag is set, the data quality will likely be reduced, but it can still be processed to create irradiances.

Any value of `euv_c1_dt_tmp_dn` above 8 deg C (greater than 37,240 DN) will set the HighTemperature flag. If this flag is set, the data quality will likely be reduced, but it can still be processed to create irradiances.

Any value of the filtered and decoded data (S) that is greater than or equal to the saturation value in `exis_fm1_euvsc_saturation.cal` for any diode in the blue wing masked pixels will set the SignalHighBlueWing flag. This indicates bad data is sneaking through the filtering. Process into an irradiance anyway. The same is true for the red wing and the h and k lines, that is, process into irradiance anyway.

The value of the FlatfieldChirpWarning flag is in the telemetry. If set this packet may produce low quality results. Until the chirp is measured, we recommend processing anyway whether the flag is set or not set.

If the `euv_c_det_chg` (DetectorChangeCount) value is less than the number reported in Table 19 then set the DetChangeCountNotValid flag, and process into an irradiance anyway.

#### 5.11.1.1 Special Note about Pointing Flags

These flags can only be set after the SPS pointing angles are averaged over the EUVS-C integration period.

Unlike the 3 pointing-related flags defined in the XRS flags section 4.6.1.1, EUVS-C only defines 2 regions distinguished by the pointingBad flag. The limits for the pointingBad flag are initially set to +/- 0.8 degrees. Once on orbit these need to be updated. There is no FOV correction for EUVS-C, but pointing beyond a certain range will introduce clipping of the sun by internal baffles. When the pointingBad flag is set, EUVS-C data may be processed, but results should not be used in the spectral model calculation.

#### 5.11.1.2 Special Note about DataNotGood Flags

The DataNotGood flags can be partially set during telemetry decomposition. These derived flags use many of the above flags, and other flags calculated later, and other telemetry values that are not flags themselves. Here we present only those flags that have already been set or are included in the telemetry packet.

The DataNotGood flags are set if the `euvscPixelMode` is not data minus reference. Also, these flags are set in accordance with Table 19. The flags are set if `exs_sl_pwr_ena` is set (Flatfield power is on is the LSB of StimLampCtrl) and `exs_sl_sel` is either EUVSC\_PRI or EUVSC\_RED (4 or 0). The flags are set if any of these conditions are met.

PointingBad is set, LowTemperature is set, HighTemperature is set, FlatfieldChirpWarning is set, DetChangeCountNotValid is set, euv\_c\_tl\_ivtm0 or euv\_c\_tl\_ivtm1 (Integration Time Warning) is set, euv\_c\_tl\_ivmbe is set (EDAC multibit error), exs\_tl\_fov\_offpt (Offpoint Maneuver) is set, exs\_tl\_fov\_lunar (lunar transit) is set, exs\_tl\_fov\_eclip (eclipse) is set, euv\_c\_integ\_tm is not equal to 3.

We have opted to not include the planetaryTransit flag in the DataNotGood flags, since the measurements are not affected significantly enough by the tiny partial blockage of Venus or Mercury.

The rest of the specific contributions to DataNotGood flags are in the next section.

### 5.11.2 Flags Set After Evaluation of Eq. 5.12

Specifically, this is the real signal above the dark subtracted background. This is where SignalLow flags can be set.

Any value in the blue wing mask that is less than or equal to zero will set the SignalLowBlueWing flag. Processing into irradiance should continue. Set the SignalLow flags for the red wing and h and k lines similarly.

The line-specific DataNotGood flags can then be determined.

### 5.11.3 Flags Set After Evaluation of Eq. 5.17

Recall the result of Eq. 5.17 is the NOAA Mg II ratio, so all information is available to calculate the remaining flags. Refer to definitions in Table 19 EUVS-C measurement flags.

The DataNotGoodHLine, DataNotGoodKLine, DataNotGoodBlueWing, DataNotGoodRedWing, and RadioNotGoodMg flags are described in Table 19.

## 6.0 Creating the Spectrum

EXIS does not directly measure the entire solar spectrum. To reduce complexity and increase reliability, the spectrum is created based on a proxy model. The measured set of proxies is all provided by EXIS. The model directly computes the broadband irradiances for the bands listed in Table 23.

The EUVS and XRS combined measure 10 different solar emissions that represent four temperature regions of the solar atmosphere, as summarized in Table 21.

i	Wavelength (nm)	EXIS Subsystem	Solar Region Represented
1	0.05-0.4	XRS-A	Hot Corona
2	0.1-0.8	XRS-B	Hot Corona
3	25.6	EUVS-A	Transition Region
4	28.4	EUVS-A	Corona
5	30.4	EUVS-A	Transition Region
6	117.5	EUVS-B	Chromosphere
7	121.6	EUVS-B	Transition Region
8	133.5	EUVS-B	Chromosphere
9	140.5	EUVS-B	Transition Region
10	Mg II C/W ratio	EUVS-C	Chromosphere

**Table 21 Solar Emissions Measured by EXIS**

The EUVS Level 1b data product is based on an empirical proxy model that calculates the full spectrum in 5-nm bins from a combination of the emissions measured by EXIS. At any given time, only four proxy measurements are necessary for the model (one each from the chromosphere, transition region, corona, and hot corona); however, for simplicity the model has been formulated to use all ten measurements. There are times when data from various subsystems are going to be absent due to calibration activities (e.g. dark, gain, and flatfield calibrations) while other subsystems will be available. This formulation for the model allows for these cases while still producing a data product, albeit of reduced accuracy, by simply selecting a different set of lookup table values for each case.

The exception is the H I Lyman-alpha emission. When available, the direct measurement average from EUVS-B is reported.

## 6.1 Proxy Model Inputs

The proxy model requires several proxies as input. These must be extracted from the processed EUVS-A, B, C, and XRS-B channels described in previous sections. There are a total of 10 possible measurements that may be used: XRS-A, XRS-B, 25.6, 28.4, 30.4, 117.5, 121.6, 133.5, 140.5 nm, and the NOAA Mg II core to wing ratio. The model may use any combination of these to determine the irradiance in a 5 nm bin.

## 6.2 Proxy Model Mathematical Description and Algorithm Design

The proxy model flow is shown in Figure 21.

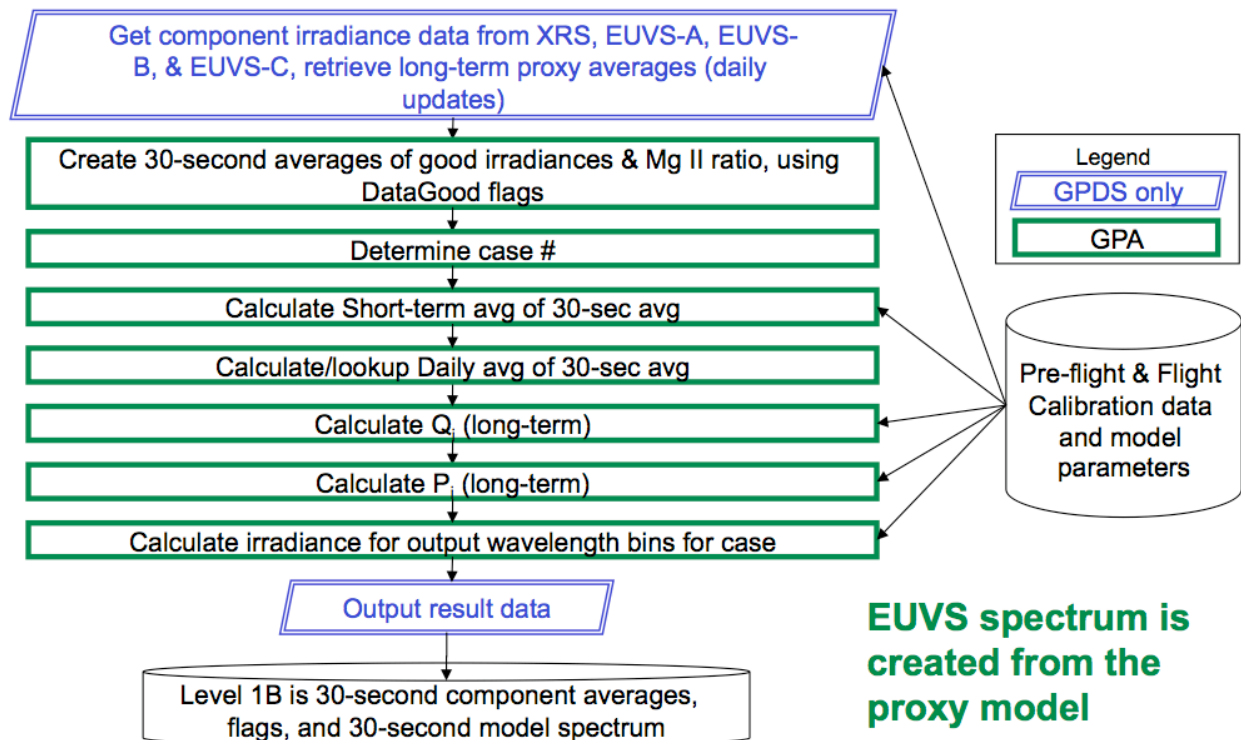


**Figure 21. Model Spectrum Algorithm Flow**

This is described in somewhat more detail in the following pseudocode.

```
#Main thread
  lookupOneAu(time)

#EUVS model thread
  model.loadConfigurationFiles()
  model.loadData()
  model.create30SecondAverages() // only over good data
  model.determineCaseNumber() // based on the good 30-sec avgs
  model.calculateShortTermAverages()
  model.calculatePreviousDayAverages() // only updated once per day
  model.calculateProxyQ() // short-term proxies
  model.calculateProxyP() // solar-cycle proxies
  model.calculateModelIrradiances() // uses case number
  model.createOutput()
```

The equation for the EUVS level 1b spectral data product is shown in Eq. 6.1.

**Eq. 6.1** 
$$E(\lambda_{5nm}, t) = A(\lambda_{5nm}) + \sum_{i=1}^{10} j_i(\lambda_{5nm}) \cdot P_i^{m_i}(t) + \sum_{i=1}^{10} k_i(\lambda_{5nm}) \cdot Q_i^{n_i}(t)$$

**Eq. 6.2** 
$$P_i(t) = \frac{\langle E_i(t) \rangle - E_{min,i}}{E_{min,i}}$$



**Eq. 6.3** 
$$Q_i = \frac{E_i(t) - \langle E_i(t) \rangle}{\langle E_i(t) \rangle}$$

In Eq. 6.1,  $E$  is the irradiance at a particular time ( $t$ ) in a 5-nm wavelength ( $\lambda_{5nm}$ ) bin.  $A$  is the solar minimum reference value for that bin. The summations ( $i$ ) are over the ten measurements. The  $P_i$  are proxies calculated from the ten measurements for a slower time-averaged variability. The  $Q_i$  are the proxies for the faster time variability to allow the model to react to flares. The  $j_i$  and the  $k_i$  are the scaling factors between the proxies and the irradiance in the wavelength bin. The  $m_i$  and  $n_i$  are the exponents of power law relationships between the proxies and the irradiance in the output wavelength bins. The  $j_i$ , and  $k_i$ , are semi-static lookup table parameter values (to be provided in CDRL 79) for the nominal operation case and each of the possible calibration cases of available subsystem measurements. The  $A$ ,  $m_i$ , and  $n_i$  are semi-static lookup table parameter values (to be provided in CDRL 79) and are the same for all cases listed in Table 22.

The slower time-averaged proxies,  $P_i(t)$ , capture variability that occurs slowly over hours, but is an enhancement over the solar minimum values. These proxies are the left side of by Eq. 6.2, where  $\langle E_i(t) \rangle$  is the measured value for the proxy wavelength time-averaged over the previous fixed number of hours (provided in CDRL 79) and  $E_{min,i}$  is the solar minimum reference value for that proxy wavelength (also provided as a lookup table in CDRL 79).

Fast time proxies,  $Q_i$ , capture irradiance enhancements that occur quickly, such as during solar flares, and are shown in Eq. 6.3, where  $E_i(t)$  is the 30-second average value for the proxy wavelength and the  $\langle E_i(t) \rangle$  are the same time-averaged values used in calculating the  $P_i(t)$ .

Note that the lyman-alpha output bin is the exception to this proxy model. We recommend calculating all of the proxy model bins, then replacing the lyman-alpha bin with the measurement of lyman-alpha from EUVS-B if it is good. The EUVS-B directly measures Lyman-alpha, and since this emission line dominates the entire area around Lyman-alpha, it shall replace the model output bin when it is available. The measurement will be used in the output, provided it's 30-second average is flagged as good.

The different cases for the lookup table values based on available of the measured proxies are summarized in Table 22. Only the nominal operations case will meet all of the accuracy requirements for the EUVS data product.

Case	Description	EUVS Product Quality
1	All subsystems available (nominal operations)	Best
2	121.6 nm not available (geocoronal absorption)	Reduced
3	EUVS-A and EUVS-B not available (gain calibration)	Reduced
4	EUVS-C not available	Reduced
5	EUVS-A not available	Reduced
6	EUVS-B not available	Reduced
7	XRS not available	Reduced
8	EUVS-A, EUVS-B, and EUVS-C not available	No useful EUVS spectrum

**Table 22 Proxy Data Availability Cases**

The accuracy of the model output is based on the accuracy of the proxies. The case number corresponds to the frequency of occurrence. Most of the time, case 1 is used, with 2 occurring during a period each day.

## 6.3 Proxy Model Algorithm Steps

### 6.3.1 Solar Minimum Reference

Each proxy is calculated using processed measurements from EXIS and a reference solar minimum value. The reference solar minimum values will be provided in CDRL 79 as an ASCII file for use in real-time. These are Semi-static Parameters.

### 6.3.2 Averaging to Create Proxies

The irradiances and Mg II ratio results from each of the good integrations are first averaged over the 30-second time interval spanning either the first 30 seconds in a UTC minute or the last 30 seconds in a minute. The center time for the EUVS model product is always 15 or 45 seconds past the minute. All integrations with center times that are greater than or equal to 0 and less than or equal to 30 seconds past the UT minute should be in the product corresponding to the center time of 15 seconds. The integrations with center times that are greater than or equal to 30 and less than or equal to 60 seconds should be in the product corresponding to the center time of 45 seconds. The 30-second averages are then averaged over a “short” time interval specified in CDRL 79. No attempt is made to account for integrations spanning the time boundary. All timestamps generated by EXIS represent the end of an integration period. The data that are available and time stamped within the data product time interval are added together and divided by the number available as shown in Eq. 6.4. If the geocorona flag is set, then the Lyman-alpha line irradiance must be treated as missing. The proxy averages should not include Lyman-alpha line irradiances during the geocorona time period. When the euvs\_md flag is set to “Cal” or “Diag”, all EUVS data is suspect and needs to be excluded from the proxy averages. Onboard stored command tables that are triggered such as for daily calibrations, weekly calibrations, maneuvers, etc. will set the euvs\_md flag to “Cal”. If there is no valid/good data for a 30-second time interval, such as in case #8, then the model shall return fill values. The fill-value is expected to be -999999, but any large negative number could represent missing data.

Eq. 6.4

$$P = \frac{1}{N} \sum_{j=1}^N P_j$$

Additional proxy averages are needed for the model that span longer time periods. These time periods may range from several hours up to 1-day.

### 6.3.2.1 Daily Averages

In order to support the bootstrap degradation algorithm, the daily averages of all good irradiances from EUVS-A, EUVS-B, and the Mg II core to wing ratio shall be calculated and provided in the level 1b data product. Daily averages shall only include values that have a corresponding DataNotGood value that indicates the measurement is good. As with proxy averaging, the daily average must exclude the Lyman-alpha line during the geocorona. The daily averages also must exclude EUVS line irradiances when the euvs\_md flag is set to "Cal" or "Diag". This is an average over the previous UT day interval spanning 24 hours that only includes irradiance data from normal solar observations. This is an average over the previous UT day interval spanning 24 hours. The reported values in current products correspond to the previous UT day, so it is the same for all output times within the same UT day.

### 6.3.3 Spectral Bins

The spectrum is calculated using the wavelength bins described in Table 23. This exceeds the requirement specified in EXISPOD107. From 5 to 35 nm, the output bins are required to be no larger than 10 nm. The 5 nm bin sizes satisfy this requirement. From 35 to 115 nm, the output bins are required to be no larger than 40 nm. The 5 nm bin sizes satisfy this requirement. The hydrogen Lyman-alpha band is required to be less than 10 nm. This dominating solar line is directly measured by EUVS-B, so instead of using a model for this bin, the direct measurement is passed through (see Figure 8).

Start wavelength (nm)	Stop wavelength (nm)	EXISPORD107 bin requirement
5	10	5-35 nm: 10 nm minimum bins or smaller
10	15	
15	20	
20	25	
25	30	
30	35	
35	40	35-115 nm: 40 nm minimum bins or smaller
40	45	
45	50	
50	55	
55	60	
60	65	
65	70	
70	75	
75	80	
80	85	
85	90	
90	95	
95	100	
100	105	
105	110	
110	115	121.6 nm: 10 nm minimum FWHM bin or smaller
117	127	

**Table 23 Spectral bin ranges**

## 6.4 Proxy Model Output

The proxy model will produce a wavelength-ordered spectrum that corresponds to the wavelength bins described in Table 23. The bin order is the same as the table.

## 6.5 EUVS Data Product

The EUVS data product shall contain a timestamp and the irradiance spectrum as defined in Table 23. In addition to the spectrum, the data product shall contain the measured irradiances from the 7 directly measured irradiance bands from EUVS-A and B with associated timestamps at each processing interval. The EUVS data product shall also contain the XRS-B primary irradiances over each processing interval. Furthermore, the EUVS data product shall contain the two Mg II core to wing ratios: the EXIS ratio (Eq. 5.16) and the NOAA ratio (Eq. 5.17).

Each measurement shall have a corresponding timestamp. Since the detector integration times are not all the same, timestamps are needed for: the model spectrum, XRS-B irradiances, EUVS-A and B irradiances and the Mg II ratios. The EUVS product shall contain a flag indicating if the SPS pointing angles (a, b) are valid and within 1 arcminute of zero over the measurement.

The spectral accuracy is determined by another program (see section 9.3.1) to avoid impacting the run-time performance.

Flag Name	Value (1/0)	Description/Explanation
XrsIntegrationFlags	NA	An array of flag tables representing each XRS integration as specified in Table 7.
EuvsAIntegrationFlags	NA	An array of flag tables representing each EUVS-A integration as specified in Table 11.
EuvsBIntegrationFlags	NA	An array of flag tables representing each EUVS-B integration as specified in Table 14.
EuvsCIntegrationFlags	NA	An array of flag tables representing each EUVS-C integration as specified in Table 19.
PointingBad	Bad/Good	Logical OR of all the pointing flags in XrsIntegrationFlags, EuvsAIntegration, EuvsBIntegrationFlags, and EuvsCIntegrationFlags. The pointing of EXIS is both known and within the valid calibration range over the 30 second interval.
FilterPositionNotSolar	NotPrimary/PrimaryScience	Logical OR of all the FilterPositionNotSolar from EuvsA, B, and C IntegrationFlags. The filter wheel position has many values, but only one is designated primary science.
LowTemperature	Low/Good	Logical OR of all the LowTemperature flags for XRS, EUVS-A, EUVS-B, and EUVS-C. If any are bad, then the whole thing is bad.
HighTemperature	High/Good	Logical OR of all the HighTemperature flags for XRS, EUVS-A, EUVS-B, and EUVS-C.
SignalLowXrsA	Low/Not Low	The 30-second time average of the integrated signal from the primary XRS-A channel is distinguishable from zero.
SignalLowXrsB	Low/Not Low	The 30-second time average of the integrated signal from the primary XRS-B channel is distinguishable from zero.
SignalLow256	Low/Not Low	The 30-second time average of integrated signals is distinguishable from zero.
SignalLow284	Low/Not Low	The 30-second time average of integrated signals is distinguishable from zero.
SignalLow304	Low/Not Low	The 30-second time average of integrated signals is distinguishable from zero.
SignalLow1175	Low/Not Low	The 30-second time average of integrated signals is distinguishable from zero.
SignalLow1216	Low/Not Low	The 30-second time average of integrated signals is distinguishable from zero.
SignalLow1335	Low/Not Low	The 30-second time average of integrated signals is distinguishable from zero.

SignalLow1405	Low/Not Low	The 30-second time average of integrated signals is distinguishable from zero.
SignalHighXrsA	High/Not high	The 30-second time average of integrated signals is below the saturation value.
SignalHighXrsB	High/Not high	The 30-second time average of integrated signals is below the saturation value.
SignalHigh256	High/Not high	The 30-second time average of integrated signals is below the saturation value.
SignalHigh284	High/Not high	The 30-second time average of integrated signals is below the saturation value.
SignalHigh304	High/Not high	The 30-second time average of integrated signals is below the saturation value.
SignalHigh1175	High/Not high	The 30-second time average of integrated signals is below the saturation value.
SignalHigh1216	High/Not high	The 30-second time average of integrated signals is below the saturation value.
SignalHigh1335	High/Not high	The 30-second time average of integrated signals is below the saturation value.
SignalHigh1405	High/Not high	The 30-second time average of integrated signals is below the saturation value.
IntTimeWarningXrs	Bad/Good	At least one of the XRS integrations was truncated (Logical OR of XRS Integration TimeWarning from InvalidFlags).
IntTimeWarningEuvsA	Bad/Good	At least one of the EUVS-A integrations was truncated (Logical OR of EUVS-A Integration TimeWarning from InvalidFlags).
IntTimeWarningEuvsB	Bad/Good	At least one of the EUVS-B integrations was truncated (Logical OR of EUVS-B Integration TimeWarning from InvalidFlags).
IntTimeWarningEuvsC	Bad/Good	At least one of the EUVS-C integrations was truncated (Logical OR of EUVS-C Integration TimeWarning from InvalidFlags).
FlatfieldChirpWarning	Bad/Good	At least one of integration may contain a flatfield flash (Logical OR of XRS flatfield chirp from InvalidFlags in XRS, EUVS-A, EUVS-B, or EUVS-C)
OffpointManeuver	Bad/Good	Maneuver in-progress, logical OR of all OffPoint from XRS, EUVS-A, EUVS-B, EUVS-C packets.
PlanetTransit	Bad/Good	Mercury or Venus is between EXIS and the sun, logical OR of all PlanetTransit from XRS, EUVS-A, EUVS-B, EUVS-C packets.
LunarTransit	Bad/Good	The moon is interfering with solar observations, logical OR of all LunarTransit from XRS, EUVS-A, EUVS-B, EUVS-C packets.
Eclipse	Bad/Good	The earth is interfering with solar observations, logical OR of Eclipse from XRS, EUVS-A, EUVS-B, EUVS-C packets.

FOVFlagsUnknown	Bad/Good	Logical OR from XRS, EUVS-A, EUVS-B, EUVS-C packets.
DataNotGoodXrsA	Bad/Good	Logical OR of DataNotGoodA from individual integrations within the 30-second period
DataNotGoodXrsB	Bad/Good	Logical OR of DataNotGoodB from individual integrations within the 30-second period
DataNotGood256	Bad/Good	Logical OR of DataNotGood256 from individual integrations within the 30-second period
DataNotGood284	Bad/Good	Logical OR of DataNotGood284 from individual integrations within the 30-second period
DataNotGood304	Bad/Good	Logical OR of DataNotGood304 from individual integrations within the 30-second period
DataNotGood1175	Bad/Good	Logical OR of DataNotGood1175 from individual integrations within the 30-second period
DataNotGood1216	Bad/Good	Logical OR of DataNotGood1216 from individual integrations within the 30-second period
DataNotGood1335	Bad/Good	Logical OR of DataNotGood1335 from individual integrations within the 30-second period
DataNotGood1405	Bad/Good	Logical OR of DataNotGood1405 from individual integrations within the 30-second period
PrimaryCActive	On/Off	Only one EUVS-C channel will be powered on most of the time, designated the primary. If the primary channel is off, then set this flag to the Off value. The detector change count flag prevents multiple good C channel measurements from being available in the same 30 seconds period.
SecondaryCActive	On/Off	IF the EUVS-C secondary channel is powered on, set this flag.
RatioNotGoodMg	Bad/Good	Logical OR of RatioNotGoodMg from individual integrations within the 30-second period

**Table 24 EUVS measurement flags**

The EUVS data 30-second cadence product content is also displayed in Table 25.

Variable	Units	Data type	Needed for	Description
Irradiance Spectrum	W/m <sup>2</sup> /nm	23 x 32-bit float	L1b product	Irradiance from Spectrum Model wavelength bins, one number per 5-nm bin including the lyman-alpha bin (23 total)
WavelengthLow	nm	23 x 16 bit int	L1b product	Integer wavelength of the low edge for each irradiance bin defined in Table 23.
WavelengthHigh	nm	23 x 16 bit int	L1b product	Integer wavelength of the high edge for each irradiance bin defined in Table 23.
CaseNumber	NA	byte	L1b product	EUVS model case number described in Table 22.
QualityFlags	NA	64-bit int	L1b product & diagnostics	The derived 30-second flags defined in Table 24. These range from PointingBad through RatioNotGoodMg. Individual integration flags are not necessary in the L1b product, and are listed lower in this table.
XRSA	W/m <sup>2</sup>	32-bit float	L1b product	30-second averaged irradiance from XRS-A
XRSB	W/m <sup>2</sup>	32-bit float	L1b product	30-second averaged irradiance from XRS-B
E256	W/m <sup>2</sup>	32-bit float	L1b product	30-second averaged irradiance from EUVS-A 25.6 nm
E284	W/m <sup>2</sup>	32-bit float	L1b product	30-second averaged irradiance from EUVS-A 28.4 nm
E304	W/m <sup>2</sup>	32-bit float	L1b product	30-second averaged irradiance from EUVS-A 30.4 nm
E1175	W/m <sup>2</sup>	32-bit float	L1b product	30-second averaged irradiance from EUVS-B 117.5 nm
E1216	W/m <sup>2</sup>	32-bit float	L1b product	30-second averaged irradiance from EUVS-B 121.6 nm
E1335	W/m <sup>2</sup>	32-bit float	L1b product	30-second averaged irradiance from EUVS-B 133.5 nm
E1405	W/m <sup>2</sup>	32-bit float	L1b product	30-second averaged irradiance from EUVS-B 140.5 nm
RatioMgIIExis	NA	32-bit float	L1b product	30-second averaged Mg II core to wing ratios from EXIS
RatioMgIINOAA	NA	32-bit float	L1b product	30-second averaged Mg II core to wing ratios scaled to NOAA trend
QProxyXRSA	NA	32-bit float	Diagnostics	Short-term XRS-A proxy, $Q_i(t)$
QProxyXRSB	NA	32-bit float	Diagnostics	Short-term XRS-B proxy, $Q_i(t)$
QProxy256	NA	32-bit float	Diagnostics	Short-term 25.6 nm proxy, $Q_i(t)$
QProxy284	NA	32-bit float	Diagnostics	Short-term 28.4 nm proxy, $Q_i(t)$



QProxy304	NA	32-bit float	Diagnostics	Short-term 30.4 nm proxy, $Q_i(t)$
QProxy1175	NA	32-bit float	Diagnostics	Short-term 117.5 nm proxy, $Q_i(t)$
QProxy1216	NA	32-bit float	Diagnostics	Short-term 121.6 nm proxy, $Q_i(t)$
QProxy1335	NA	32-bit float	Diagnostics	Short-term 133.5 nm proxy, $Q_i(t)$
QProxy1405	NA	32-bit float	Diagnostics	Short-term 140.5 nm proxy, $Q_i(t)$
QProxyMgIINOAA	NA	32-bit float	Diagnostics	Short-term Mg II core to wing ratio (NOAA) proxy, $Q_i(t)$
PProxyXrsA	NA	32-bit float	Diagnostics	Long-term XRSA proxy, $P_i(t)$
PProxyXrsB	NA	32-bit float	Diagnostics	Long-term XRSB proxy, $P_i(t)$
PProxy256	NA	32-bit float	Diagnostics	Long-term 25.6 nm proxy, $P_i(t)$
PProxy284	NA	32-bit float	Diagnostics	Long-term 28.4 nm proxy, $P_i(t)$
PProxy304	NA	32-bit float	Diagnostics	Long-term 30.4 nm proxy, $P_i(t)$
PProxy1175	NA	32-bit float	Diagnostics	Long-term 117.5 nm proxy, $P_i(t)$
PProxy1216	NA	32-bit float	Diagnostics	Long-term 121.6 nm proxy, $P_i(t)$
PProxy1335	NA	32-bit float	Diagnostics	Long-term 133.5 nm proxy, $P_i(t)$
PProxy1405	NA	32-bit float	Diagnostics	Long-term 140.5 nm proxy, $P_i(t)$
PProxyMgIINOAA	NA	32-bit float	Diagnostics	Long-term Mg II core to wing ratio proxy, $P_i(t)$
Daily256	W/m <sup>2</sup>	32-bit float	L1b product & diagnostics	The daily average irradiance for solar measurements from the previous day. This is used in the bootstrap degradation algorithm described in section 9.1.4
Daily284	W/m <sup>2</sup>	32-bit float	L1b product & diagnostics	The daily average irradiance for solar measurements from the previous day. This is used in the bootstrap degradation algorithm described in section 9.1.4
Daily304	W/m <sup>2</sup>	32-bit float	L1b product & diagnostics	The daily average irradiance for solar measurements from the previous day. This is used in the bootstrap degradation algorithm described in section 9.1.4
Daily1175	W/m <sup>2</sup>	32-bit float	L1b product & diagnostics	The daily average irradiance for solar measurements from the previous day. This is used in the bootstrap degradation

				algorithm described in section 9.1.4
Daily1216	W/m <sup>2</sup>	32-bit float	L1b product & diagnostics	The daily average irradiance for solar measurements from the previous day. This is used in the bootstrap degradation algorithm described in section 9.1.4
Daily1335	W/m <sup>2</sup>	32-bit float	L1b product & diagnostics	The daily average irradiance for solar measurements from the previous day. This is used in the bootstrap degradation algorithm described in section 9.1.4
Daily1405	W/m <sup>2</sup>	32-bit float	L1b product & diagnostics	The daily average irradiance for solar measurements from the previous day. This is used in the bootstrap degradation algorithm described in section 9.1.4
DailyRatioMgIINOAA	NA	32-bit float	L1b product & diagnostics	The daily average irradiance for the Mg II ratio from the previous day. This is used in the bootstrap degradation algorithm described in section 9.1.4
previousDay	Days	32-bit float	L1b product	Previous day center (noon UT) in days since the epoch. This corresponds to the center of the UT day used in the daily average calculations.
a	degrees	32-bit float	Diagnostics	Averaged dispersion direction pointing angle from SPS
b	degrees	32-bit float	Diagnostics	Averaged cross-dispersion direction pointing angle from SPS
a_GT	degrees	32-bit float	Diagnostics	Averaged SUVI Guide Telescope angle along SPS alpha direction (yaw)
b_GT	degrees	32-bit float	Diagnostics	Averaged SUVI Guide Telescope angle along SPS beta direction (pitch)
AU_factor	AU	32-bit float	L1b product	The 1-AU correction factor that could be multiplied by the irradiances to remove the distance-effect of earth orbiting the sun.

day	Days	32-bit float	L1b product	Days since the epoch at the CENTER time of the integration
time	Seconds	32-bit float	L1b product	Seconds of the UT day representing the CENTER of the 30-second window (interval end time minus 15 seconds)
euvsa_temp	degrees C	32-bit float	L1b product & diagnostics	30-second average of EUVS-A detector temperature
euvsb_temp	degrees C	32-bit float	L1b product & diagnostics	30-second average of EUVS-B detector temperature
euvsc_temp	degrees C	32-bit float	L1b product & diagnostics	30-second average of EUVS-C1 detector temperature
euvsv_filter_position	NA	byte	L1b product & diagnostics	EUVS filter absolute step number (euv_fw_step_num)
EUVSA	NA	30 x Table size	Diagnostics	Array containing the contents of Table 12 from each integration in the 30 second time period.
EUVSB	NA	30 x Table size	Diagnostics	Array containing the contents of Table 15 from each integration in the 30 second time period.
EUVSC	NA	Number of integrations x Table size	Diagnostics	Array containing the contents of Table 20 from each integration in the 30 second time period.

**Table 25 EUVS data product contents**

If all integrations for EUVS-A, EUVS-B, and EUVS-C have the same value for euv\_fw\_step\_num, then that value is reported in euvsv\_filter\_position. If any one of these does not agree with the others, then set the euvsv\_filter\_position to 255. This is a value that is outside the possible range of the filter since there are only 108 possible steps (0-107). The filter positions are listed for each channel in Table 26.

## 7.0 GPDS System Description

The Ground Processing Demonstration System (GPDS) is a computer workstation that will demonstrate the algorithm feasibility. It is currently expected to be an Intel-based computer running GNU-Linux. The system hardware is described in Appendix A - Table 27.

## 8.0 SPS Processing

### 8.1 Detector Measurements

The SPS detector exists to provide pointing information for EXIS that is used for processing the science data from all of the other channels. While SPS is not itself a science measurement, it must be processed

to obtain pointing angles that are directly used for the field-of-view correction factors in the measurement equations for the science channels (see sections 4.4.8 and 5.3.12). The SPS also provides a reference bore sight for direct mapping of the measured ground alignments to the flight instrument on-orbit.

The SPS detector data comes from a quadrant diode detector connected to an ASIC, similar to the XRS. The SPS has a field-of-view (FOV) of approximately  $\pm 3.5$  degrees, and is designed to be sensitive to visible light. The purpose for the SPS is to provide pointing information to support EXIS processing. Sun light passes through an aperture and filter onto the diodes producing currents. The values of these signals are used to determine the pointing.

The SPS will be operated such that a pointing measurement is obtained four times per second. Each quadrant is expected to read approximately 49,000 DN every quarter second while pointed straight at the sun. Since the SPS electronics is based on the XRS, the ASIC has 6 outputs. The first four of those represent the quadrant diode measurements, and the remaining two are from precision resistors. The precision resistor measurements can be disregarded.

As with XRS, the SPS has a commanded IDAC setting (for the ASIC) that does not exactly correspond to the value obtained (offset) during dark collection. This will be calibrated during testing and adjusted if necessary on-orbit during instrument commissioning (PLT).

As with XRS, the SPS can be commanded into a calibration state where charge is injected into the circuit to provide an internal calibration for the electronics. This should only be performed when SPS is not pointed at the sun. The telemetry mnemonic to determine if SPS has been commanded to produce calibration signals is `sps_runctrlmd`.

Over the course of a year the total signal measured by the SPS (the sum of the quadrants) will vary together with the earth-sun distance variation. This is the 1-AU effect. As the mission progresses, the total signal may also decrease as the filter degrades. This is expected to be on the order of less than 1% per year, but the magnitude variation of the total signal does not strongly affect the pointing determination. This assumes that the detectors change together. A similar instrument on another spacecraft has shown a decrease in signal of less than 2% over 9 years of operation in low earth orbit with a lower duty cycle.

## 8.2 Mathematical Description

The mathematical description of the SPS processing is shown in the following equations. First, the signal current in each quadrant diode is calculated. Similar to the XRS algorithm, the raw signals are divided by the integration time, multiplied by the gain correction, and then the dark is subtracted.

**Eq. 8.1** 
$$C'_i = \left( \frac{S_i}{\Delta t} \cdot G_i \right) - C_{Dark,i}$$

**Eq. 8.2** 
$$G_i = G_{preflight,i} \cdot f_{G,i} \cdot f_{Lin,i}$$

As with the XRS, the gain has a long-term component that will be updated using the on-board charge injection calibration.

**Eq. 8.3** 
$$C_{Dark,i} = C_{elect,i} + C_{therm,i}$$

Note that unlike the XRS, there is no radiation background subtraction. The SPS has no in situ measurement of the background radiation. Furthermore, the diodes are physically adjacent to each other in a quadrant package, such that the radiation contribution is likely to be uniform over all quadrants. Finally, the absolute value is of no interest, and the pointing information is derived from differencing the diode values (this is clear upon inspection of Eq. 8.5).

Next calculate the total signal,  $T$ , from the individual quadrant signals,  $C'_i$ .

**Eq. 8.4** 
$$T = \sum_i C'_i$$

If  $T$  is less than the threshold, then EXIS is not pointed at the sun center within 3 degrees. The threshold will be defined in CDRL 79 and is expected to be approximately 4 nA, but depends on instrument performance so it needs to be measured using post-launch test phase cruciform maneuver data.  $T$  is the normalizing factor for determining the dimensionless parameters  $a$  and  $b$  that span the range of values from -1 to +1. The detector/filter combination is designed such that the solar signals are much larger than the dark subtraction (about 50,000 to about 15).

**Eq. 8.5** 
$$a = \frac{(C'_1 + C'_2) - (C'_3 + C'_4)}{T}$$

$$b = \frac{(C'_1 + C'_4) - (C'_2 + C'_3)}{T}$$

The flight layout of the diodes is shown in Figure 22.

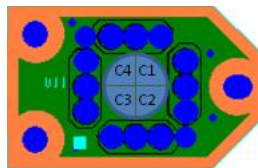


**Figure 22 SPS diode layout on the flex circuit.**

The parameters  $a$  and  $b$ , are then used to lookup the pointing angles  $\alpha$  and  $\beta$ , in degrees.

### 8.2.1 Implementation Recommendation

The pointing angles can be determined by 2 lookup tables, with one for  $\alpha$  (using  $a$ ) and another for  $\beta$  (from  $b$ ). We plan to create a uniformly sampled table with 2001 samples (centered on zero) for each angle. The index into the table is then calculated as shown in Eq. 8.6.

**Eq. 8.6**

$$\alpha = Table[Round(a \cdot n) + n]$$

$$\beta = Table[Round(b \cdot n) + n]$$

The floating point values of  $a$  and  $b$  are multiplied by 1000 ( $n$  in the equation), rounded to an integer, and then added to 1000. The result is the index into the lookup table.

### 8.2.2 Dependency Analysis

The terms in the equations for SPS are inter-related. The dependency is shown graphically in Figure 23.

## SPS Dependency Graph

Dependent Terms



Independent terms



Dependency hierarchy is a planar directed acyclic graph

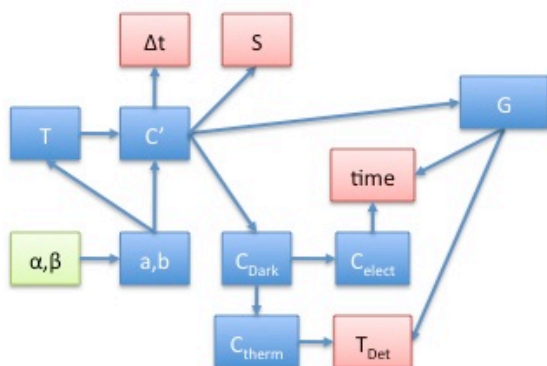


**Figure 23 SPS dependency graph**

The dependency graph is useful for identifying connectedness of the terms in the equations. Items with more connectedness are more complex than items with fewer connections. The acyclic property of the graph ensures that no terms are dependent in a way that would cause an infinite loop. This implies that there is no circular dependence in the equations.

Reversing the arrows of Figure 23 creates a rooted-tree as shown in Figure 24. Starting with any independent term and following arrows will eventually terminate at the pointing angle results.

## SPS Rooted Tree

Dependent Terms



Independent terms



Rooted tree shows all paths terminate at the pointing angles

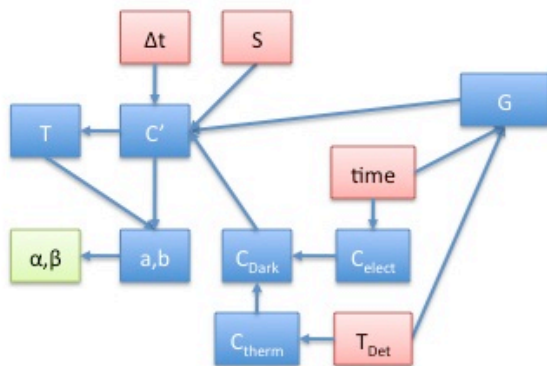


**Figure 24 SPS rooted dependency tree**

The arrows emanating from “time” (meaning long-term) require off-line analysis. These long-term components can only be measured when the SPS is pointed away from the sun and no light is on the detectors.

### 8.3 SPS Algorithm Steps

#### 8.3.1 Packet Decomposition

The SPS packet is organized similarly to the XRS packet. Details are incorporated into the command and telemetry handbook (EXIS CDRL 43).

#### 8.3.2 Signal, S

The corrected signals,  $S_i$ , from each quadrant are directly extracted from the packet with the mnemonics `sps_cnt_ch0` through `sps_cnt_3`. Disregard `sps_cnt_ch4` and `sps_cnt_5`, as these are precision resistors and do not provide pointing, or anything else useful.

The magnitudes of the signal for SPS will be very large (~ 50,000 DN/quarter second).

### 8.3.3 Integration Time

This is the same as 4.4.4 except that the default integration rate is 4 Hz or 0 DN.

### 8.3.4 Gain, G

The gain correction is identical to the gain correction for XRS. Refer to section 4.4.5. The temperature needed for the lookup table is `sps_dt_tmp_dn`. Note that there may be different conversions for EXIS side a power and side b power (indicated by `exs_ps_pb_stat`).

The absolute preflight gain calibration parameters to the linear fit will be provided in CDRL 79. These are Static Parameters that can only be determined during pre-flight calibration activities.

The relative change in gain over time is initially set to 1.0 and should remain at 1.0 until the gain has been proven to change. This is a Semi-static Parameter.

The relative linearity should be 1.0. This is a Static Parameter.

### 8.3.5 Dark, $C_{\text{Dark}}$

The dark is the sum of contributions from the electrometer offset and thermal contribution.

#### 8.3.5.1 Electrometer Offset, $C_{\text{elect}}$

The electrometer offsets are identical to XRS. Refer to section 4.4.6.1.1. The commanded electrometer offsets are `sps_idac_ch0` through `sps_idac_ch3`.

#### 8.3.5.2 Thermal Contribution to Dark, $C_{\text{therm}}$

The temperature dependence of the diodes will be calibrated on the ground. This value will be a lookup table based on the diode temperature. The temperature needed for the lookup table is `sps_dt_tmp_dn`. This table will be a set of Static Parameters provided in CDRL 79.

### 8.3.6 Implementation Recommendations

An overview of the process is shown in the following pseudocode.

```
#Main thread
    sps.extractPacket(packet)

#SPS thread
    sps.loadConfigurationFiles()
    sps.applyGain()
    sps.applyDarkDiodeCorrections()
    sps.calculateNormalizedPointing()
    sps.calculatePointingAngles()
    sps.createOutput()
    sps.printProcessedData()
```

The SPS packet processing is summarized in Figure 25.



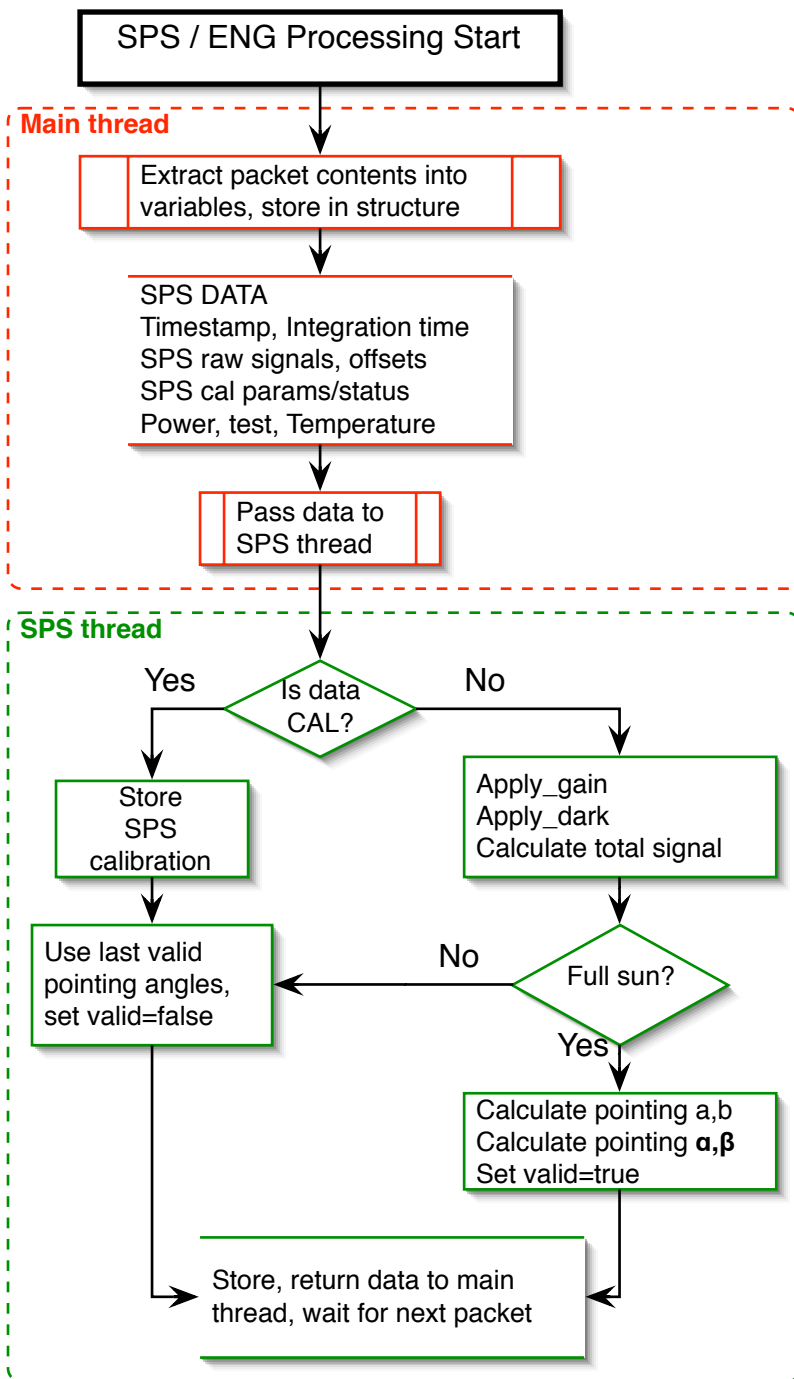
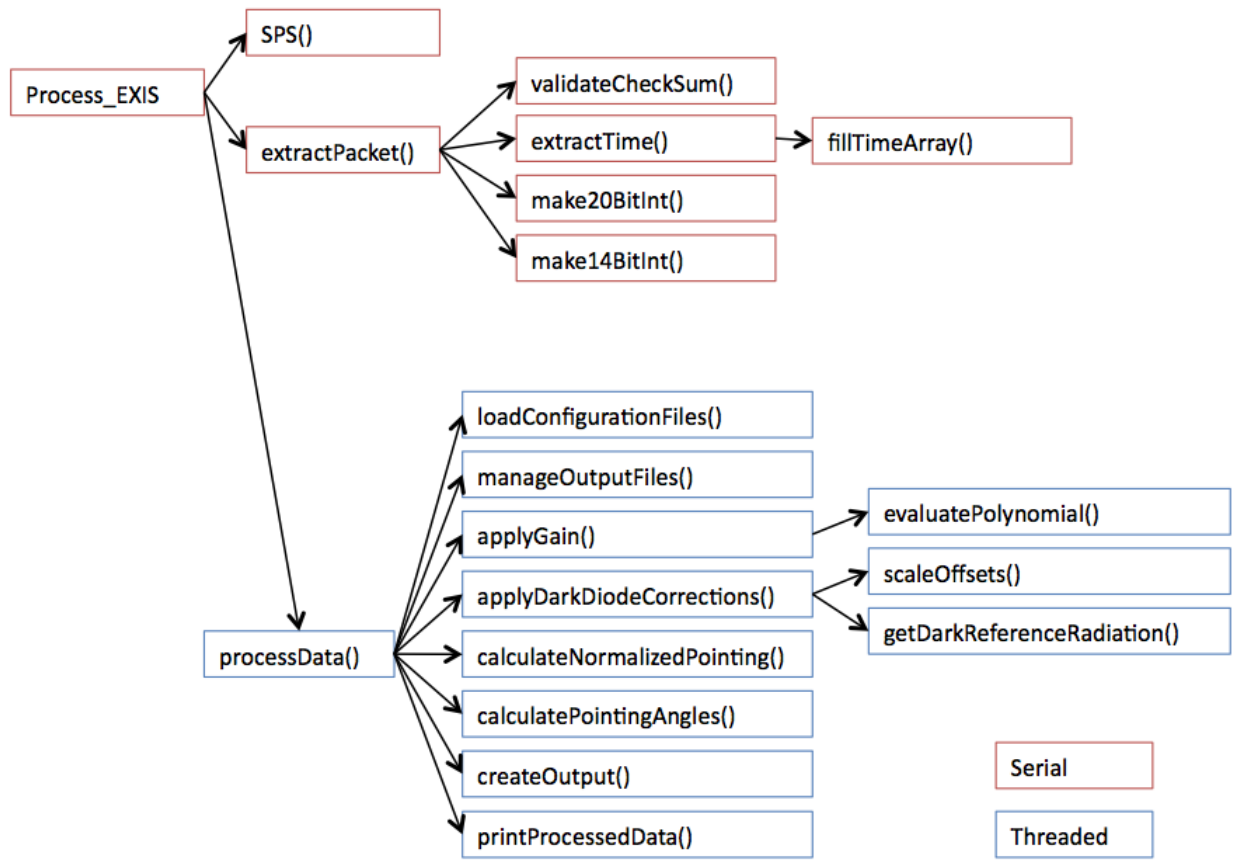


Figure 25. SPS Processing Flow



**Figure 26. SPS Functions**

SPS packet information is stored in the XRS level 1b product.

## 8.4 EXIS Orientation and Roll Angle

The EXIS orientation is required to be provided in the XRS data product to support level 2+ flare location algorithms. All angles could be determined from a quaternion, but this is not provided to EXIS on board the spacecraft. Since the spacecraft quaternion will not be provided in EXIS telemetry, it is now the responsibility of the ground system contractor to provide EXIS orientation angles in the XRS data products.

The orientation of the EXIS optical axes (defined by a and b) to the sun directly impacts the ability to determine level 1b irradiance in addition to flare location using the XRS quadrant diodes. These two angles are measured by the SPS and are used in the calculation of the FOV correction, so these are readily available from the level 1b processing.

The roll angle is the last angle required, and it is not used to generate the level 1b irradiances. However, without the roll angle (not measured by EXIS), the flare location could be determined to be on the wrong side of the sun (East-West). The roll angle is also necessary for SUVI processing, so the angular

determination made to support level 1b SUVI processing could be made available to the XRS processing. The details of determining the roll angle are beyond the scope of this document. The details of calculating the EXIS roll angle relative to the solar spin axis may or may not be covered in an upcoming document by Lockheed Martin.

The quaternion convention is described in “Coordinate System Standards GOES-OT-10-0069.doc” in section 6. Basically, it follows the convention from Wertz (Spacecraft Attitude Determination and Control, 1978) and additionally constrains the 4<sup>th</sup> term to be positive, similar to the convention used by TIMED.

Note that the roll angle has no relationship to earth. It is affected by spacecraft orientation, the solar panel angle, and the solar pointing platform to which EXIS is mounted.

## 9.0 Maintaining Calibration, Long-Term Stability

Certain tasks must be performed on a daily basis in order to maintain the absolute calibration accuracy over the life of the instrument. Other tasks are less frequent, but no less important. These include analyzing data collected during spacecraft maneuvers. Note that these calibration algorithm are not part of the Level 1b product generation, however, these algorithm are necessary to keep the calibration files and parameters up-to-date. If these off-line algorithms are not performed and used to maintain the calibration accuracy, then EXIS products will likely fail to meet the accuracy requirements.

### 9.1 Daily Calibration Analysis Routines

This section describes the algorithms needed to perform the routine analysis of calibration corrections that change over time.

#### 9.1.1 Flatfield

The flatfield correction is calculated from the curve fit parameters for each diode that are stored in an ASCII file. Each channel will have parameters stored in a separate file. The file is created by the analysis procedure to satisfy the function shown in Eq. 9.1, where the  $p$  terms are variable parameters, and  $t$  is time in days since an epoch. Time is described in more detail in Appendix E - Time. For this function, the epoch is defined as the first date of the desired fit range.

$$\text{Eq. 9.1} \quad f_{FF} = p_0 + p_1 \cdot \exp\left(\frac{-t - p_2}{p_3}\right) + (p_4 \cdot t)$$

The function allows for the flexibility to use purely exponential behavior, or a linear behavior, or a mixture. The results of the analysis procedure should be reviewed carefully to ensure that the long-term behavior does not extrapolate to unrealistic numbers. The analysis procedure will perform multiple curve fits and choose the best combination of curve fit parameters. One curve fit is a straight line ( $p_1=0$ ), another is an exponential, and the third is the combination.

It is important to note that the data used in the curve fit should be divided by the integration time, and multiplied by the gain.

#### 9.1.1.1 EUVS-A and EUVS-B

The first step involves retrieving the raw data with flatfield flags available. The data are first filtered to remove data that is not identified as having the flatfield LED powered on for the channel. The primary LED and the redundant LED must be tracked separately since these generate different illumination patterns. Furthermore, the first integrations collected during the flatfield exposures may be partial, so the flatfield change counter can be used to remove the first 2 integrations to prevent these, from biasing the results. Recall that since the flatfield change counter increments for each quarter second tick, a value greater than 8 should be sufficient to ensure no partial LED exposure are included for EUVS-A and B.

First divide the raw diode signals in the packet by the integration time (refer to Eq. 4.19). Apply the gain correction to each diode. Subtract the dark correction for the temperature (use the same gain correction). Average and store the results for each diode. Repeat for the previous 3-6 months. This requires some finesse, since a time interval that is too short may have poor statistics, and a period that is too long may not fit the recent data very well. Perform the appropriate curve fit of the diode average vs. days since the epoch for each diode. Compare the results with the previous calibration table values to identify large changes. Store the results as an updated calibration table. When the day boundary is crossed, the new table will take effect.

Initially,  $p_0=1$ ,  $p_1=0$ ,  $p_3=10000$ ,  $p_4=0$ , and  $p_2$  is initially set to  $(-t)$ .

The flatfield trend will change based on exposure to the sun, so the on-orbit storage period may not accurately reflect the gradual changes the detectors will experience during the initial activation period.

#### 9.1.1.2 EUVS-C

The main process for EUVS-C is largely the same as EUVS-A. Periodically, the EUVS-C detector will be dark when the filter wheel is moved to the appropriate position. When dark, the flatfield LEDs can be used to illuminate the detector array with a constant wavelength light. These measurements shall be analyzed off-line to determine updates to the flatfield correction tables used in the Ground Processing Algorithm. The off-line analysis will consist of performing curve fits over each pixel as a function of time using flatfield data collected over the previous 3-6 months. As with EUVS-A, the duration is a trade-off between getting good statistics and fitting the recent trend well.

The time-dependence of the flatfield will be used to correct for shape-dependent changes in the detector counts. Initially, the flatfield correction is expected to have some characteristic shape for each detector based on preflight calibration (refer to calibration data book).

Flatfields will be collected for each LED (2) and each detector (2). The choice of a primary detector will be based on preflight calibration. The choice of the primary LED to use for trending will also be chosen during ground testing. Due to physical placement, the LEDs will produce a different initial pattern on each detector. The flatfields are only really useful when compared to the reference flatfield values, so the flatfields collected in-flight will be divided by the reference flatfield (provided in the calibration data book) to keep most numbers around 1.0. Those relative flatfields are used in the curve fitting.

### 9.1.2 Dark Electrometer Offset

Off-pointing is needed to obtain dark values in-flight for XRS and SPS after the door is opened. This requires coordination with the spacecraft and SUVI. Details will be recorded in the Operations Handbook (CDRL 120).

EUVS A and B can obtain dark measurements at any time by moving the filter mechanism to the proper position. This does not affect other instruments or the spacecraft, but it will impact the EUVS-C measurements since they share a filter mechanism. The filter wheel positions are such that only one of the detectors A, B, or C is allowed to be dark. Each must collect dark sequentially.

Once dark measurements are available, the electrometer offset values can be verified and, if necessary, adjusted. If the offset values calculated do not match the expected values from ground calibration, then a constant should be added/subtracted to bring the ground calibration into agreement.

If the dark values are zero, then the IDAC setting should be adjusted so the dark values can be measured. We recommend communicating with the instrument vendor (LASP) if the IDAC setting needs to be changed, since this is not expected on orbit.

### 9.1.3 Relative Gain

The relative gain change is tracked throughout the mission using built-in current sources. Operationally, a set of calibration tables are activated that insert reference currents into the circuit chain. An offline analysis routine is executed to analyze on-board detector changes using the reference currents. This is necessary to track changes in the detector electronics that affect the relative gain. No adjustments to the instrument operation can be done to moderate/mitigate gain changes, but it can be tracked and corrected in the GPA. This calibration shall be performed when the filter is in the dark position for EUVS-A, and EUVS-B on a regular (perhaps weekly) basis. Since EUVS-A and EUVS-B share a filter wheel mechanism and one gain electrical circuit, and only one of them can be completely dark at a time during the gain calibration. The other channel will be in the sun during the gain, and should be discarded. It is neither useful for gain nor for solar observations when this happens. The diodes remain part of the circuit

chain, so the detectors need to be dark to prevent time-varying signals in the results. Since the XRS and SPS cannot be put into a dark state without off-pointing, these channels will be measured less regularly (expected quarterly). Details about frequency of operation will be recorded in the operations handbook.

This offline calibration routine will look for data patterns that consist of two sets of charge injection or charge-ramp measurements with two different ramp rates plus dark measurements preferably from both before and after the charge-ramp measurements. An RTS is expected to trigger this sequence of events, and set the cal flag in telemetry.

The on-board calibration requires the relevant ASIC channel to be in the dark state, with no solar (or flatfield LED) light striking the detectors. Perhaps 60 seconds of dark data collection with a 1 Hz cadence may be necessary to thermally stabilize. Only the last 51 seconds of data should be used. The remaining dark measurements are then averaged together. The average represents the quantity  $N_{offset\_before}$ . Similar post-charge injection dark measurements are also processed in the same fashion to obtain  $N_{offset\_after}$ . From these two dark measurements, the average is  $N_{offset}$ .

Based on circuit analysis and laboratory measurements, a semi-empirical relationship has been found that allows tracking changes in the gain. The relationship between the calibration parameters, the measurements, the gain, and a leakage current,  $I_B$  is shown in Eq. 9.2.

$$\text{Eq. 9.2} \quad \left( \frac{N_1 - N_{offset}}{\Delta t_1} \right) G + I_B = Cap \cdot \frac{dV_1}{dt_1}$$

$G$  represents the gain (fC/DN),  $Cap$  is the capacitance of the ASIC internal calibration capacitor (a constant),  $dV/dt$  is the configurable voltage ramp rate of the calibration circuit, and  $t$  is the integration time of the measurement (approximately 0.96 seconds). The values with subscripts of "1" correspond to one charge-ramp configuration (the one with the lowest value of  $N$ ). For one charge-ramp configuration set, each measurement (in DN) is represented as  $N$ . Many measurements are necessary to decrease the uncertainty of the average values of  $N$  to achieve better than 2% (1-sigma) statistics for the gain calibration. Approximately 60 1-Hz samples will be collected for charge-ramp configuration #1, and this analysis will ignore the first 9 samples. The remaining samples are then averaged, and the result is  $N_1$ . One of the configuration parameters used in the charge-ramp is  $dV/dt$ . This quantity is calculated using two telemetry items as shown in Eq. 9.3.

$$\text{Eq. 9.3} \quad Steptime_1 \equiv (cal\_t\_step_1 + 1) \cdot 0.00002$$

$$\frac{dV_1}{dt_1} = 5 \cdot \frac{\left( \frac{cal\_v\_step_1 + 1}{4096} \right)}{Steptime_1}$$

Additional useful quantities are shown in Eq. 9.4, where  $Nsteps$  is the number downward voltage steps in the calibration ramp,  $Steptime$  is the number of seconds elapsed in each step, and  $Dt$  is the actual

integration time for the downward portion of the calibration ramp. The value of the integration time that is in the packet is only valid when data is being collected through the diodes, and does not represent the actual integration time for the gain calibration.

$$\text{Eq. 9.4} \quad Nsteps_1 \equiv \frac{(cal\_v\_max_1 - cal\_v\_min_1)}{(cal\_v\_step_1 + 1)}$$

$$\Delta t_1 = Nsteps_1 \cdot Steptime_1$$

It is convenient to track changes in ratios, to map ground measurements to flight measurements, so we rewrite Eq. 9.2 as Eq. 9.5.

$$\text{Eq. 9.5} \quad \left( \frac{N_1 - N_{offset}}{\Delta t_1} \right) \left( \frac{G}{Cap} \right) + \left( \frac{I_B}{Cap} \right) = \frac{dV_1}{dt_1}$$

Note that Eq. 9.5 contains two unknown,  $G/Cap$  and  $I_B/Cap$ . Using the second charge-ramp data set, reduced similarly to the first set, we can solve for the ratio  $G/Cap$  as in Eq. 9.6.

$$\text{Eq. 9.6} \quad \left( \frac{G}{Cap} \right) = \frac{\left( \frac{dV_2}{dt_2} - \frac{dV_1}{dt_1} \right)}{\left( \frac{N_2 - N_{offset}}{\Delta t_2} \right) - \left( \frac{N_1 - N_{offset}}{\Delta t_1} \right)}$$

Similarly, a solution for the leakage current can be determined as in Eq. 9.7.

$$\text{Eq. 9.7} \quad \left( \frac{I_B}{Cap} \right) = \left( \frac{dV_1}{dt_1} \right) - \left( \frac{N_1 - N_{offset}}{\Delta t_1} \right) \left( \frac{G}{Cap} \right)$$

Once  $G/Cap$  is determined, it should be calculated the same way, using the same charge-ramp settings to look for long-term changes. This ratio is expected to be stable to better than 2%, and if it changes by more than 2%, then the relative gain used in the GPA should be updated. The value reported in the calibration file described in section 4.4.5.1.2, is the ratio of the result of Eq. 9.6 divided by the initial value ( $G_0/Cap_0$ ) provided in CDRL 79, the calibration data book. After each relative gain calibration is performed, the table of values is updated with another row.

For EUVS-A and B, recall that all ASICs for both detectors are controlled together. If EUVS-A is in the dark position and a gain calibration is initiated, then EUVS-B data will be corrupted and is unusable, since it contains the solar signals plus the current from the charge injection circuit. Similarly, if EUVS-B was in the dark position and a gain calibration is initiated, then EUVS-A data will be corrupted and is unusable. This is a design “feature” of EXIS, since there is no position where more than one channel can be in the dark position.

### 9.1.4 Degradation Bootstrap Algorithm

This section summarizes the bootstrap degradation description part of a presentation from Sept 15-17, 2008 at the EXIS ISR. This technique was also presented at the EXIS PDR. In flight, this technique was replaced with simpler methods. For EUVS-A, relative filter changes are measured during daily calibrations and used to fit long-term degradation corrections. For all EUVS-B lines, a custom NCEI model was developed driven the Mg II index. The method described here was not used.

The bootstrap degradation technique relies on using long-term measurements. Short-term solar variations observed over less than 30 days are not significant enough to determine long-time degradation changes. The bootstrap degradation analysis uses daily averages of proxy values (not the level 1b high-cadence measurements) of all the good solar measurements. All comparisons are performed using proxies, not irradiances.

First measure something that is degradation independent. The Mg II core-to-wing index is a well-established chromospheric proxy. It was originally developed using the Nimbus SBUV solar data (Heath and Schlesinger, JGR, 1986) and continues to the present with daily measurements from SBUV-2, SORCE, and GOME. As long as the instrument degradation is linear with wavelength, then the Mg II core-to-wing ratio is "degradation free". The Mg II h and k emission lines vary around 12% over the solar cycle relative to the photospheric continuum wing regions.

The next step in the bootstrap technique involves measuring something that varies like the Mg II core-to-wing ratio, with the same instrument that measures transition region emissions. EUVS-B measures C II and C III emissions that are chromospheric in origin, like the Mg II core-to-wing ratio. EUVS-B also measures transition region emissions from H I and Si IV. The degradation of the EUVS-B chromospheric lines is evident when long-term comparisons (>3 solar rotations) are made to the Mg II core-to-wing proxy. With known degradation measured for chromospheric lines, a similar comparison can be made for the chromospheric lines and transition region lines. Now the transition line degradations are known.

The third step involves measuring something that varies like the transition region with the same instrument that measures the corona. EUVS-A measures transition region lines (He II) and the corona (Fe XV). The transition region line comparisons of H I and Si IV to He II determines the degradation of He II. The corrected transition region lines are compared to the Fe XV line to determine coronal line degradation.

A daily routine is executed to perform the degradation analysis. This is performed using daily averages of the fully processed results of: Mg II core to wing ratio, all directly measured lines from EUVS-A (3), and EUVS-B (4).



### 9.1.5 EUVS-A Filter Degradation

There are 108 steps for the filter wheel (euv\_fw\_step\_num). There are approximately 3.33333 degrees per step. While EUVS-B and EUVS-C have no filters in the wheel, there are 24 separate filters for EUVS-A located in different positions of the filter wheel. Step numbers range from 0-107 while each filter occupies about 3 positions. The center position of each filter is designed to have no glint or obstructions, but the others for each filter are partially blocked by the holder that fixes the filter to the wheel. The step numbers that correspond to valid solar positions are 3, 6, 12, 15, 21, 24, 30, 33, 39, 42, 51, 57, 60, 66, 69, 75, 78, 84, 93, and 105. Some larger gaps are caused by the filter wheel frame support structure. One of these filter step numbers will be designated the primary science position.

In Table 26, the EUVS absolute filter step numbers for each position are shown along with the information about the optical channels. This information was taken from LASP document #110565 rev B. For EUVS-B, EUVS-C1, and EUVS-C2 the “open” state indicates a clear path for light to the detectors. For EUVS-A the “open” state indicates there is a clear, unobstructed, glint-free path for in-band light to get to the detector. The “darkpri” state denotes the preferred dark position for a given detector. States designated as “bad” indicate that either no measurement, or a degraded measurement is possible. The “bad” positions should be discarded. Certain “dark” states are possible that are not “darkpri” because another channel is obstructed in some way making that particular position undesirable. There is one “darkpri” position for each detector. We use EUVS-A filter # -1 to designate a position that is not capable of providing solar measurements.

STEP SIZE: 3.33333 DEGREES/STEP  
 ROTATION DIRECTION: CW, MOTOR SHAFT RIGHT HAND RULE. MOTOR SHAFT POINTS IN -X DIRECTION, EXIS COORDINATES.

Green: Preferred position, no obstructions  
 Yellow: Channel A Filter Frame center rib causes obstruction. Light could still get to detector, but seriously degraded.  
 Orange: An edge is within the Glint FOV, but outside the science FOV. These positions may experience glint problems.  
 Red: An edge is partially or fully obscuring the Science FOV.  
 Gray: Dark positions

True Darks	Step #	EUVS-A Filter #	EUVS-A State	EUVS-B State	EUVS-C1 State	EUVS-C2 State	Notes
A-DARK	0	-1	DARKPRI	OPEN	OPEN	OPEN	"HOME" OR "LAUNCH" POSITION. OPTICAL FIDUCIAL 1
	1	-1	BAD	OPEN	OPEN	OPEN	
	2	-1	BAD	OPEN	OPEN	OPEN	
	3	23	OPEN	OPEN	OPEN	OPEN	
	4	-1	BAD	OPEN	OPEN	OPEN	
	5	-1	BAD	OPEN	OPEN	OPEN	

	6	22	OPEN	OPEN	OPEN	OPEN	
	7	-1	BAD	OPEN	OPEN	OPEN	
	8	-1	BAD	OPEN	OPEN	OPEN	
	9	-1	DARK	BAD	OPEN	OPEN	
	10	-1	BAD	BAD	OPEN	OPEN	
	11	-1	BAD	DARK	OPEN	OPEN	
B-DARK	12	21	OPEN	DARKPRI	OPEN	OPEN	
	13	-1	BAD	BAD	OPEN	OPEN	
	14	-1	BAD	BAD	OPEN	OPEN	
	15	20	OPEN	OPEN	OPEN	OPEN	
	16	-1	BAD	OPEN	OPEN	OPEN	
	17	-1	BAD	OPEN	OPEN	OPEN	
	18	-1	DARK	OPEN	OPEN	OPEN	
	19	-1	BAD	OPEN	OPEN	OPEN	
	20	-1	BAD	OPEN	OPEN	OPEN	
	21	19	OPEN	OPEN	OPEN	OPEN	
	22	-1	BAD	OPEN	OPEN	OPEN	
	23	-1	BAD	OPEN	OPEN	OPEN	
	24	18	OPEN	OPEN	OPEN	OPEN	
	25	-1	BAD	OPEN	OPEN	OPEN	
	26	-1	BAD	OPEN	OPEN	OPEN	
	27	-1	DARK	OPEN	OPEN	BAD	OPTICAL FIDUCIAL 2
	28	-1	BAD	OPEN	OPEN	BAD	
	29	-1	BAD	OPEN	OPEN	BAD	
C2 DARK	30	17	OPEN	OPEN	OPEN	DARKPRI	
	31	-1	BAD	OPEN	OPEN	BAD	
	32	-1	BAD	OPEN	OPEN	BAD	
	33	16	OPEN	OPEN	OPEN	BAD	
	34	-1	BAD	OPEN	BAD	OPEN	
	35	-1	BAD	OPEN	BAD	OPEN	
	36	-1	DARK	OPEN	BAD	OPEN	
	37	-1	BAD	OPEN	OPEN	OPEN	
	38	-1	BAD	OPEN	OPEN	OPEN	
	39	15	OPEN	OPEN	OPEN	OPEN	
	40	-1	BAD	OPEN	OPEN	OPEN	
	41	-1	BAD	OPEN	OPEN	OPEN	
	42	14	OPEN	OPEN	OPEN	OPEN	
	43	-1	BAD	OPEN	OPEN	OPEN	
	44	-1	BAD	OPEN	OPEN	OPEN	
	45	-1	DARK	BAD	OPEN	OPEN	
	46	-1	BAD	BAD	OPEN	OPEN	
	47	-1	BAD	BAD	OPEN	OPEN	
	48	13	OPEN	BAD	OPEN	OPEN	
	49	-1	BAD	OPEN	OPEN	OPEN	
	50	-1	BAD	OPEN	OPEN	OPEN	
	51	12	OPEN	OPEN	OPEN	OPEN	
	52	-1	BAD	OPEN	OPEN	OPEN	
	53	-1	BAD	OPEN	OPEN	OPEN	
	54	-1	DARK	OPEN	OPEN	OPEN	
	55	-1	BAD	OPEN	OPEN	OPEN	

	56	-1	BAD	OPEN	OPEN	OPEN	
	57	11	OPEN	OPEN	OPEN	OPEN	
	58	-1	BAD	OPEN	OPEN	OPEN	
	59	-1	BAD	OPEN	OPEN	OPEN	
	60	10	OPEN	OPEN	OPEN	OPEN	
	61	-1	BAD	OPEN	OPEN	BAD	
	62	-1	BAD	OPEN	OPEN	BAD	
	63	-1	DARK	OPEN	OPEN	BAD	
	64	-1	BAD	OPEN	BAD	OPEN	
	65	-1	BAD	OPEN	BAD	OPEN	
C1 DARK	66	9	OPEN	OPEN	DARKPRI	OPEN	
	67	-1	BAD	OPEN	DARK	OPEN	
	68	-1	BAD	OPEN	BAD	OPEN	
	69	8	OPEN	OPEN	BAD	OPEN	
	70	-1	BAD	OPEN	OPEN	OPEN	
	71	-1	BAD	OPEN	OPEN	OPEN	
	72	-1	DARK	OPEN	OPEN	OPEN	
	73	-1	BAD	OPEN	OPEN	OPEN	
	74	-1	BAD	OPEN	OPEN	OPEN	
	75	7	OPEN	OPEN	OPEN	OPEN	
	76	-1	BAD	OPEN	OPEN	OPEN	
	77	-1	BAD	OPEN	OPEN	OPEN	
	78	6	OPEN	OPEN	OPEN	OPEN	
	79	-1	BAD	OPEN	OPEN	OPEN	
	80	-1	BAD	OPEN	OPEN	OPEN	
	81	-1	DARK	OPEN	OPEN	OPEN	
	82	-1	BAD	OPEN	OPEN	OPEN	
	83	-1	BAD	OPEN	OPEN	OPEN	
	84	5	OPEN	OPEN	OPEN	OPEN	
	85	-1	BAD	OPEN	OPEN	OPEN	
	86	-1	BAD	BAD	OPEN	OPEN	
	87	4	OPEN	BAD	OPEN	OPEN	
	88	-1	BAD	BAD	OPEN	OPEN	
	89	-1	BAD	BAD	OPEN	OPEN	
	90	-1	DARK	BAD	OPEN	OPEN	
	91	-1	BAD	OPEN	OPEN	OPEN	
	92	-1	BAD	OPEN	OPEN	OPEN	
	93	3	OPEN	OPEN	OPEN	OPEN	
	94	-1	BAD	OPEN	OPEN	OPEN	
	95	-1	BAD	OPEN	OPEN	OPEN	
	96	2	OPEN	OPEN	OPEN	BAD	
	97	-1	BAD	OPEN	OPEN	BAD	
	98	-1	BAD	OPEN	OPEN	BAD	
	99	-1	DARK	OPEN	OPEN	BAD	
	100	-1	BAD	OPEN	OPEN	OPEN	
	101	-1	BAD	OPEN	BAD	OPEN	
	102	1	OPEN	OPEN	BAD	OPEN	
	103	-1	BAD	OPEN	OPEN	OPEN	
	104	-1	BAD	OPEN	OPEN	OPEN	
	105	0	OPEN	OPEN	OPEN	OPEN	

	106	-1	BAD	OPEN	OPEN	OPEN	
	107	-1	BAD	OPEN	OPEN	OPEN	

**Table 26 EUVS absolute filter step numbers and positions.**

The primary science position filter will degrade slowly over time. This degradation will be measured by moving the filter to a low-duty cycle, secondary filter position. Provided the sun does not change significantly during the solar measurements collected during exposure of the secondary filter, the ratio of the measurement currents ( $C''$  as defined in Eq. 5.6) provide a direct measure of the filter degradation for each line.

The filter degradation is a function of wavelength, so there will be different degradation corrections for each line in EUVS-A.

We recommend that an analyst perform this comparison on a weekly or bi-weekly basis to keep changes to the degradation small. Furthermore, these filter transmission comparisons can be corrupted by solar flares, so a person should identify measurements that are suspect and remove them when determining a trend.

Over time (say 3 months), the filter ratios should be plotted to determine a trend. If the trend is a smooth curve, then the daily degradation correction values can be computed in advance, and compared against future ratios.

## 9.2 Other Calibration Analysis Routines

### 9.2.1 Cruciform and FOV

Spacecraft cruciform scans and FOV mapping data are analyzed off-line. These will be performed during PLT, possibly multiple times, in order to determine inter-channel alignment relative to the SPS, and ground calibration results.

The cruciform allows the chance to determine the optical edges that are used for estimating any small launch shifts from the ground calibration. The cruciform also allows the direct measurement of any possible in-band light “burn-in” effects particularly on 30.4 and 121.6 nm.

The length of the outer parts of the cruciform provides additional dark measurements for XRS. This may exceed the number of dark measurements produced during the off-point maneuver, so these dark data should be analyzed for XRS when possible.

We recommend that an analyst determine the optical edges from cruciform maneuvers manually, since solar activity (such as flares) will negatively impact the results. If a flare occurs during the maneuver, then the ratio will be thrown off, giving incorrect results. Initially, we define the optical edges as the half-power points of the measurement current ratios ( $C''$  as defined in Eq. 5.6) to the center point. This will produce

a trapezoidal-like structure when viewed as a function of angle. As the center point degrades, the off-center areas will artificially increase, resulting in a possible small increase in optical edges.

If the sun is constant over the FOV map, then the relative measurement current variations to center pointing should be compared to the FOV correction being applied. When the confidence in the map data collected is high, and the variations differ from the applied FOV correction by more than 2% within one degree of center pointing, then the FOV correction should be updated. Recall that EXISPORD 142 required the response variation across the sensor field-of-view to deviate by no more than 5% peak-to-peak.

### 9.2.2 Inter-comparisons

Where possible, similar measurements should be compared. The most obvious example of this lies in the twin redundant EUVS-C detectors, with redundant optical paths. Unfortunately, only one of these can be used at a time. It is useful to look for long-term differences between the channels.

### 9.2.3 EUVS-C Flatfield

Initial flatfield comparison to ground measurements is needed to determine if changes have occurred since the last ground check.

## 9.3 Special Routines

This section describes routines that are not necessarily run frequently or regularly.

### 9.3.1 Accuracy

The EXISPORD11 defines accuracy.

“Accuracy: Refers to the error in a measurement, that is the difference between the measured and true value. It includes both systematic and random errors. Systematic errors must be estimated from an analysis of the experimental conditions and techniques. Random errors can be determined, and reduced, through repeated measurements under identical conditions and a Standard Deviation calculated.”

We shall interpret the EXISPORD definition of accuracy in the context of the National Institute for Standards and Technology (NIST) recommendations. The recommendation is published in NIST Technical note 1297, 1994 edition and is available for download from the NIST web site (<http://physics.nist.gov/Pubs/guidelines/sec5.html>). In practical terms, we define a working definition of accuracy as the NIST combined standard uncertainty in the EXIS irradiances. Henceforth, accuracy is synonymous with uncertainty.

The accuracy of the measurements is not calculated within the GPA processing for two reasons. First, the accuracy is not expected to change significantly over short time periods since the calibration uncertainty is likely the largest uncertainty source. Second, the accuracy calculation would slow down the GPA

execution since it involves more calculations than the irradiance. If processing performance were not a concern, then we would recommend calculating the NIST combined standard uncertainty in every measurement.

Rather than possibly impacting the execution time of the GPA calculating numbers that change very slowly, we recommend performing the accuracy calculations in a separate off-line procedure. This allows more advanced tools to be used (for example Matlab, IDL, etc) to simplify the software development.

### 9.3.1.1 XRS Accuracy

EXISPORD80 states: "The accuracy of the XRS irradiance products at the beginning of normal operations shall be 20%, 1 sigma, for irradiance greater than 20 times the minimum irradiance specified in EXISPORD65."

Disregard all long wavelength irradiances that are less than B2.0 (2e-7), and disregard all short wavelength irradiances that are lower than 2e-8 W/m<sup>2</sup>.

The uncertainty equations for XRS are represented in steps for clarity, similar to the irradiance equations. First calculate the uncertainty,  $u_C$ , in the corrected current, (C).

$$\text{Eq. 9.8} \quad u_C = C \cdot \sqrt{\left(\frac{u_S}{S}\right)^2 + \left(\frac{u_{\Delta t}}{\Delta t}\right)^2 + \left(\frac{u_G}{G}\right)^2}$$

As in section 4.3, S is the signal from telemetry,  $\Delta t$  is the integration time, and G is the gain. Each of these terms has an uncertainty. The uncertainty in the signal is 2 DN. The uncertainty in the integration time is 10 microseconds (from GIRD445). The uncertainty in G is required to be less than 2%. This indicates that the uncertainty in the signal is most important for count rates less than 100 DN, and the uncertainty of the gain is most important for signals larger than 100 DN.

$$\text{Eq. 9.9} \quad u_{C'} = \sqrt{(u_C)^2 + (u_{C_{Dark}})^2}$$

The uncertainty in the dark corrected current ( $C'$ ) is shown in Eq. 9.9. It depends on the uncertainty in the current, and the uncertainty in the total dark correction ( $C_{Dark}$ ). The uncertainty in the dark includes a contribution from the Amplifier noise and the Shot noise. Neither of these appears in the irradiance calculation, but these increase the uncertainty. The values of amplifier noise and shot noise will be provided in CDRL 79.

$$\text{Eq. 9.10} \quad (u_{Dark,ij})^2 = u_{elect,ij}^2 + u_{them,ij}^2 + u_{Rad,ij}^2 + u_{Amp,ij}^2 + u_{Shot,ij}^2$$

$$u_{C''} = u_{C'} \text{ for solar minimum diodes}$$

$$\text{Eq. 9.11} \quad u_{C''} = \sqrt{\sum_{j=1}^4 (u_{C'})^2} \text{ for quadrant diodes}$$

The NIST combined standard uncertainty (or accuracy) of the XRS irradiance is calculated in Eq. 9.12, with the irradiance,  $E$ , appearing on the right side. The first ratio term is the relative uncertainty in the total current. The second ratio term is the relative uncertainty in the responsivity, expected to be less than 12%. The third ratio term is the relative uncertainty in the field of view correction, expected to be less than 2%. Of course, the relative (or fractional) uncertainty is found by dividing both sides by the irradiance ( $E$ ).

$$\text{Eq. 9.12} \quad u_E = E \cdot \sqrt{\left(\frac{u_{C''}}{C''}\right)^2 + \left(\frac{u_R}{R}\right)^2 + \left(\frac{u_{f_{FOV}}}{f_{FOV}}\right)^2}$$

This can alternatively be expressed as a percentage.

$$\text{Eq. 9.13} \quad \% = 100 \cdot \frac{u_E}{E}$$

Note that the uncertainty in responsivity, and the responsivity itself are determined in pre-flight ground calibration and are static parameters.

### 9.3.1.2 EUVS-A Accuracy

The EUVS-A accuracy is calculated for each of the 4 irradiances using the method described for XRS (see section 9.3.1.1). We start with calculating the uncertainties in the diode current,  $C_{ij}$ .

$$\text{Eq. 9.14} \quad u_{C_{ij}} = C_{ij} \cdot \sqrt{\left(\frac{u_{S_{ij}}}{S_{ij}}\right)^2 + \left(\frac{u_{\Delta t}}{\Delta t}\right)^2 + \left(\frac{u_{G_{ij}}}{G_{ij}}\right)^2 + \left(\frac{u_{f_{FFij}}}{f_{FFij}}\right)^2}$$

The first ratio is the relative uncertainty in the diode counts. The relative uncertainty in integration time and gain are next followed by the relative uncertainty in the flatfield correction factor. The uncertainty in the corrected current ( $C'$ ) can now be calculated.

$$\text{Eq. 9.15} \quad u_{C'_{ij}} = \sqrt{\left(u_{C_{ii}}\right)^2 + \left(u_{C_{SL,ii}}\right)^2 + \left(u_{C_{OS,ii}}\right)^2 + \left(u_{C_{Dark,ii}}\right)^2}$$

The additive terms are uncertainties in the diode current, scattered light, order sorting, and dark. The dark uncertainty contains contributions from Amplifier noise and Shot noise, although these do not appear in the irradiance calculation. These two terms will be provided in CDRL 79.

$$\text{Eq. 9.16} \quad \left(u_{Dark,ij}\right)^2 = u_{elect,ij}^2 + u_{them,ij}^2 + u_{Rad,ij}^2 + u_{Amp,ij}^2 + u_{Shot,ij}^2$$

**Eq. 9.17** 
$$u_{C'_i} = \sqrt{\sum_j (u_{C'_{ij}})^2}$$
 for quadrant diodes

The uncertainty in the measurement current ( $C''$ ) is shown in Eq. 9.17 (for line  $i$ ). The uncertainty in the irradiance from each line is calculated according to Eq. 9.18.

**Eq. 9.18** 
$$u_{E_i} = E_i \cdot \sqrt{\left(\frac{u_{C''_i}}{C''_i}\right)^2 + \left(\frac{u_{R_i}}{R_i}\right)^2 + \left(\frac{u_{f_{FOV,i}}}{f_{FOV,i}}\right)^2 + \left(\frac{u_{f_{Degrad,i}}}{f_{Degrad,i}}\right)^2 + \left(\frac{u_{\lambda_i}}{\lambda_i}\right)^2}$$

The relative uncertainty in responsivity is a Static Parameter determined in preflight calibration and recorded in the calibration data books (CDRL 79).

### 9.3.1.3 EUVS-B Accuracy

The EUVS-B accuracy is calculated for each of the 3 irradiances using the method described for EUVS-A (see section 9.3.1.2). The uncertainties are calculated exactly the same way with the order sorting uncertainty set to zero.

### 9.3.1.4 EUVS-C Accuracy

The accuracy of the Mg II core-to-wing ratio is calculated using a method similar to the ones described for XRS and EUVS-A. The uncertainties in the two Mg II lines, and the red and blue wing are separately determined. These are then combined into the combined uncertainty of the Mg II core-to-wing ratio. First we calculate the uncertainty in the estimate for data numbers ( $D$ ) in every pixel.

**Eq. 9.19** 
$$u_{D_j} = D_j \cdot \sqrt{\left(\frac{u_{S_j}}{S_j}\right)^2 + \left(\frac{u_{f_{Lin,j}}}{f_{Lin,j}}\right)^2 + \left(\frac{u_{f_{FF,j}}}{f_{FF,j}}\right)^2}$$

This is used to calculate the uncertainty in pixel signal ( $D'$ ).

**Eq. 9.20** 
$$u_{D'_j} = D_j \cdot \sqrt{(u_{D_j})^2 + (u_{D_{SL,j}})^2 + (u_{Dark,j})^2}$$

We can now calculate the uncertainty in the red and blue wings. As with EUVS-A, there are contributions to the uncertainty in the dark that are not present in the irradiance.

**Eq. 9.21** 
$$(u_{Dark,ij})^2 = u_{elect,ij}^2 + u_{them,ij}^2 + u_{Rad,ij}^2 + u_{Amp,ij}^2 + u_{Shot,ij}^2$$

**Eq. 9.22** 
$$u_{D'_i} = \frac{\sqrt{\sum_j [(W_{ij})^2 \cdot (u_{D'_j})^2]}}{\left(\sum_j W_{ij}\right)^2}$$
 where  $i = \begin{cases} blue_{wing} \\ red_{wing} \end{cases}$



Additionally, we can now calculate the uncertainty in the core lines using the fit parameters ( $p$ ) and the associated uncertainties from the fit.

$$\text{Eq. 9.23} \quad u_{D_i''} = \sqrt{2\pi \cdot \left[ p_{2,i}^2 \cdot u_{p_{0,i}}^2 + (p_{0,i}^2 \cdot p_{3,i}^2) u_{p_{2,i}}^2 \right] + (2\pi \cdot p_{2,i}^2 + N_i^2) u_{p_{3,i}}^2}$$

The uncertainty in the Mg II ratio can be written in terms of the wings and core contributions.

$$\text{Eq. 9.24} \quad u_R = R \cdot \sqrt{\left( \frac{u_{D_h''}^2 + u_{D_k''}^2}{(D_h'' + D_k'')^2} \right) + \left( \frac{u_{D_{blue}}^2 + u_{D_{red}}^2}{(D_{blue}'' + D_{red}'')^2} \right)}$$

### 9.3.1.5 EUVS Product Accuracy

The accuracy of the EUVS irradiance products shall be within 20% of the actual irradiance (EXIS245). The EUVS irradiance accuracy is calculated for each spectral band reported in the product.

First the uncertainty in each proxy is calculated.

$$\text{Eq. 9.25} \quad u_{P_i} = P_i \cdot \sqrt{\left( \frac{u_{E_i}}{E_i} \right)^2}$$

The uncertainties from the proxy values are used to estimate the uncertainty in the 5 nm bins results. This uncertainty only includes the uncertainties from the proxies that are used in creating the 5 nm bin model irradiance.

$$\text{Eq. 9.26} \quad u_{E(\lambda)} = \sqrt{(u_{Model(\lambda)})^2 + \sum_{i \text{ used in } \lambda} (u_{P_i})^2}$$

The model uncertainties shall be provided in CDRL 79.

## 9.3.2 Signal to Noise

The EXISPORD has requirements for verification of signal-to-noise. This section describes methods for estimating the signal to noise that could prove useful in monitoring product quality.

### 9.3.2.1 XRS Signal to Noise

The requirement stated in EXISPORD83 is “The signal level shall be such that at minimum (threshold) irradiance levels, the mean signal shall be greater than the standard deviation of the data (instrument noise) over a 10-minute interval.”

An off-line procedure could verify this requirement only during solar minimum conditions. However, the signal-to-noise is a possible metric for tracking sudden detector changes (not anticipated). We recommend calculating the signal-to-noise ratio every day.

First, we conceptually divide each day into non-overlapping 10-minute intervals (144). Each interval is then used to calculate the corresponding 10-minute average of the good solar measurements, and the associated 10-minute standard deviation of those same good measurements. The signal-to-noise ratio is then the average divided by the standard deviation.

The requirement is met for all periods when the ratio is greater than 1.0.

This should be calculated for the primary and secondary irradiance measurements for XRS-A and XRS-B. This provides a noise comparison between channels measuring the same wavelengths. The primary irradiances should always meet the requirement, but the secondary irradiances may not under both low and high solar activity conditions. Note that care must be exercised to prevent divide-by-zero errors. For the extreme high solar activity case, one or both of the secondary irradiance channels may saturate, resulting in zero standard deviation due to the instrument design. For the extreme low solar activity case, the solar maximum channels will become the secondary irradiances and may fail to meet the requirement since the mean irradiance may be comparable to the noise. However, the solar minimum channels are included in EXIS specifically for the purpose of measuring low signals. The primary irradiances should always meet this requirement.

### 9.3.2.2 EUVS Signal to Noise

The requirement stated in EXISPOD125 is "The signal level shall be such that at minimum (threshold) irradiance levels, the mean signal is greater than the standard deviation of the data (instrumental and out of band background noise) over a 10-minute interval".

Since the EUVS product is the result of a model, the noise contribution due to random noise arises solely from the direct detector measurements. Further although the model depends on the XRS-B (long) channel, it will not be discussed here since it was treated separately in section 9.3.2.1.

For the EUVS-A and EUVS-B irradiances, the signal to noise ratio is calculated the same way as described for the XRS. First, a day of measurements is divided into 10-minute intervals. For each interval, the mean and standard deviation are calculated, then the signal to noise ratio is calculated as the mean value divided by the standard deviation. The requirement is satisfied for all signal to noise ratios that are larger than 1.

For EUVS-C, the signal is not directly accessible from the Mg II core-to-wing ratio because it is a derived quantity. Recall that the Mg II h and k lines are not directly integrated, but rather fit to a Gaussian, the random noise in the core line pixels is even further suppressed (due to partial cancellation). If the integrated h and k line count rates, and the red and blue wing count rates separately exceed the signal to noise of 1, then the requirement is met for EUVS-C. For each 10-minute interval, the average h signal, k signal, red signal, and blue signal can be separately differenced from the background signal. These are then averaged and divided by their respective standard deviations.

## Appendix A - GPDS Description

The Ground Processing Demonstration System (GPDS) is a computer with the following physical characteristics.

Vendor: Sun Microsystems

Model: x2270

OS: GNU-Linux Red Hat 5, kernel 2.6.18

Compiler: GCC 4.4.1 Compiler

CPU: 2.67 GHz Intel Xeon X5550 quad-core (Nehalem) processor

Memory: 12 GB (1333 DDR3)

Basic Items	Description
CPU	Intel 2.67 GHz Xeon X5550
Memory	6 GB minimum
Network	3 GbE ports 1 talks to OIS 1 talks to LASP LAN 1 is reserved for off-site configuration (NIST or I&T networks)
Hard Drive	SATA II or SAS (3Gb/sec) 500 GB capacity or greater
OS	RedHat Enterprise Linux 5

Table 27 GPDS Hardware Description

## Appendix B - Polynomial Conversions

Some corrections (say  $V$ ) may best be represented as one or more polynomial conversions. The polynomial coefficients,  $C_i$ , are used in the polynomial evaluation along with some parameter  $X_{raw}$ . The mathematical formula is given by the following equation.

Eq. 9.27 
$$V = \sum_{i=0}^n C_i \cdot X_{raw}^i$$

Note that the equation represents a polynomial of degree  $n$ . In general, care must be taken to ensure that only the valid range of the polynomial is calculated. Most polynomial coefficients are not valid over the entire range of  $X_{raw}$ . For example, for very large values of  $X_{raw}$ , the exponentiation operation could cause an overflow condition.

## Appendix C - Calibration Coefficients and Lookup Tables

This polynomial evaluation process is generic. It may be used for the evaluation of calibration corrections as well, such as dark, which is expected to be smoothly changing over temperature. The coefficients,  $C_i$ ,

may be determined using either analysis of the calibration measurements collected by personnel from the engineering division at LASP, or from manufacturer specifications, or through component calibration analysis. Some of these coefficients may be subject to update in orbit.

An alternative to polynomial evaluation is a lookup table. Depending on the table size, it may be faster to use lookup tables instead of polynomial evaluation. Lookup tables allow for changes to be more easily incorporated later without the need for changing the code. This will be determined on a case-by-case basis after relevant calibration data has been collected and analyzed. The major drivers in making this determination are table size (smaller is best), and complexity of the correction function (simpler is better).

For example, the temperatures are converted from DN to degrees based on ground calibration measurements. Since the temperature DN ranges from 0-65535 (16 bits), this is a good candidate for a lookup table (see 4.4.1.1). The temperatures will vary from integration to integration, so the expensive calculation would need to be performed for every packet. However, a lookup table allows the OS to take advantage of memory locality to reference pre-calculated results from table. In this temperature example, the table would be loaded into an array, and the software would use the temperature DN value as the index into the array to retrieve the precomputed result, with no interpolation necessary. Specifically, every temperature that is possible to receive has already been converted to degrees C. Similarly, the XRS dark and pre-flight gain corrections have already been computed for every possible temperature DN value.

## **Appendix D - Astronomical Unit Correction (1-AU)**

A series of yearly tables of 1-AU correction factors are supplied for a specific instant of each day representing 0 UTC. The correction tables each contain 1 year of correction factors with the first row corresponding to 0:00:00 UTC on January 1, and the last row corresponding to 0:00:00 UTC on January 1 of the following year. The first column is the day of year, the second column is the correction at the start of each UTC day. The rest of the columns are the coefficients of a least squares fit to a polynomial over the course of that UTC day, with the fraction of day (0.0-1.0) as the abscissa. It is recommended that the implementer determine the 1-AU correction factor for the center time of the integration (as a day fraction) by evaluating the polynomial for that instant. The values represent the multiplicative correction ( $1/r^2$ ) from the center of the earth to the center of the sun.

The data for these corrections are included as ASCII files bundled into a zip file (1auCorrections.zip) in the bill of materials with this Agile document. The corrections provided span 2001 through 2050.

The 1-AU corrections provided are derived from the VSOP 87 algorithm [see Bretagnon P. and Francou G., *Astronomy and Astrophysics*, **202**, p309-315, 1988]. It has been shown that this choice of algorithm agrees with the best JPL ephemeris within about 75 km over the last 5 years or about 0.7 ppm. This formulation is reported to provide accurate longitudes to 0.005 arc-seconds from 1900-2100. The solution

is accurate to within 1 arc-second at the year 4000. These solutions were used as the starting point for the calculation of the polynomial curve fits.

## **Appendix E - Time**

The time specified in the CCSDS packet secondary header is offset from Universal Coordinated Time (UTC) by 12 hours. This packet secondary header times are formatted using the so-called day-segmented-time format.

In the GOES-R packet convention, the first field is the number of days since the epoch Jan. 1, 2000 at 12:00:00 UT (range is 0-16,777,215 possible in 24-bits), the number of milliseconds in the shifted day (0-86,399,999 usually, but 32-bits are allocated), and the number of microseconds since the last millisecond (0-999, but 16-bits are allocated). From these fields we calculate the timestamp in UTC seconds of day by subtracting half a day. The seconds of day values range from 0 to 86400, ignoring leap seconds.

However, Julian dates are compatible with UTC noon-time as the start of day. The Julian date at the GOES time epoch of 12:00:00 UTC on Jan 1, 2000 is 245145.0. Conversion of the GOES-R timestamp to Julian date involves adding this constant to the day counter and adding the milliseconds counter divided by 86,400,000.

Note that the integer leap seconds added to atomic time are undefined for Julian dates, since days are equal length. It is recommended that a function be used with a leap second flag to calculate the day fraction.

## **Appendix F - Spacecraft Telemetry**

Some telemetry items may be necessary for processing of higher-level EXIS products (level 2+). Those telemetry items shall be provided from the spacecraft. The only item that has been identified, currently, is the spacecraft roll-angle with respect to the solar north pole. This could be calculated from the attitude quaternion, but since the roll angle of SUVI will be required for SUVI processing, it may be easier to obtain from other processing software produced by the ground systems contractor. It is the responsibility of the ground system contractor to provide orientation information to the level 2 processing, specifically, the EXIS pointing angles plus the roll angle of EXIS about the line of sight to the center of the sun relative to solar north. These have no relation with earth axes.